ABSTRACT

Title of Thesis:	GENETIC CONTROL OF FLOWERING TIME IN A SOFT RED WINTER WHEAT DOUBLED HAPLOID POPULATION
	Daniela Michelle Miller, Master of Science, 2015
Thesis Directed By:	Dr. José Costa, Department of Plant Science and Landscape Architecture

Flowering time in wheat is regulated mainly by response to seasonal environmental cues and controlled by the photoperiod and vernalization pathways. Allelic diversity in genes controlling these pathways is used by breeders to adapt wheat for optimal yield in a broad range of environments. This study characterized genetic loci influencing heading date in a soft red winter wheat doubled haploid population. Two photoperiod insensitivity alleles, *Ppd-A1a* and *Ppd-D1a*, were found to have major effects in eight field locations. The *Ppd-A1* locus explained up to 16.8% of variation in heading date, whereas the *Ppd-D1* locus explained up to 39.7%. In reduced vernalization greenhouse experiments, a QTL in the same region as the *VRN-A1* gene explained up to 42.4% of variation in heading date, suggesting that the population differed in this region. Assays for previously-described allelic diversity in the *VRN-A1* gene, however, did not detect any polymorphism between parents of the population.

GENETIC CONTROL OF FLOWERING TIME IN A SOFT RED WINTER WHEAT DOUBLED HAPLOID POPULATION

by

Daniela Michelle Miller

Thesis submitted to the Faculty of the Graduate School of the
University of Maryland, College Park, in partial fulfillment
of the requirements for the degree of
Master of Science
2015

Advisory Committee:
Professor Dr. José Costa, Chair
Dr. Shunyuan Xiao
Dr. Jianhua Zhu

Acknowledgements

I would like to acknowledge my colleague Yaopeng Zhou for his continued advice and support during my time in the Master's program. His intelligence and persistence, as well as direct assistance, were indispensable to me and I thank him for his continued support. I would also like to acknowledge Mohammed Guedira, Gina Brown-Guedira, and Mai Xiong at North Carolina State University and the USDA-ARS Eastern Regional Small Grains Genotyping Lab in Raleigh, NC. From long-distance advice on designing my greenhouse experiments to hands-on training in the lab and assistance in analyzing results, their support has been integral to my success. Thanks to my collaborators Dr. Shiaoman Chao and Dr. Gina Brown-Guedira or USDA-ARS, without whose genotyping assistance this project could not have been possible. Also, thanks to Dr. Paul Murphy and Virginia Verges for their cooperation in growing two additional field environments in North Carolina and Argentina; Paul Murphy also for the original development of the DH population. Further, I would like to acknowledge the help of our Field Technician Aaron Cooper for planting, harvesting, maintaining plots, and collecting heading date data at our Eastern Shore field locations, as well as Laura Brockdorff and Philip Clements in collecting data for the 2014 greenhouse experiment. Lastly, but most importantly, I would like to acknowledge my major professor, Dr. José Costa, for not only his support in my research but for giving me a more global view of the importance of wheat breeding through travel, connections, and many insightful discussions.

Table of Contents

List of Tables

List of Figures

Chapter 1: Literature Review

Introduction

Wheat is one of the world's most important cereals, providing over 20% of the total caloric and protein intake of the world's population. It is the staple food for more than 40 countries and over 35% of the world's population (Bushuk 1998). In 2013, global production of wheat was 713,182,914 Tonnes, grown from southern latitudes in Argentina and Australia through Russia and Canada in the north (Food and Agriculture Organization, faostat.fao.org). Wheat's global importance is awarded by its ability to grow in a wide range of environments.

Global demand for wheat is predicted to increase at a faster rate than the annual genetic gains currently realized. Therefore, improvements in genetic yield potential must be accelerated to avoid the destruction of natural landscapes to create farmland (Reynolds et al. 2009). Climate change is predicted to further exacerbate global food insecurity (Wheeler & von Braun 2013). Yields of the major crops grown in Africa and South Asia may decline under climate change by an average of 8% by the 2050s; in Africa alone, wheat yields are predicted to drop by 17% (Knox et al. 2012). Serious improvements in yield potential will be required to combat these losses.

Wheat's ability to fine-tune its phenology to its environment by responding to changing day length and temperature has been integral to its adaptation to diverse

climates. Optimized phenological patterns have been cited as a primary means to raise the yield potential in wheat (Reynolds et al. 2009). Better understanding the genetic basis of wheat's response to these environmental signals, and exploiting the genetic diversity at loci controlling these traits, will enable breeders to help wheat adapt to future climates and increase yields.

Wheat Evolution and Domestication

Modern wheat cultivars are usually one of two species: hexaploid bread wheat (*Triticum aestivum*, $2n = 6x = 42$, AABBDD) and tetraploid durum wheat (*T. durum*, $2n = 4x = 28$, AABB) used for pasta and other semolina products. These polyploid wheats evolved from inter-specific hybridization events between three diploid ancestors: *T. uratu*, *Aepilops speltoides*, and *Ae. tauschii*. The progenitors of the A (*T. uratu*, $2n = 2x = 14$) and B (*Ae. speltoides*, $2n = 2x = 14$) genomes in wheat diverged ~7 million years ago; the D progenitor (*Ae. tauschii*) emerged 1-2 million years later through homoploid hybridization between *T. uratu* and *Ae. speltoides* (Marcussen et al. 2014). About 300,000-500,000 years ago, polyploid hybridization between *T. uratu* and *Ae. speltoides* produced wild emmer wheat (*T. dicoccoides*, $2n = 4x = 28$, genome AABB; Petersen et al. 2006; Marcussen et al. 2014).

About 10,000 years ago, hunter-gatherers began cultivating wild wheats in the Fertile Crescent. In about a thousand years, their selections gradually created domesticated einkorn wheat (*T. monococcum*, 2n = 2x = 14, genome AmAm) and domesticated emmer wheat (*T. dicoccum*, 2n = 4x = 28, genome AABB; Feldman &

Kislev 2015). A second hybridization between domesticated emmer and *Ae. Tauschii* ($2n = 2x = 14$, genome DD), created hexaploid spelt wheat (*T. spelta*, $2n = 6x = 42$, genome AABBDD). This cross occurred about 9,000 years ago, after emmer wheat cultivation expanded eastwards from the Fertile Crescent into the natural habitat of *Ae. tauschii*, to the south and west of the Caspian Sea (Peng et al. 2011; Dvorak et al. 1998). Selection has since created hexaploid bread wheat as we know it today (*T. aestivum*, $2n = 6x = 42$, genome AABBDD). Major genes selected for under domestication transformed the brittle rachis to no longer shed its seeds at maturity, while glumes were weakened and hulls removed to enhance threshability (Peng et al. 2011).

Wheat exemplifies the positive correlation between ploidy and success as a crop. In almost all areas where domesticated einkorn (AA) and emmer (AABB) wheat were grown together, emmer became the primary cereal. Today, 95% of wheat is hexaploid bread wheat (AABBDD), while 5% is tetraploid durum wheat (AABB). Allopolyploidy (inter-specific hybridization) increases likelihood of success by converging genomes previously adapted to different environments in a single organism, thus creating the potential for the adaptation to a wider range of environmental conditions. Compared with tetraploid wheat, *T. aestivum* has broader adaptability to different photoperiod and vernalization requirements; improved tolerance to salt, low pH, aluminum, and frost; better resistance to several pests and diseases; and extended potential to make different food products (Dubcovsky & Dvorak 2007).

Regulation of Flowering Time in Wheat

Flowering time of wheat is determined both physiologically and in response to environmental cues such as exposure to cold temperatures (vernalization) and duration of daylight (photoperiod). These responses are regulated through three groups of genes: earliness per se genes (*Eps* genes), vernalization response genes (*VRN* genes), and photoperiod response genes (*Ppd* genes) (Snape et al. 2001). *Eps* genes are purely physiological and control the rate of plant development independent of environmental influence. *VRN* genes control flowering time in response to exposure to cold temperatures. *Ppd* genes control flowering time relative to day length (photoperiod). Working together in a complex network, *VRN* and *Ppd* genes enable the plant to fine-tune itself to its environment and flower at the optimal time for fitness (Snape et al. 2001).

Earliness per se

Eps is a quantitative trait controlled by polygenes with small effect, and can only be evaluated in the absence of photoperiod and vernalization effects. *Eps* plays a minor role in the regulation of flowering time as compared to vernalization and photoperiod; it is a quantitative trait controlled by polygenes with small effect that can only be determined when the requirements of vernalization and photoperiod have been fulfilled (Kamran et al. 2014; Kato & Wada 1999). No *eps* genes have been cloned to date. A major e*ps* QTL on chromosome 1DL of winter wheat is associated

with 3 to 5 days earlier flowering regardless of photoperiod (Zikhali et al. 2014). There has been little effort in characterizing eps QTL as they tend to have relatively minor effects and are difficult to characterize.

Vernalization

Vernalization is the "acquisition or acceleration of the ability to flower by a chilling treatment" (Chouard 1960). Vernalization requirements are common in cold-adapted plants, protecting floral meristems of many annuals and perennials from winter damage. This helps the plants maximize fitness and yield in their respective environments. In wheat, vernalization response is regulated by the vernalization genes *VRN-1*, *VRN-2*, and *VRN-3*. Each gene has three homoeologous copies across the three genomes (A, B, D) of wheat. Spring and winter growth habit is defined by whether the plant requires vernalization to flower.

The *VRN-1* loci are the primary target of vernalization (Li & Dubcovsky 2008; Shitsukawa et al. 2007). The *VRN-1* locus in diploid wheat (*T. monococcum*) encodes a MADS-box transcription factor that is orthologous to *Arabidopsis thaliana* meristem identity gene *APETALA1* (*AP1*; Yan et al. 2003). In *A. thaliana, AP1* acts in concert with *APETALA2* (*AP2*) to establish a determinate floral meristem, transitioning the plant from the vegetative to reproductive phases (Irish & Sussex 1990).

Cultivars carrying recessive alleles at all *VRN-1* loci show winter growth habit, requiring vernalization to flower; carrying the dominant *Vrn-1* allele at any of

the three loci confers a reduced vernalization requirement and a spring growth habit (Tranquilli & Dubcovsky 2000). Spring habit has been associated with large deletions in the first intron of *VRN-A1, VRN-B1,* and *VRN-D1*, removing a 2.8-kb segment highly conserved between different recessive alleles for winter habit (Fu et al. 2005). Expression profile analysis of *VRN-D1* of diploid wheat (*T. monococcum*) shows that transcripts increase proportionally to duration of vernalization; however, *VRN-D1* was not transcribed in unvernalized winter types (Yan et al. 2003). Vernalization acts as a trigger for the transcription of *VRN-1*, thus promoting flowering in winter habit plants.

Duration of vernalization requirement within winter wheat is also largely controlled by allelic variation at *VRN-1* loci. In a doubled haploid soft red winter wheat population, an A/C SNP polymorphism in an intron of *VRN-B1* was associated with a difference of 30 days in heading date between alleles after a short (4-week) vernalization treatment (Guedira et al. 2014). Increased copy number of *VRN-A1* has also been found to confer an increased requirement for vernalization (Diaz et al. 2012). The allelic diversity in the *VRN-A1* gene offers fine-tuneability of flowering time to breeders. In a diverse set of 683 wheat genotypes, the allele phases in the *VRN-1* genes showed the strongest associations with geographic origins of genotypes, suggesting that *VRN-1* is a major determinant of environmental adaptability (Kiss et al. 2014).

VRN-2 is a dominant gene for winter growth habit; a single functional copy of *VRN-2* on any genome will repress flowering (Yan et al. 2004). The *VRN-2* loci are

located on the group 5 chromosomes and encode ZCCT zinc finger transcription factors that down-regulate *VRN-1* and *VRN-3*, promoters of flowering (Yan et al. 2003; Yan et al. 2004; Yan et al. 2006). *VRN-2* has no clear orthologs in *A. thaliana* or rice. *VRN-2* is down-regulated by cold exposure, enabling increased *VRN-1* transcription with increased duration of vernalization. Loss-of-function *VRN-2* did not require vernalization to flower, suggesting that *VRN-2* function is essential to winter growth habit (Yan et al. 2004). *VRN-1* and *VRN-2* interact epistatically to determine vernalization requirement (Tranquilli & Dubcovsky 2000; Fu et al. 2005).

VRN-3, also known as *TaFT1*, encodes a RAF kinase inhibitor-like protein orthologous to *FLOWERING LOCUS T* (*FT*) in *A. thaliana* (Yan et al. 2006). *FT* is tightly regulated by seasonal cues, controlled by at least five activators and five repressors from the vernalization, photoperiod, and autonomous pathways. *FT* acts as a mobile signal to initiate the reproductive phase. The protein is made in the leaves and transported to the meristem, where it creates a complex with *FLOWERING LOCUS D (FD)* and activates *AP1* and other meristem identity genes (Andrés & Coupland 2012).

VRN-3 promotes flowering in wheat by up-regulating *VRN-1* transcription (Yan et al. 2006). *VRN-3* is repressed by high levels of *VRN-2*; expression of *VRN-3* increases after vernalization has significantly downregulated *VRN-2* (Yan et al. 2006). Additionally, *VRN-3* is up-regulated by the photoperiod gene *Ppd-1* under long day conditions (Yan et al. 2006; Beales et al. 2007). *VRN-3* acts as an integrator of the vernalization and photoperiod pathways, placing *VRN-3* at the center of the gene

network regulating flowering time. This is comparable to the central role of orthologous *FT* in *A. thaliana* (Yan et al. 2006; Distelfeld, Li, and Dubcovsky 2009).

Photoperiod

Plants can also respond to changes in day length; this phenomenon is known as photoperiodism. Most ancestral wheat is photoperiod sensitive (PS), meaning that induction of flowering is accelerated under exposure to long days (16+ hours). PS is advantageous in winter wheats grown in cooler environments because it helps the plant maximize its time growing in ideal spring temperatures, enabling higher yield. Natural mutations in the genes controlling photoperiod introduced neutrality to day length, known as photoperiod insensitivity (PI). PI brings great yield advantages in regions with hot, dry summers because the plant can flower and mature before the onset of harsh summer conditions (Kato and Yokoyama 1992; Worland 1996).

Response to day length is controlled by the *Photoperiod-1* (*Ppd-1*) gene family, comprised of three homoeologous loci on the group 2 chromosomes (*Ppd-A1* on chromosome 2A, *Ppd-B1* on chromosome 2B, and *Ppd-D1* on chromosome 2D) (Distelfeld et al. 2009). These genes are in the pseudo-response regulator (*PRR*) family and are homologous to *Ppd-H1*, a *PRR* gene that regulates photoperiod response in barley (*Hordeum vulgare* L.; Beales et al. 2007; Turner et al. 2005). PRR proteins are a class of genes involved in circadian clock function, characterized by a pseudo-receiver domain on the N-terminal end and a CCT motif at the C-terminal end (Nakamichi et al. 2005).

In barley, reduced responsiveness to long days in a *ppd-H1* mutant was found to be caused by altered circadian expression of the photoperiod pathway gene *CONSTANS* (*CO*), which reduced expression of its downstream target, *FT* (Turner et al. 2005). In *Arabidopsis*, *CO* encodes a nuclear protein containing zinc fingers that activates transcription of *FT* (Putterill et al. 1995; Suarez-Lopez et al. 2001). Expression of *CO* is regulated by the circadian clock such that *CO* expression peaks during daylight hours only under long day (16+ hours) conditions (Suarez-Lopez et al. 2001). *CO* protein is degraded by the proteasome in the morning or in darkness, allowing *CO* to only persist when expression peaks in the evening are stabilized by light under long day conditions (Valverde et al. 2004). *Ppd-1* genes and *CO* homologs in wheat have not yet been cloned, but colinearity and homology with barley and *Arabidopsis* suggest that they function similarly (Beales et al. 2007).

Mutations conferring PI have been found on all three homeologous *Ppd-1* genes of wheat (Beales et al. 2007; Wilhelm et al. 2009; Diaz et al. 2012). These genes are given an '*a*' suffix to represent the insensitive phenotype, whereas sensitive phenotypes are given suffix '*b*' (McIntosh et al. 2003). The most-widely used source of PI in wheat is a 2,089 bp deletion upstream of the *Ppd-D1* coding region, the semi-dominant *Ppd-D1a* allele (Worland et al. 1998; Beales et al. 2007). In a diverse set of global wheat cultivars, the *Ppd-D1a* allele was carried on 57% of the cultivars (Kiss et al. 2014). The deletion is associated with misexpression of *Ppd-D1*, which lead to lower *TaCO* expression and higher expression of *VRN-3* (*TaFT*) in long or short days (Beales et al. 2007).

Deletions in the 5' UTR region upstream of the *Ppd-1* coding region is common among PI alleles. A 1,027 bp deletion and 1,117 bp deletion that included 886 bp common to each other as well as the deletion in *Ppd-D1a* (Wilhelm et al. 2009). These deletions were also associated with increased expression of *VRN-3* (*TaFT*), especially during daylight hours (Wilhelm et al. 2009). *Ppd-B1a* insensitivity is associated with a 308 bp insertion in the 5' upstream region of *Ppd-B1* in the cultivar 'Winter-Abukumawase' (Nishida et al. 2013). PI is also associated with a 1,085 bp deletion in the 5' upstream region of *Ppd-A1* in the insensitive cultivar 'Chihokukomugi' (Nishida et al. 2013).

The *Ppd-B1* locus is highly variable, often based on copy number. In a diverse set of 683 global wheat cultivars, 22% of genotypes carrying the *Ppd-B1a* PI allele had 11 different versions: nine versions were identified based on copy number and junction structure, and two genotypes had null copies of the *Ppd-B1* gene (Kiss et al. 2014). Increase in copy number of *Ppd-B1* is associated with the earlier flowering phenotype (Diaz et al. 2012). PS genotypes (*Ppd-B1b* allele) have a haploid copy number of one; PI (*Ppd-B1a* allele) genotypes have been reported with two to four copies of *Ppd-B1* (Diaz et al. 2012; Kiss et al. 2014). The minor and incremental effects of *Ppd-B1a* copy number variation allows for precise tailoring of crops to flower at the best times for their environments.

Quantitative Traits

Most crop traits of agronomic importance are quantitative traits, including yield, quality, some types of disease resistance, and flowering time. Quantitative traits (e.g. 'polygenic' or 'complex' traits) are controlled by gene differences at several (sometimes many) loci, most of which have small effects. Quantitative traits vary continuously rather than discretely. The expected Mendelian ratios are not observed for quantitative traits segregating in a population because they are controlled by many genes rather than single genes. Individual loci controlling a quantitative trait are called quantitative trait loci (QTL). Locating QTL is done using quantitative genetics.

Quantitative genetics is the study of the inheritance of quantitative traits. Quantitative genetics differs from Mendelian genetics in two major ways: 1) traits must be measured, not classified; and 2) populations, not individuals, must be studied, since Mendelian ratios cannot be observed. However, the inheritance of quantitative differences still occurs by means of genes, and these genes are subject to the Mendelian laws of transmission. Thus, quantitative genetics can be considered an extension of Mendelian genetics. A chromosomal region linked to or associated with a marker which affects a quantitative trait was defined as a quantitative trait loci (QTL) (Geldermann 1975). The identification of QTLs requires large populations where the trait of interest is measured (phenotyping) and genetic variation is screened (genotyping) for each individual in the population.

Genetic Markers

Genetic markers represent genetic differences between individuals that can be used to detect allelic variation in genes underlying traits of interest. Typically, genetic markers do not represent target genes themselves, but can be used as experimental probes or tags to keep track of an individual, a tissue, cell, nucleus, chromosome or gene (Xu 2010). Genetic markers are particularly useful if they reveal differences between individuals. The different forms of a marker are called 'alleles.' Genetic markers with multiple alleles within a population of individuals are considered 'polymorphic' markers, whereas 'monomorphic' markers are the same across the entire population. Markers are either dominant (having only two alleles) or codominant (numerous alleles; Collard et al. 2005).

Polymorphism and abundance are important attributes of genetic markers (Tanksley 1993). Genetic markers must be polymorphic to be useful, because there is no segregation in the population if there is no allelic variation, and without segregation no linkage tests can be done to locate QTLs. Abundance of (polymorphic) markers is an important attribute to consider when selecting genetic markers to use. It is theoretically possible to detect all QTLs affecting a quantitative trait if enough polymorphic markers are scattered across the genome. Increased abundance of markers increases the likelihood of detecting a QTL and improves resolution of its location (Tanksley 1993).

Morphological Markers

The earliest genetic markers were physiological features linked to genes of interest, called morphological markers. Morphological markers represent genetic polymorphism, but are visible as differences in appearance. Mendel's round/wrinkled peas in his classic pea experiment represented a morphological marker: round vs. wrinkled. Morphological markers are beneficial in that they are easily detectable in the field, but their usefulness is limited by the small number of unique morphological markers that can be recorded in a population. Further, morphological markers can be influenced by environmental factors or the developmental stage of the plant, creating ambiguity (Winter & Kahl 1995).

RFLPs

The rapid advancement of DNA technologies allowed a shift from the use of morphological markers to the use of DNA markers. The earliest DNA markers used were DNA restriction fragment length polymorphisms (RFLPs), used to create linkage maps of the human genome (Botstein et al. 1980). RFLPs are created by digesting purified DNA with specific restriction enzymes that cut the DNA strand wherever there is a recognition site sequence. These recognition sequences are typically four to eight base pairs long and are known for each restriction enzyme used. The digestion products, known as restriction fragments, are then electrophoresed on agarose gel; however, they appear as a smears because of the large number of fragments. Therefore, fragments must be visualized using the Southern

blotting method (Southern 1975). Polymorphism is revealed by the variable lengths of restriction fragments. RFLPs provide useful markers for comparative and synteny mapping, but they are time-consuming, require large amounts of high quality DNA, have low genotyping throughput, and are very difficult to automate (Xu 2010).

AFLPs

The concept of RFLPs was improved upon in the early 1990s by the introduction of amplified fragment length polymorphism (AFLP; Vos et al. 1995). AFLPs also exploit the polymorphism revealed by variable-length restriction fragments, but combines this with polymorphism caused by the hybridization of arbitrary PCR primers. In the AFLP method, whole genome DNA is digested with specific restriction enzymes, ligated, pre-amplified, then selectively amplified using a primer that includes an arbitrary, non-degenerate 'selective' sequence (Vos et al. 1995). Electrophoresis of these products reveals polymorphism.

SSRs

Microsatellites, or simple sequence repeats (SSRs), grew in popularity as a genetic marker in the 1990s, and are still widely employed to provide 'anchors' to genetic linkage maps in organisms that do not have reference genomes. SSRs are tandemly repeated units of short nucleotide motifs that are 1-6 bp long (Xu 2010). They are particularly valuable genetic markers because of their high level of allelic variation, with rates of mutation at around $4\times10^{4} – 5\times10^{6}$ per allele and per

generation (Xu 2010). SSR loci are individually amplified, using PCR pairs with primers unique to both flanking DNA sequences. Polymorphism is determined by the number of repeats and is revealed by the variable length of amplification products. SSR products can be separated by gel electrophoresis or by automation. While SSRs are labor-intensive to run, even when automated, they are reliable markers once developed, characterized by their high variability, reproducibility, co-dominant nature, locus specificity, and random dispersion throughout most genomes (Xu 2010).

SNPs

Single nucleotide polymorphisms (SNPs) are considered to be the ultimate genetic marker because they are the smallest unit of inheritance: a nucleotide base. A SNP is defined as an individual nucleotide base difference between two DNA sequences (Xu 2010). For variation at any specific locus to be considered a SNP, variation must occur here for at least 1% of the population (Xu 2010). SNPs can occur anywhere in the genome: in coding, non-coding, and intergenic regions. However, SNPs tend to be found at a lower frequency around centromeric regions, which also tend to contain few transcribed genes (Schmid et al. 2003). SNPs have become the most highly-sought after genetic marker and there are a number of assays used to genotype them.

Genotyping-by-Sequencing (GBS) has recently been introduced as a method to discover large numbers of SNPs in high diversity species with complex genomes, such as wheat (Elshire et al. 2011; Poland et al. 2012). GBS library construction

requires restriction digestion and targeted amplification. The process is expedited by the use of a barcoding system. Genomic DNA is digested with specific restriction enzymes; repetitive regions of the genome can be avoided and low copy regions can be targeted by selecting appropriate restriction enzymes. Adapters, selected to include a barcode just upstream of the restriction enzyme cut site, are ligated to digest products. DNA is pooled and purified, and PCR is performed to increase the sample pool. PCR primer pairs are selected to contain complementary sequences to amplify restriction fragments with ligated adapters. The resulting amplified fragment sample pools constitute a GBS library (Elshire et al. 2011).

Once constructed, libraries are sequenced, and raw sequence data is filtered based on barcode, quality, and presence of expected remnant of restriction enzyme cut site. Filtered reads are trimmed to 64 bases, including cut site, and aligned to a reference genome (Elshire et al. 2011). Potential SNP loci can be identified by scanning the aligned reads of different genotypes for polymorphic loci. Because a reference map is only necessary around restriction sites, GBS is particularly advantageous when studying organisms lacking a complete reference genome.

Bi-Parental Mapping Populations

Locating quantitative trait loci (QTLs) using linkage mapping requires precise genetic stocks, known as mapping populations. Typically, these are bi-parental populations: a group of sibling lines derived from a cross between two parents of interest. Careful consideration should be taken when selecting the parents of a

mapping population. Parents should differ significantly for the trait of interest. Often, it is beneficial for the parents to be adapted to similar environments and remain fairly consistent for other quantitative traits, as these differences may make it more difficult to isolate the effects of the trait of interest. Mapping populations can be classified into two major groups based on the stability of their genetics: segregating populations and stable populations.

Segregating Populations

The earliest mapping populations used were segregating populations, meaning that their genetics were unstable. A common segregating population used was F2 populations, derived from first generation of self-pollination after the original cross is made. F2s are advantageous because of their quick generation time, but the genetics within these populations will change with each generation. Therefore, F2 populations can only be grown in one location during one growing cycle, making them impossible to replicate or retest. Stable (non-segregating) populations are preferable because their genetics are consistent and they can be replicated as many times as desired across environments, growing seasons, and laboratories (Xu 2010).

Stable Populations: Recombinant Inbred Lines (RILs)

Recombinant inbred lines (RILs) are generated by continuous inbreeding starting from an F2 population until homozygosity is reached. The rate of approach to homozygosity depends on the number of heterozygous loci in the initial progeny

and, when linked loci are involved, the recombination frequencies between linked loci. The lower the recombination frequency, the more rapidly the population becomes homogenized. For self-pollinated plants, continuous inbreeding is done following two different methods: bulking and single seed descent (SSD). Using the bulking method, F2 progeny are bulk planted and harvested until F5 to F8. In SSD, one or several seeds are harvested from each plant starting in the F2 generation and are grown until F5 to F8. Once the RILs attain homozygosity, the genetic combinations of both parental genomes represented in individual F2 plants are each represented by a RIL.

Stable Populations: Doubled Haploids (DHs)

Doubled haploid production creates stable populations within a much shorter generation time than RILs, by utilizing haploid copies of the F2 generation of a cross. Induction of haploidy can be done using a number of methods, often suited to a specific plant. In wheat, one of the common methods is by wheat x maize crosses. The hybrid embryos contain one haploid chromosome set from each parent, but the maize chromosomes are lost after the first few cell division cycles, producing a haploid set of wheat chromosomes (n=1, x=3, 21, genome ABD). Almost all embryos abort when left to develop on the plant, but when grown in spikelet culture, about 25% are recovered (Laurie & Bennett 1988). Very young haploid plants are then treated with colchicine to induce chromosome doubling. The resultant DH lines are stable in that they display both complete homogeneity and homozygosity within

lines. DH populations are ideal because of their short generation time; the whole process of DH population production can be done within a year, whereas RIL populations need to be grown for at least six generations before stable genetics are attained. This also makes them cheaper and less labor-intensive to develop than RILs. However, a setback of DHs when compared to RILs are that they have a much lower recombination frequency. DHs contain immortalized F2 genetics, representing only one recombination event, whereas RILs have as many recombination events as the number of generations they are grown. This generally allows for better linkage maps to be produced from RILs than DHs because linkage maps are built based on recombination frequencies. To compensate for this, larger DH populations can be used. Still, DH populations are convenient and widely-used mapping populations.

QTL Mapping

A quantitative trait locus (QTL) is a region of a chromosome (usually defined by linkage to a DNA marker) that has a significant effect on a quantitative trait (Tanksley 1993). Once a mapping population has been genotyped and phenotyped, determining the location of a QTL requires two steps: linkage map construction and QTL mapping. A linkage map functions as a 'road map' of the chromosomes of the two different parents of a mapping population, indicating the location and relative genetic distances between markers along chromosomes (Paterson 1996). It is important to note that genetic distances are not the same as physical distances on a chromosome, but rather represent locations of markers relative to another, as

calculated statistically. Linkage maps can be used to identify chromosomal locations containing QTL associated with the trait of interest.

The underlying assumption of using marker loci to detect QTL is that linkage disequilibrium (LD; the nonrandom association of alleles at different loci in a population) exists between alleles at the marker locus and alleles of the linked QTL (Tanksley 1993). In bi-parental mapping populations, LD primarily occurs by recombination (crossing-over) of chromosomes during meiosis (Collard et al. 2005). When crossing-over occurs, two chromosomes intertwine and exchange ends of one chromosome with the other; this process can happen repeatedly on the same chromosome (Hartl & Jones 2001). Crossing-over results in the recombination of parental genotypes. The greater the distances between markers, the greater the likelihood of recombination occurring during meiosis. Markers and/or genes that are close together (e.g. 'tightly linked') are transmitted together more frequently from parent to progeny.

Recombination within a population can be used to infer genetic distance between markers. Recombination fractions are calculated using the frequency of recombinant genotypes: as recombination increases, the recombination fraction increases, and the markers are interpreted as being farther apart. Marker combinations that have a recombination fraction of 50% are considered 'unlinked,' and are assumed to be located on different chromosomes or very far apart of the same chromosome (Collard et al. 2005; Hartl & Jones 2001).

Mapping functions are used to convert recombination fractions into units of genetic distance ('map units,' centiMorgans [cM]). The two most commonly used mapping functions are the Haldane and Kosambi mapping functions. The Kosambi mapping function assumes that recombination events influence the occurrence of adjacent recombination events, while the Haldane mapping function assumes no interference (Hartl & Jones 2001).

Once a linkage map is constructed, QTL mapping can be used to correlate regions of the genome with a trait of interest. To map a QTL, the population is first partitioned into different genotypic classes based on genotypes at a marker locus, then correlative statistics are used to determine whether the individuals of different genotype classes differed significantly with respect to the trait being measured (Tanksley 1993). This process happens iteratively for each marker (or set of markers) across the constructed linkage map.

The simplest approach to mapping QTL analyzes data one marker at a time. This is referred to as single point analysis and does not require a complete linkage map. The magnitude of a QTL is typically underestimated using this method, and QTL without tightly-linked markers often go undetected (Tanksley 1993). Interval analysis was developed to overcome these limitations (Lander & Botstein 1989). Interval analysis analyzes sets of linked markers simultaneously with regard to their effects on quantitative traits, allowing compensation for recombination between markers, thereby increasing power to detect a QTL. The first QTL mapping study using a complete linkage map was published in 1988 (Paterson et al. 1988), using

interval analysis and RFLP markers with an interspecific backcross population of tomato (Paterson et al. 1988)

QTL mapping scans across intervals to find evidence for QTL with large logarithm of odds (LOD) scores related to a particular trait. LOD is the logarithm of the odds ratio, calculated as the likelihood of linkage versus likelihood of no linkage. An LOD value of 3 indicates that linkage between loci is 1000 times more likely than no linkage. A threshold LOD of 3 is widely accepted in the field as an indicator of presence of a real QTL. Once QTL have been mapped, polymorphism at flanking markers can be used to track presence of the QTL in breeding populations.

Marker-Assisted Selection

Fundamentally, plant breeding is the process of selecting specific plants with desirable traits; the goal of the plant breeder is to assemble more desirable combinations of genes into new genotypes. In conventional breeding of inbreeding plants, crosses are made between genotypes that contain different target traits. With increasing generations, progeny of these crosses are selected based on agronomic traits, resistance to various stresses, and quality. These evaluations are typically done visually in the field or greenhouse or using lab methods, and are time- and labor-consuming. The full process of developing and evaluating a new cultivar takes 5-10 years and considerable expense (Collard & Mackill 2008).

Marker-assisted selection (MAS) is the use of DNA markers to increase the efficiency and precision of plant breeding. Once QTL have been mapped and tightly-

linked DNA markers identified, these markers can be used to 'tag' the presence/absence of specific alleles in a gene of interest and tracked in resultant populations. An ideal DNA marker is tightly-linked to the target loci, preferably less than 5 cM genetic distance, and is highly polymorphic in breeding materials (Collard & Mackill 2008).

There are many advantages of MAS versus conventional phenotypic selection. Selections can be made with single plants as early as the seedling stage, and phenotypic selection can be replaced with genetic selection. This is particularly useful in early generations and with traits that are particularly costly or time-consuming to measure (i.e. *Fusarium* head blight resistance, cereal cyst nematode resistance; Collard & Mackill 2008). MAS can be used to minimize 'linkage drag', the transfer of undesireable genes along with the introgression of target genes from wild relatives (Collard et al. 2005). Additionally, different genes and traits can be manipulated simultaneously, enabling efficient 'pyramiding' of multiple genes for resistance to specific pathogens within the same elite cultivar (Dubcovsky 2004). As genotyping costs continue to decrease, costs of phenotyping many traits quickly outweigh costs of screening populations using MAS. GBS offers the ultimate tool for MAS, simultaneously discovering new markers and genotyping breeding populations rapidly and at low-cost (He et al. 2014).

MAS is a molecular breeding method. However, unlike transgenic methods, alleles that are incorporated by MAS are typically already present within the gene pool of a particular crop, or a relative of it, and are transferred by meiotic

chromosome recombination. Transferred alleles reside at their natural chromosome locations, minimizing the risk of gene silencing, public disapproval, and extensive regulation that are characteristic of transgenic crops (Dubcovsky 2004). MAS is not a new method of plant breeding, but an improvement and expansion of conventional plant breeding.

Chapter 2: Genetic Control of Flowering Time in a Soft Red Winter Wheat Doubled Haploid Population

Introduction

Wheat is the staple food for more than 40 countries and over 35% of the world's population, providing over 20% of the total caloric and protein intake of the world's population (Bushuk 1998). It is widely grown from southern latitudes in Argentina and Australia through Russia and Canada in the north (Food and Agriculture Organization, faostat.fao.org). Exploiting genetic diversity in genes controlling flowering time, via the photoperiod and vernalization response pathways, breeders have adapted wheat to this broad range of environments. For example, photoperiod insensitivity from *Ppd-D1a*, derived from Japanese varieties Akakomugi or Saitama 27, was widely employed in European winter wheats, providing yield advantages of over 35% in Southern Europe and 15% in Central Europe (Worland 1996). Especially at lower latitudes, this insensitivity enables winter wheats to flower before the onset of hot, dry summer conditions that negatively impact yield. Shuttle breeding, a technique developed by Dr. Norman Borlaug and employed by the CIMMYT International Maize and Wheat Research Center, in which breeding populations were grown during two growing seasons per year—one in the cooler highlands of Obregón, Mexico in the summer and one in warmer lowlands during the winter, enabled accelerating plant breeding, but also indirectly selected for photoperiod insensitivity, as this brought better adaptability and higher yields in the

spring-sown crop in Obregón. The hexaploid nature of wheat enables further fine-tuning as there are three homoeologous copies of the genes involved in these pathways, one on each of its three genomes, which can each function differently.

The phenology of wheat influences key traits in wheat, including yield, disease resistance, and heat- and drought-stress tolerance. Optimized phenological patterns for a particular growing environment allows for the maximum partitioning of available assimilates to the spikes, improving grain yield (Reynolds et al. 2009). Earlier flowering time helps protect winter wheat spikes from grain-infecting pathogens like *Fusarium* head blight, by enabling an "escape" from the pathogen by flowering and beginning to mature before the onset of optimal warm, humid environmental conditions for pathogen growth in late-spring/early summer. Mondal et al. (2015) found that the entries that had best yields in both heat- and drought-stress environments also had earlier heading dates than average, suggesting there is a benefit to earlier heading in environments where these stresses are common.

Optimizing phenological patterns may become increasingly challenging in the face of climate change. Understanding the genetic basis of flowering time control and the range of variation available to wheat breeders is particularly important as high summer temperatures in wheat growing regions are likely to become more prevalent with climate change (Beales et al. 2007). Increasing the known allelic diversity at photoperiod and vernalization gene loci will enable a broader range of adaptation to be employed by breeders. Understanding the effects of different alleles at these loci, on their own and in varying combinations, on heading date is essential to enable

continued breeding for higher yields in increasingly variable environmental conditions. In this study, I examined the effect of different combinations of alleles of flowering time genes in a doubled haploid soft red winter wheat population, and characterized its vernalization response.

Materials and Methods

Plant Materials

A bi-parental doubled haploid (DH) mapping population of 124 soft red winter wheat (SRWW) experimental lines was derived from MD01W233-06-1 and SS8641 using the wheat × maize wide cross method at the North Carolina State University in Raleigh, NC.

MD01W233-06-1 (hereby referred to as MD233) was released by the Maryland Agricultural Experiment Station in 2009. MD233 (PI658682) was selected as an F3:5 selection from the cross of SRWW cultivar 'McCormick' (VA92-51-39 (IN71761A4-31-5-48//VA71-54-147/'McNair 1813')/AL870365 ('Coker 747*2/'Amigo')) (PI632691, Griffey et al., 2005) with SRWW cultivar 'Choptank' ('Coker 9803'/'Freedom') (PI 639724, Costa et al., 2006). MD233 carries native *Fusarium* head blight resistance, with no Sumai 3 alleles. MD233 has a slightly delayed maturity, heading on average six days later than Coker 9553 (Costa et al., 2010).

SS8641, originally named GA 96229-3A41, was developed at the University of Georgia. It is derived from the cross 'GA 881130 ('KSH8998 / FR 81-10 // Gore')/2*GA 881582'. Both KSH8998 and FR 81-10 were developed for enhanced disease resistance by transferring disease resistance genes from *Ae. tauschii* (for Hessian fly resistance gene *H13*), *Ae. ventricosa* (leaf rust resistance gene Lr37) and *T. persicum* (stripe rust resistance gene *Yr17*). SS8641 has early maturity, similar to that of 'AGS2000' (Johnson et al., 2007).

Characterization of Known Alleles Regulating Flowering Time

Targeted genotyping of specific vernalization (*VRN*) and photoperiod (*Ppd*) genes was performed using the parental genotypes, MD233 and SS8641. All three homoeologous copies of *VRN-1* and *Ppd-1* were characterized using allele-specific assays to determine which known alleles may be present in this population. Genes, alleles genotyped, and references are given in Table 2.1.

Marker Discovery and Genotyping

The MD233 × SS8641 population was genotyped using single nucleotide polymorphisms (SNPs), simple sequence repeats (SSRs), and a morphological marker, to provide wide genome coverage. One morphological marker was used based on coleoptile color: MD233 had a red coleoptile and SS8641 had a clear coleoptile; this marker was segregating in the population, was scored on seedlings, and reported as the 'Rc' marker. The bulk of the markers were SNPs, which were

Table 2.1. Description of KASP assays used to characterize MD233 and SS8641. KASP detected allelic variants at *VRN-A1*, *VRN-B1*, *VRN-D1*, *Ppd-A1*, *Ppd-B1*, and *Ppd-D1*. KASP assays do not include tail sequences.

Locus	Allele(s) assayed	Marker ID	Primer name	Primer Sequence	Reference
Vrn-A1	Vrn-A1a	wMAS000033	Vrn-A1_9K0001_AL2	GAGTTTTCCAAAAAGATAGATCAATGTAAAC	Brown-Guedira,
			Vrn-A1_9K0001_AL1	AGAGTTTTCCAAAAAGATAGATCAATGTAAAT	unpublished
			Vrn-A1_9K0001_C1	GTTAGTAGTGATGGTCCAATAATGCCAAA	
	Vrn-A1b	wMAS000035	Vrn-A1b-Marq_AL2	GTTTTGGCCTGGCCATCCTCA	Yan et al. 2004
			Vrn-A1b-Marq_AL1	GTTTTGGCCTGGCCATCCTCC	
			Vrn-A1b-Marq_C1	TATCAGGTGGTTGGGTGAGGACGT	
	vrn-A1	vrn-A1exon4	Vrn-A1_Exon4_F1	AGGCATCTCATGGGAGAGGATC	Diaz et al. 2012
	exon 4_C/T		Vrn-A1_Exon4_F2	CAGGCATCTCATGGGAGAGGATT	
			Vrn-A1_Exon4_R	CCAGTTGCTGCAACTCCTTGAGATT	
	vrn-A1	vrn-A1exon7	Vrn-A1_Exon7_F1	TGAGTTTGATCTTGCTGCGCCG	Diaz et al. 2012
	exon 7_G/A		Vrn-A1_Exon7_F2	CTGAGTTTGATCTTGCTGCGCCA	
			Vrn-A1_Exon4_R	CTTCCCCACAGCTCGTGGAGAA	
Vrn-B1	Vrn-B1a	Vrn-B1_I_D	Vrn-B1_D_A2	GGCAGCTAATGTGGGGTAGTCT	Brown-Guedira,
			Vrn-B1_D_C1s	ATTCGTATTGCTAGCTCCGGCCAT	unpublished
			Vrn-B1_I_ALG	CAACCTCCACGGTTTCAAAAAGTAG	
			Vrn-B1_I_C1	ATATTTACTAAGCAGCGGTCATTCCGAT	
	Vrn-B1b	wMAS000037	Vrn-B1_B_ALC	GCGCAAGCGGGAGCTACATC	Santra et al. 2009
			Vrn-B1_B_ALG	TGCGCAAGCGGGAGCTACATG	
			Vrn-B1_B_C1	GCCATGAACAACAAAGGGGGTGGT	

Table 2.1, continued. Description of KASP assays used to characterize MD233 and SS8641. KASP detected allelic variants at *VRN-A1*, *VRN-B1*, *VRN-D1*, *Ppd-A1*, *Ppd-B1*, and *Ppd-D1*. KASP assays do not include tail sequences.

Locus	Allele(s) assayed	Marker ID	Primer name	Primer Sequence	Reference
Vrn-B1	Vrn-B1c	Vrn-B1_C	Vrn-B1_C _ALT	CCTAAACAGGGGCAGAACACTA	Milec et al. 2012
			Vrn-B1_C _ALG	CCTAAACAGGGGCAGAACACTG	
			Vrn-B1_C _C	GACCCCAGGGCCTATGAATGTAATT	
	vrn-B1_intron1_A/C	TaVrn-B1_1752	TaVrnB1_1752_AF2	GGAATGACCGCTGCTTAGTAAATATA	Guedira et al. 2014
			TaVrnB1_1752_CF1	GGAATGACCGCTGCTTAGTAAATATC	
			TaVrnB1_1752_R	GATTTAGCACCTCAACATACAGGTCT	
Vrn-D1	Vrn-D1a	wMAS000039	Vrn-D1-D1a_A_ALC	ATCATTCGAATTGCTAGCTCCGC	Fu et al. 2005
			Vrn-D1-D1a_A_ALG	ATCATTCGAATTGCTAGCTCCGG	
			Vrn-D1-D1a_A_C	GCCTGAACGCCTAGCCTGTGTA	
Ppd-A1	Ppd-A1a.1	Ppd-A1prodel	Ppd-A1prodel_AL2	GCGGCGAGCCGGTTAATCG	Nishida et al. 2013
			Ppd-A1prodel_AL1	TTTCGGTGTTTGACTTCAGGCG	
			Ppd-A1prodel_C1	GTGGCGTACTCCCTCCGTTTCTT	
Ppd-B1	Ppd-B1a Chinese Spring truncated copy	wMAS000027	TaPpdBJ001tR	GACGTTATGAACGCTTGGCA	Nishida et al. 2013
			TaPpdBJ001iR	CCGTTTTCGCGGCCTT	
			TaPpdBJ001tF	GGGTTCGTCGGGAGCTGT	
	Ppd-B1a Chinese Spring intercopy	TaPpdBJ002	TaPpdBJ002F	GCTCCCGTCCCCGATAAA	Nishida et al. 2013
			TaPpdBJ002R	TGCATGGCTTAGGTGTCCCT	
Ppd-D1	Ppd-D1a Ciano67 promoter deletion	wMAS000024	TaPpdDD001RI	CAAGGAAGTATGAGCAGCGGTT	Nishida et al. 2013
			TaPpdDD001RD	AAGAGGAAACATGTTGGGGTCC	
			TaPpdDD001FL	GCCTCCCACTACACTGGGC	

detected using the Illumina 9K iSelect Assay, Kompetitive Allele Specific PCR (KASP) assays, and genotyping-by-sequencing (GBS). The population and parents, 126 genotypes total, were grown in 96-well trays to collect tissue for DNA extraction. Leaf cuttings were taken at the 2-leaf stage, collecting approximately 25 mg of leaf tissue. Genomic DNA extraction was performed following the protocol of Pallotta et al. (2003) at the USDA-ARS Eastern Regional Small Grain Genotyping Lab at Raleigh, NC.

SSR markers were selected from (Roder et al. 1998; Somers et al. 2004; Song et al. 2005), including: wmc474, wmc471, gwm272, gwm11, barc170, barc45, wmc496, barc164, wmc273, barc163, barc101, wmc278, barc100, barc12, barc80, barc10, barc28, barc127, barc147, barc137, gdm136, barc59, gwm111, gwm149, gwm260, gwm261, gwm282, gwm304, and gwm319. These markers were selected either because they are tightly linked to QTLs of interest, or to provide marker coverage in areas of the genome known to have low marker density. Genotyping of SSR markers was done at the USDA-ARS Eastern Region Small Grain Genotyping Lab in Raleigh, NC, following the protocols described in Kang et al. (2011). Sizing of PCR products was performed using an ABI3130xl Genetic Analyzer (Applied BioSystems, Foster City, CA); analysis of PCR fragments was performed using GeneMarker 1.60 software (SoftGenetics, LLC, State College, PA).

For SNP discovery, the population was genotyped using the wheat 9K iSelect Beadchip Assay (Illumina Inc., San Diego, CA, USA), which contains 9,000 potential SNP markers. The assay was developed by the International Wheat SNP Consortium

and was run at the USDA Northern Central Small Grains Genotyping Lab in Fargo, ND under direction of Dr. Shiaoman Chao. SNP genotyping calls were made by Dr. Brown-Guedira at the USDA-ARS Eastern Region Small Grain Genotyping Lab in Raleigh, NC using GenomeStudio v2011.1 software (Illumina, San Diego, CA), as described in (Cavanagh et al. 2013).

KASP (Kompetitive Allele Specific PCR) assays (LGC Genomics, Middlesex, UK) were used to target specific genes of interest or to provide genome coverage in areas with low marker density provided by the 9K assay. KASP markers used were either designed by USDA Regional Genotyping Labs (IWB49398, TaPpdDD001, TaPpd-A1prodel, sbv5D_6060) or selected from (Wilkinson et al. 2012), including: BS00081724, BS00024094, BS00021850, BS00024015, BS00022436, BS00023944, BS00047797, BS00064002, BS00024118, BS00117841, BS00098495, BS99999954, BS00065928, BS99999957, BS00036421, BS99999964, BS00024014, BS99999971, BS00122945, BS99999998, and BS00022283.

Genotyping-by-sequencing (GBS) was employed to allow the incorporation of previously-unknown SNP markers. GBS analysis was done following the protocols of Elshire et al. (2011). A SNP array was developed by restriction enzyme digestion and targeted PCR amplification. Sequencing was done on an Illumina 2500 HiSeq at the Genomics Science Lab at North Carolina State University. The raw sequence data was then filtered and evaluated at the USDA-ARS Eastern Regional Small Grain Genotyping Lab in Raleigh, NC. The resultant polymorphic SNPs were used in linkage map construction and QTL analysis.

Field Trials

The MD233 × SS8641 DH population was evaluated in the field in eight environments across the Eastern US and Argentina, from 2011 to 2014. Each location-year combination was treated as a unique environment. In three environments, the population was planted as single 1.2m long rows with three replications: Salisbury, MD, 2011; Salisbury, MD, 2012; and 9 de Julio, Buenos Aires, Argentina, 2012. In the five remaining environments, the population was grown as yield plots, comprised of seven 3.6 m long rows, with two replications: Clarksville, MD, 2013; Clarksville, MD, 2014; Queenstown, MD, 2013; Queenstown, MD, 2014; and Kinston, NC, 2014. All field environments were grown using a randomized complete block design. Flowering time data was collected as heading date: the date at which the spike had fully emerged from the boot (Zadoks 59) for 50% of plants within the plot (Zadoks et al. 1974). Heading dates were recorded as Julian Days, but because it is in the southern hemisphere, June 1 was treated as the first day of the year in 9 de Julio, Argentina.

Yield data was collected in all environments where yield plots were grown. Yield plots in all of these locations had harvest areas of 3.8 m^2. To obtain yield data, plots were mechanically harvested using a small plot combine (Wintersteiger Nurserymaster Elite, Ried, Austria). Plot weight and moisture-content data were collected using a HarvestMaster HM1000b (Juniper Systems, Logan, UT) attached to

the plot combine. Grain yield was measured as pounds per plot and converted to grams per square meter.

Soil fertility followed recommended best management practices for each location. All yield trials were sprayed with metconazole fungicide (Caramba®, BASF) at anthesis to reduce potential infection by *Fusarium graminearum*. Growing season rainfall and temperature data were obtained from respective research farm weather stations for Clarksville, MD; Queenstown, MD; Salisbury, MD (rainfall only); and 9 de Julio, ARG; and from National Oceanic and Atmospheric Administration (NOAA) measurements for Kinston, NC and Salisbury, MD (National Climatic Data Center 2011, 2012, 2014). Soil data was collected from the National Cooperative Soil Survey (USDA-NRCS 2015) and from information provided by the National Agricultural Technology Institute (INTA) of Argentina for the 9 de Julio location.

Greenhouse Experiments

To facilitate the controlled study of flowering time response to different vernalization conditions, the MD233 × SS8641 population was evaluated in two greenhouse experiments in College Park, MD in 2013-2014 and 2014-2015. The population was grown under different vernalization treatments, with seeds exposed to cold temperatures (4˚C) for 2-, 4-, 6-, or 8-week periods. Seeds of approximately the same size were germinated in paper towels modified with a wick, partially immersed with water, in a controlled growth chamber for 2-, 4-, 6-, or 8-week vernalization

treatments at 4˚C. Seeds were germinated during vernalization treatment in the fall, and transplanted to the greenhouse in early to mid-winter, depending on when their vernalization treatment was complete. Once vernalization treatments were complete, seedlings of similar size were transplanted into plastic containers filled with Metro-Mix PX1 organic substrate (Sun Gro Horticulture Canada Ltd.). Both years had six replicate plants for each DH line, assorted in a randomized complete block design. Each pot was treated with imidacloprid insecticide (Marathon®, OHP) and lime ($CaCO_3$) to control pests and increase the slightly-acidic substrate pH. Triadimefon fungicide (Strike®, OHP) was used during the experiment to manage powdery mildew (*Erysiphe graminis* f.sp. *tritici*).

In 2013-2014, plants from 2-, 4-, 6-, and 8-week treatments were grown in the greenhouse with a 16 hour photoperiod at 24˚C during the day and 18˚C at night in 587.9 cm^2 plastic containers and were hand-watered daily. In 2014-2015, plants were grown in the greenhouse with a 16 hour photoperiod at 20˚C during the day and 18˚C at night in 3.8 L plastic containers. The use of long photoperiods (16 h) was done in an attempt to minimize photoperiod effects, allowing better detection of vernalization effects. In 2014-2015, the 2-week treatment was grown on drip irrigation. The 4-week and 8-week treatments were grown under a hand-watering irrigation regime to improve plant vigor. In both years, plants were fertigated biweekly using a 15-5-15 Cal Mag special fertilizer mix at a rate of 220 ppm at 1:50. Heading date was recorded at Zadoks 59, when the spike had fully emerged from the boot on the main tiller of each plant (Zadoks et al. 1974).

Statistical Analysis

All statistical analysis of heading date data was completed using SAS version 9.3 (SAS Institute, Raleigh, NC 2013). Summary statistics were calculated using the MEANS and GLM procedures. The GLM procedure was used to calculate least square means for each phenotypic trait, which were then used for QTL mapping. Analysis of variance (ANOVA) was calculated using the MIXED procedure. Within each environment or vernalization treatment, the ANOVA model used was: heading date = genotype + block + error. Error effects were treated as random, while Genotype and Block (replication) effects were treated as fixed effects. Pearson's correlation coefficients were calculated using the CORR procedure. To compare heading date means of DHs with different allelic combinations at major flowering time loci, DHs were classified based on genotypes at these loci, and heading dates of different classes were analyzed using PROC GLM. Where significant F values were found, multiple mean comparisons were completed using the Tukey-Kramer adjustment.

QTL Mapping

SSR, SNP, and morphological marker data were combined for linkage map construction and QTL analysis. Before linkage map construction, markers were filtered and removed if they were: monomorphic; had missing data rates greater than

20%; or were distorted, differing from the expected 1:1 segregation ratio for DHs. The remaining polymorphic markers were used in subsequent genetic analysis. Linkage groups were constructed using the MAP function in IciMapping version 4.0, using a LOD threshold of 10 (Li et al., 2008). The Kosambi mapping function was used to convert recombination frequencies to centimorgans (cM). Linkage groups were assigned to chromosomes by anchoring markers shared with the published SNP consensus map (Cavanagh et al. 2013), SSR consensus map (Somers et al. 2004), and wheat POPSEQ data (http://wheat-urgi.versailles.inra.fr/). Genetic distance of markers on the same chromosome were then recalculated using the RECORD and COUNT algorithms in IciMapping version 4.0. QTL with additive effects were detected using inclusive composite interval mapping methods by the ICIM-ADD function in IciMapping version 4.0, with a walking speed of 1 cM. An LOD threshold of 3.0 was used to declare the presence of a significant QTL. The position at which the LOD score curve reached its maximum was used as the estimated location of the QTL.

Allele Discovery in *VRN-A1*

A TaqMan® assay was used to estimate *VRN-A1* gene copy number by quantitative PCR following the methods described by Diaz et al. (2012). The TaqMan® assay was run using genomic DNA isolated from seedling tissue of SS8641 and MD233 and was conducted at the USDA-ARS Eastern Regional Small Grain Genotyping Lab in Raleigh, NC. Approximately 6 kb of the *VRN-A1* gene was

amplified from MD233 and SS8641 using gene-specific primers based on the 'Triple Dirk C' *vrn-A1* winter allele (AY747600.1). Quantitative PCR of these fragments and an internal positive control was performed on a LightCycler 480 Roche. The internal positive control used was the *TaCO* gene. Copy number was estimated from the *Vrn-A1*/internal positive control ratio, calculated as ΔCT, where $\Delta CT = 2^{-(VrnA1-TaCO)}$.

Additionally, sequencing of approximately 600-bp of the *VRN-A1* first intron including the RIP-3 region was performed to determine if there was disrupted binding of a repressor. The RIP-3 region contains binding sites for the RNA-binding protein TaGRP2, which is homologous to the Arabidopsis GLYCINE-RICH RNA-BINDING PROTEIN7 (GRP7) and inhibits *VRN1* expression in the absence of cold (Xiao et al. 2014; Kippes et al. 2015). Two SNPs in the RIP-3 region of the *VRN-D4* gene and *VRN-A1* alleles of wheat varieties Jagger, Claire, and Chinese Spring have recently been characterized, which disrupt binding of TaGRP2 and induce earlier flowering (Kippes et al. 2015). PCR primer pairs were designed from the 'Triple Dirk C' *vrn-A1* sequence (AY747600.1) to target the RIP-3 binding region, using sequence data for the RIP-3 region published in Kippes et al. (2015). These primers were sent with genomic DNA of SS8641 and MD233 (4 replicates of each cultivar at 30ng/µL concentration) to Eton Bio in Research Triangle Park, NC for Sanger sequencing. Sequencing trace files were analyzed using UGene and results were aligned with each other and *vrn-A1* Triple Dirk C (AY747600.1) sequence using Clustal Omega

(Sievers et al. 2011). Sequencing results were also aligned to any matches in *T. aestivum* using NCBI-BLAST.

Results

Characterization of Known Alleles Regulating Flowering Time

Both parents of the population, SS8641 and MD233, carried recessive winter-type alleles at all three homoeologous *VRN-1* loci. In all *VRN-1* assays listed in Table 2.1, neither parent was found to have any of the insertions, deletions or SNPs in *VRN-1* genes associated with spring wheat growth habit or earlier flowering winter wheat. Polymorphisms were found at the *Ppd-A1* and *Ppd-D1* loci, which are known to control photoperiod sensitivity. *Ppd-A1* was assayed using the Ppd-A1prodel marker, which detects the presence of a 1,085 bp deletion in the 5' UTR; *Ppd-D1* was assayed using the wMAS000024 marker, which detects the presence of a 2,089 bp deletion in the 5' UTR (Nishida et al. 2013). MD233 carried the *Ppd-A1a* allele associated with photoperiod-insensitivity at *Ppd-A1*, while SS8641 carried the sensitivity allele, *Ppd-A1b*. At *Ppd-D1*, MD233 carried the sensitivity allele, *Ppd-A1b*, while SS8641 carried the insensitivity allele, *Ppd-D1a*. At *Ppd-B1*, both parents carried the allele associated with photoperiod-sensitivity, *Ppd-B1b*.

Linkage Map Construction

The DH population was analyzed with 4982 markers that were polymorphic between the two parents (4957 SNPs, 24 SSRs and 1 morphological marker). After co-segregating markers were removed, the final genetic linkage map was constructed using 860 unique markers covering a genome length of 2934.12 cM. The linkage map is summarized in Table 2.2. The average interval length on the map was 3.4 cM, which is well within the recommended map distance for QTL analysis: an average interval length less than 10 cM (Doerge 2002). This linkage map was used for subsequent QTL analysis.

Environmental Conditions

Environmental conditions of all field locations are summarized in Table 2.3.

Table 2.2. Summary of constructed chromosome linkage groups used for subsequent QTL analysis.

Chromosome	Number of Markers	Length (cM)	Average Distance Between Markers (cM)
1A	31	67.7	2.2
2A	58	123.9	2.1
3A	63	216.8	3.4
4A	43	158.3	3.7
5A	58	190.0	3.3
6A	33	95.1	2.9
7A	90	171.5	1.9
1B	47	144.1	3.1
2B	65	139.8	2.2
3B	66	134.0	2.0
4B	28	134.5	4.8
5B	64	123.2	1.9
6B	36	112.4	3.1
7B	44	177.8	4.0
1D	18	85.6	4.8
2D	34	125.9	3.7
3D	12	72.7	6.1
4D	7	76.8	11.0
5D	20	179.5	9.0
6D	22	144.6	6.6
7D	21	259.8	12.4
Whole Genome	860	2934.1	3.4

Table 2.3. Environmental conditions of eight field growing environments.

			Total Rainfall (cm)					Mean Temperature (^{o}C)				
Environment	Latitude	Soil Type	Feb	Mar	Apr	May	Jun	Feb	Mar	Apr	May	Jun
2011 Salisbury, MD	38°22'14.48"N	Fort Mott loamy sand, Arenic Hapludults	5.3	8.9	3.6	9.1	8.4	6.2	8.2	15.7	20.0	24.7
2012 Salisbury, MD	38°22'14.48"N	Fort Mott loamy sand, Arenic Hapludults	6.6	4.8	14.2	4.8	6.9	6.2	13.0	13.8	20.5	22.7
2012 9 de Julio, ARG†	35°28'53.39"S	Norumbega sandy loam, Entic Hapludoll	8.5†	8.5†	8.5†	18.4†	10.5†	13.8†	13.8†	13.8†	22.1†	21.7†
2013 Clarksville, MD	39°15'31.44"N	Glenville silt loam, Aquic Fragiudults	5.0	6.5	4.7	9.0	12.7	0.6	3.8	11.8	16.5	21.9
2014 Clarksville, MD	39°15'31.44"N	Glenville silt loam, Aquic Fragiudults	6.1	9.9	17.1	10.4	3.0*	-1.2	2.4	10.7	17.2	21.7*
2013 Queenstown, MD	38°54'43.75"N	Nassawango silt loam, Typic Hapludults	6.1	9.3	11.8	4.9	24.9	2.0	5.1	12.7	17.7	23.0
2014 Queenstown, MD	38°54'43.75"N	Nassawango silt loam, Typic Hapludults	11.3	11.9	13.2	9.3	7.0	0.9	3.8	11.7	18.2	22.2
2014 Kinston, NC	35°17'58.41"N	Norfolk loamy sand, Typic Kandiudults	6.5	14.2	11	8.9	26.3	8.4	9.8	17.9	22.9	25.4

* Temp and Precipitation data for June 2013 in Clarksville only includes June 1-18 due to equipment malfunction

† because 9 de Julio is in the Southern hemisphere, months are as follows: Feb=Jul; Mar=Aug; Apr=Sep; May=Oct; Jun=Nov

Field Trials

The DH population and parents were grown in eight field environments, typically exhibiting normal or bimodal distributions in heading date. Frequencies of DH lines at different heading dates for each environment are reported in Figure 2.1 through Figure 2.8. The parent that headed latest was not consistent across environments, with MD233 heading by an average of 4 days later than SS8641 in four environments, SS8641 heading by an average of 2 days later than MD233 in three environments, and both parents sharing the same heading date in the 2014 Clarksville, MD environment (Table 2.4). This was likely due to differential response to photoperiod signals from the two PI alleles: either *Ppd-A1a*, carried by MD233, or *Ppd-D1a*, carried by SS8641. DH lines had heading date ranges from 9 days to 31 days, the 31 day range occurring in the warmest location, 9 de Julio in the Buenos Aires Province of Argentina. Heading date means among DH lines generally aligned with the dates reported for one of the parents at that location (Table 2.4).

QTL analysis detected two QTL across all environments: one QTL near the *Ppd-A1* locus on chromosome 2A, at marker interval XPpdA1-Xsnp2461, and the other near the *Ppd-D1* locus on chromosome 2D, at marker intervals Xsnp2862-XPpdD1 or XPpdD1-Xsnp2869 (Table 2.5). Since both QTL near *Ppd-D1* share the same marker, XPpdD1, these QTL were considered to be the same locus. Because both of these reported QTL were detected at markers known to be within the *Ppd-A1*

and *Ppd-D1* genes (Table 2.1; Nishida et al. 2013), it is believed that these QTL are caused by allelic variation in these genes.

LOD scores for the *Ppd-A1* QTL ranged from 3.83 in the 2012 Salisbury, MD environment to 11.78 in the 2013 Queenstown environment, LOD scores greater than 8 were detected in all but three environments (Table 2.5). LOD scores for the *Ppd-D1* QTL ranged from 6.35 in the 2013 Clarksville, MD environment to 22.36 in the 2014 Queenstown, MD environment, with scores above 20 at three locations (Table 2.5). These high LOD scores suggest that these are major genes. The difference in LOD scores between these two loci suggests that allelic variation at *Ppd-D1* typically has a larger effect on earliness of heading date than the *Ppd-A1* locus. This conclusion is also supported by the mean heading dates of DHs when classified by alleles at *Ppd-A1* and *Ppd-D1*, as reported in Table 2.6.

ANOVA of the three-way allele combinations, at *vrn-A1* + *Ppd-A1* + *Ppd-D1* loci, reported in Table 2.6 found significant differences ($p < 0.0001$) between allele combination classes at all eight field locations. Therefore, multiple mean comparisons were calculated for these allele combinations for all locations, reported in Table 2.7. Comparisons testing *Ppd-A1a* against *Ppd-A1b* found extremely significant effects ($p < 0.001$) when tested in a background of *Ppd-D1b* and *vrn-A1-SS8641* (Table 2.7, row four). When tested in a background of *Ppd-D1b* and *vrn-A1-MD233*, significant effects were detected in all environments but one: 2014 Clarksville, MD (Table 2.7, row three). However, comparisons testing *Ppd-A1a* against *Ppd-A1b* found no significant difference when tested in a *Ppd-D1a*

Table 2.4. Summary statistics for heading date (Julian days) across eight field environments. F-values and P-values were calculated using the MIXED procedure in SAS.

Environment	Plot Type	Parental Means		DHs							
		MD233	SS8641	Mean	SD†	Range	Minimum	Maximum	CV%‡	F-value	P-value
2011 Salisbury, MD	Single row	135	125	125	2.68	13	121	134	2.14	13.80	<.0001
2012 Salisbury, MD	Single row	143	138	143	6.79	24	135	159	4.75	43.10	<.0001
2012 9 de Julio, ARG	Single row	135	134	137	6.38	31	124	155	4.67	8.18	<.0001
2013 Clarksville, MD	Yield plot	133	134	133	1.96	9	129	138	1.47	6.70	<.0001
2014 Clarksville, MD	Yield plot	142	142	142	1.72	10	137	147	1.21	5.25	<.0001
2013 Queenstown, MD	Yield plot	127	128	128	3.12	17	119	136	2.44	24.99	<.0001
2014 Queenstown, MD	Yield plot	138	141	140	1.74	9	136	145	1.24	10.06	<.0001
2014 Kinston, NC	Yield plot	115	114	115	3.62	16	107	123	3.14	117.48	<.0001

†Standard Deviation
‡Coefficient of Variation

Figure 2.1. Frequency of heading dates among DH lines in 2011 Salisbury, MD field environment.

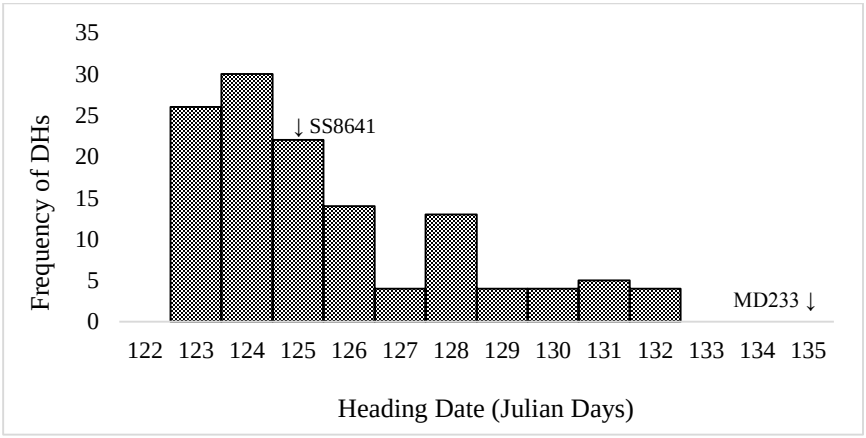

Figure 2.2. Frequency of heading dates among DH lines in 2012 Salisbury, MD field environment.

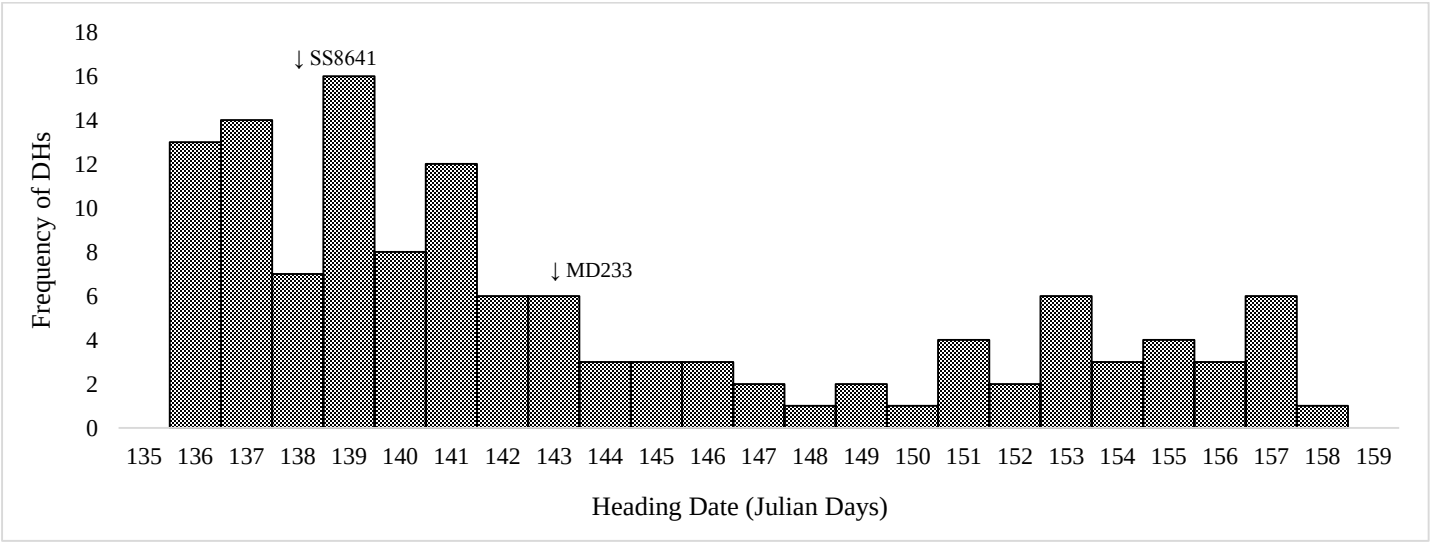

Figure 2.3. Frequency of heading dates among DH lines in 2012 9 de Julio, Buenos Aires, Argentina field environment.

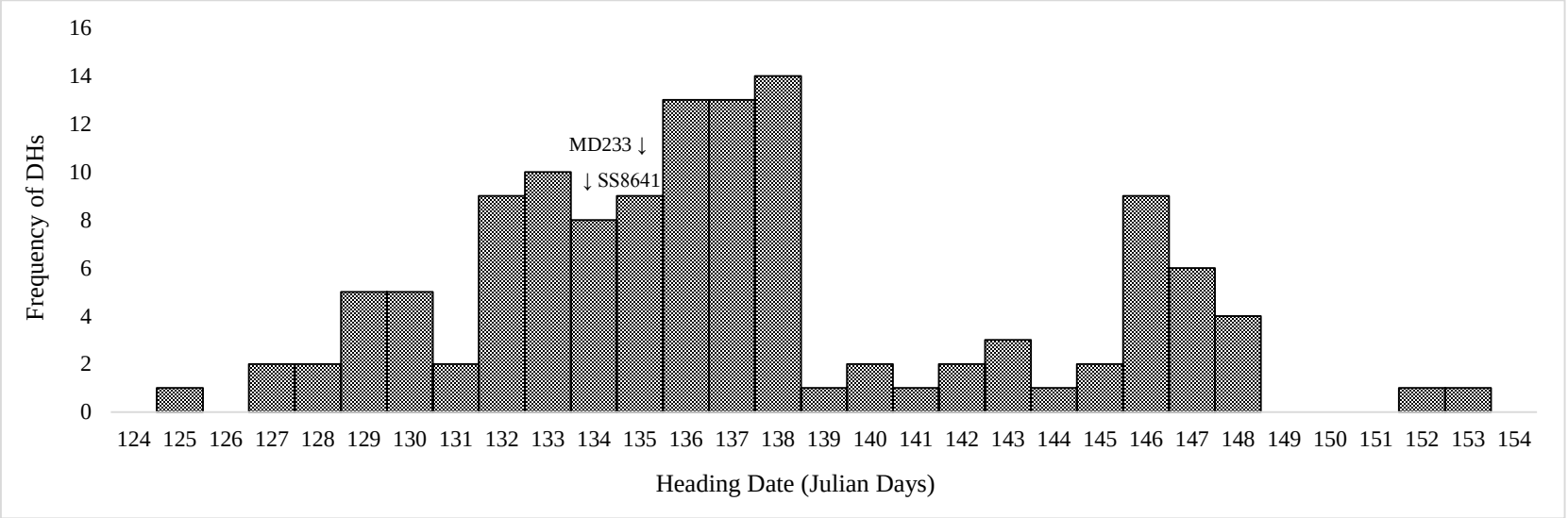

Figure 2.4. Frequency of heading dates among DH lines in 2013 Clarksville, MD field environment.

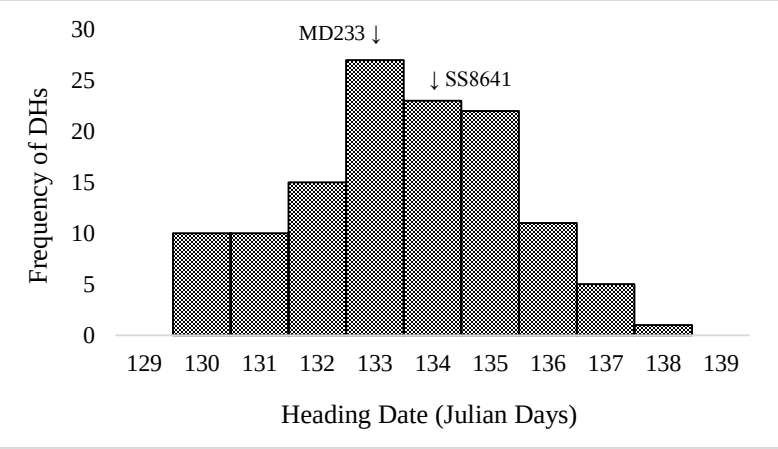

Figure 2.5. Frequency of heading dates among DH lines in 2014 Clarksville, MD field environment.

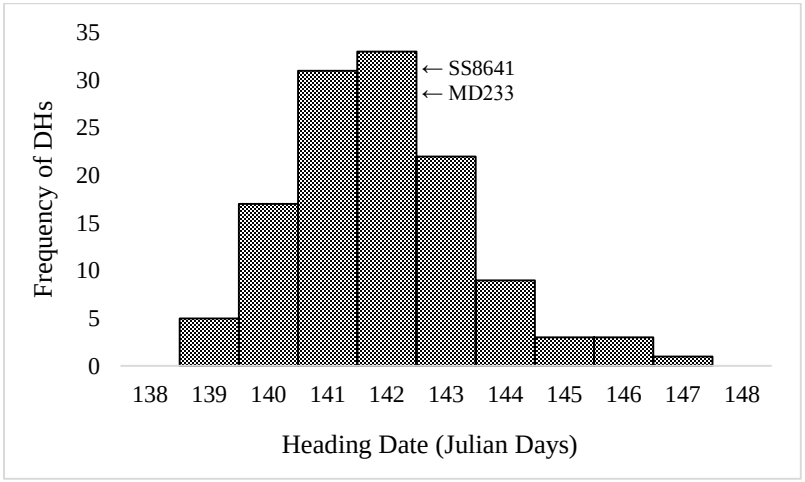

Figure 2.6. Frequency of heading dates among DH lines in 2013 Queenstown, MD field environment.

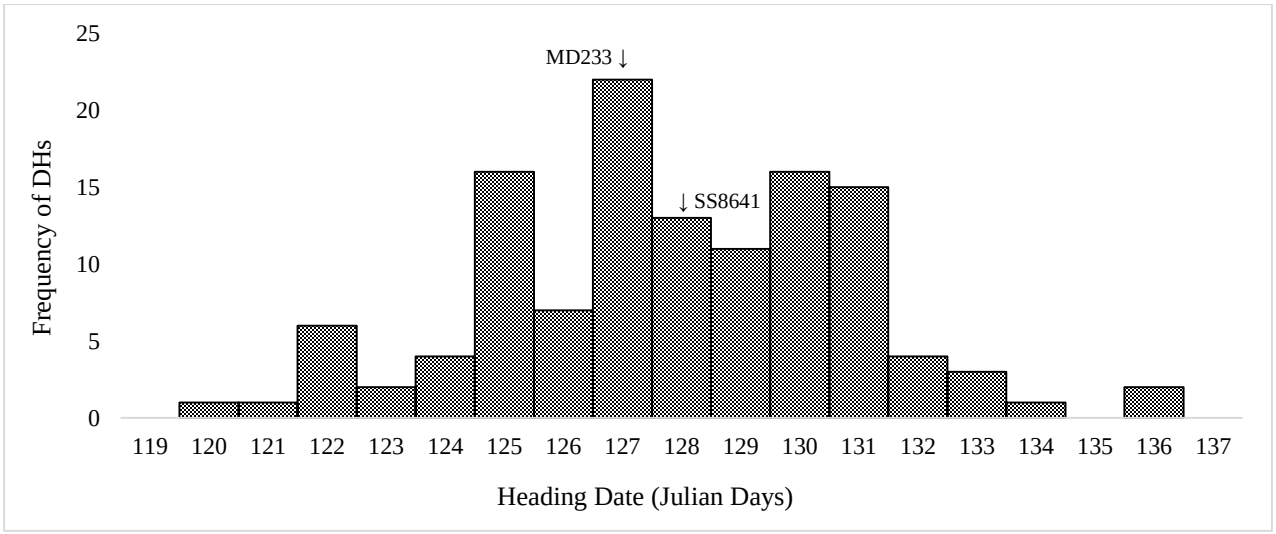

Figure 2.7. Frequency of heading dates among DH lines in 2014 Queenstown, MD field environment.

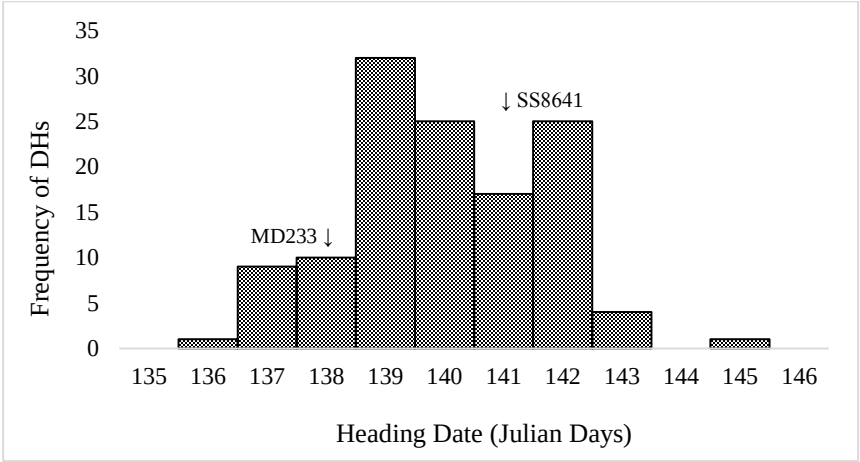

Figure 2.8. Frequency of heading dates among DH lines in 2014 Kinston, NC field environment.

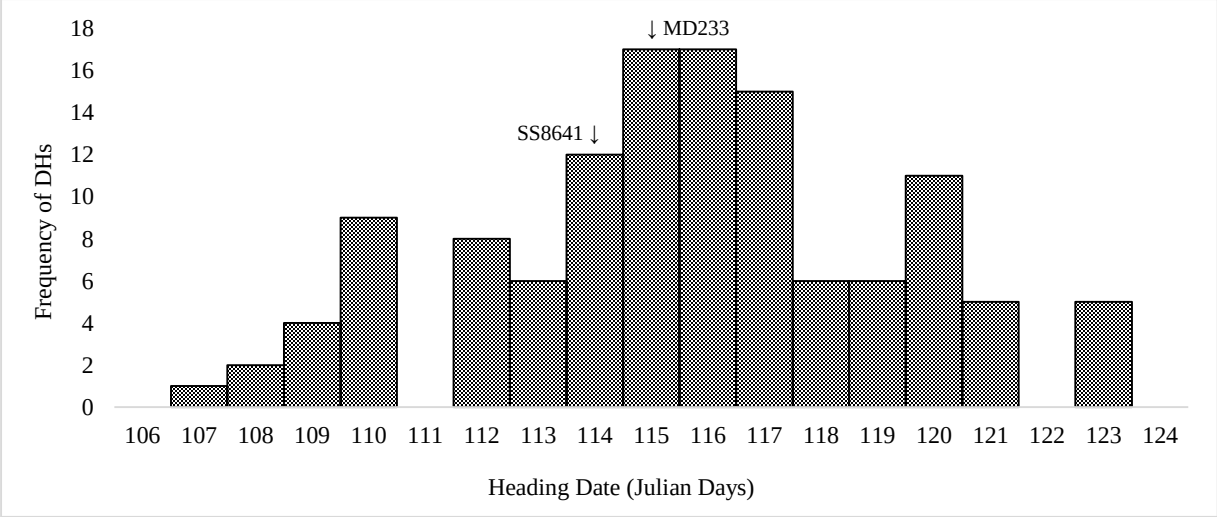

Table 2.5. QTL mapping results for all field environments.

Environment	Chromosome	Position (cM)	Left Marker	Right Marker	LOD	PVE%	Additive Effect
2011 Salisbury, MD	2A	17	XPpdA1	Xsnp2461	4.23	11.01	0.81
2011 Salisbury, MD	2D	64	XPpdD1	Xsnp2869	8.93	27.26	-1.28
2012 Salisbury, MD	2A	17	XPpdA1	Xsnp2461	3.83	9.87	2.12
2012 Salisbury, MD	2D	65	XPpdD1	Xsnp2869	9.75	31.21	-3.75
2012 9 de Julio, ARG	2A	17	XPpdA1	Xsnp2461	4.54	12.75	2.09
2012 9 de Julio, ARG	2D	66	XPpdD1	Xsnp2869	7.75	27.39	-3.06
2013 Clarksville, MD	2A	19	XPpdA1	Xsnp2461	8.07	13.69	0.68
2013 Clarksville, MD	7A	55	Xsnp324	Xbarc127	3.62	5.74	0.44
2013 Clarksville, MD	2B	63	Xsnp2786	Xsnp2777	5.86	9.67	0.57
2013 Clarksville, MD	5B	64	Xsnp823	Xsnp4059	3.79	6.08	0.45
2013 Clarksville, MD	2D	57	Xsnp2862	XPpdD1	6.35	11.52	-0.62
2013 Clarksville, MD	6D	136	Xsnp4488	Xsnp4485	8.27	14.14	0.69
2014 Clarksville, MD	2A	17	XPpdA1	Xsnp2461	8.08	14.06	0.58
2014 Clarksville, MD	4A	95	Xsnp3597	Xsnp910	4.31	6.97	0.41
2014 Clarksville, MD	2B	36	Xsnp2785	Xsnp2778	3.06	4.83	-0.34
2014 Clarksville, MD	2B	65	Xsnp2773	Xgwm319	5.16	8.65	0.45
2014 Clarksville, MD	2D	62	XPpdD1	Xsnp2869	13.46	26.19	-0.79
2013 Queenstown, MD	2A	17	XPpdA1	Xsnp2461	11.78	16.80	1.26
2013 Queenstown, MD	3A	168	Xsnp2989	Xsnp2983	4.05	4.96	0.68
2013 Queenstown, MD	5A	109	Xsnp3845	Xsnp3865	5.59	7.23	-0.83
2013 Queenstown, MD	7A	56	Xbarc127	Xsnp1376	3.50	4.38	0.65
2013 Queenstown, MD	2B	62	Xsnp2752	Xsnp2786	6.55	8.50	0.89
2013 Queenstown, MD	2D	64	XPpdD1	Xsnp2869	21.79	38.64	-1.90
2014 Queenstown, MD	2A	17	XPpdA1	Xsnp2461	11.51	16.21	0.67
2014 Queenstown, MD	7A	38	Xsnp4768	Xsnp1302	3.59	4.47	0.35
2014 Queenstown, MD	1B	26	Xsnp2213	Xsnp1707	3.21	4.02	0.33
2014 Queenstown, MD	3B	133	Xsnp3403	Xsnp3181	4.34	5.44	0.38
2014 Queenstown, MD	2D	61	Xsnp2862	XPpdD1	22.36	39.66	-1.05
2014 Kinston, NC	2A	17	XPpdA1	Xsnp2461	11.08	16.43	1.47
2014 Kinston, NC	4A	24	Xsnp3614	Xsnp3636	4.25	6.89	-0.95
2014 Kinston, NC	3B	129	Xsnp3401	Xsnp3358	3.41	4.35	0.75
2014 Kinston, NC	5B	68	Xsnp4061	Xsnp4027	4.42	5.73	0.86
2014 Kinston, NC	7B	61	Xsnp4883	Xsnp4808	3.88	4.97	-0.80
2014 Kinston, NC	2D	58	Xsnp2862	XPpdD1	20.16	35.88	-2.17

Table 2.6. Heading date mean for DHs with different genotypes and allele combinations in all field locations. Heading dates given in Julian days.

Genotype	No. of Lines	Field environment†							
		Sal_11	Sal_12	9dJ_12	Cla_13	Cla_14	Que_13	Que_14	Kin_14
MD233 (*Ppd-A1a, Ppd-D1b*)		135	143	135	133	142	127	138	115
SS8641 (*Ppd-A1b, Ppd-D1a*)		125	138	134	134	142	128	141	114
DHs	124	125	143	137	133	142	128	140	115
vrn-A1-MD233	50	125	144	137	134	141	128	140	116
vrn-A1-SS8641	67	125	142	136	133	142	127	140	115
Ppd-A1a-MD233	68	124	140	134	133	141	127	139	114
Ppd-A1b-SS8641	56	127	147	140	134	142	129	140	117
Ppd-D1a-SS8641	54	124	138	133	132	141	126	139	113
Ppd-D1b-MD233	69	127	147	140	134	142	129	141	117
vrn-A1-MD233 + Ppd-A1a + Ppd-D1a	12	123	140	134	133	140	127	138	115
vrn-A1-MD233 + Ppd-A1a + Ppd-D1b	16	125	144	137	134	142	128	140	116
vrn-A1-MD233 + Ppd-A1b + Ppd-D1a	13	124	140	135	133	141	127	139	114
vrn-A1-MD233 + Ppd-A1b + Ppd-D1b	9	129	154	145	135	143	131	142	120
vrn-A1-SS8641 + Ppd-A1a + Ppd-D1a	16	123	137	131	131	141	124	138	111
vrn-A1-SS8641 + Ppd-A1a + Ppd-D1b	21	125	140	135	133	142	127	140	115
vrn-A1-SS8641 + Ppd-A1b + Ppd-D1a	11	124	137	133	132	141	125	139	112
vrn-A1-SS8641 + Ppd-A1b + Ppd-D1b	18	129	153	145	135	143	131	142	119

†Sal_11, 2011 Salisbury, MD; Sal_12, 2012 Salisbury, MD; 9dJ_12, 2012 9 de Julio, ARG; Cla_13, 2013 Clarksville, MD; Cla_14, 2014 Clarksville, MD; Que_13, 2013 Queenstown, MD; Que_14, 2014 Queenstown, MD; Kin_14, 2014 Kinston, NC

Table 2.7. Multiple mean comparisons between DHs carrying different allele combinations across all field locations, calculated using PROC GLM with Tukey-Kramer adjustment in SAS. Bolded alleles indicate those whose effects are being compared in each test. Significance level of mean comparison is indicated by stars, where * = 0.01 < p < 0.05; ** = 0.001 < p < 0.01; *** = 0.001 < p < 0.001; **** = p < 0.0001.

	Field Environment							
Mean Comparison	Sal_11	Sal_12	9dJ_12	Cla_13	Cla_14	Que_13	Que_14	Kin_14
vrn-A1-MD233 + ***Ppd-A1a*** + *Ppd-D1b* *vrn-A1-MD233* + *Ppd-A1b* + ***Ppd-D1a***		****					**	**
vrn-A1-SS8641 + ***Ppd-A1a*** + *Ppd-D1b* *vrn-A1-SS8641* + *Ppd-A1b* + ***Ppd-D1a***	*	***				****		****
vrn-A1-MD233 + ***Ppd-A1a*** + *Ppd-D1b* *vrn-A1-MD233* + ***Ppd-A1b*** + *Ppd-D1b*	****	****	****		**	**	****	****
vrn-A1-SS8641 + ***Ppd-A1a*** + *Ppd-D1b* *vrn-A1-SS8641* + ***Ppd-A1b*** + *Ppd-D1b*	****	****	****	***	****	****	****	****
vrn-A1-MD233 + ***Ppd-A1a*** + *Ppd-D1a* *vrn-A1-MD233* + ***Ppd-A1b*** + *Ppd-D1a*								
vrn-A1-SS8641 + ***Ppd-A1a*** + *Ppd-D1a* *vrn-A1-SS8641* + ***Ppd-A1b*** + *Ppd-D1a*								
vrn-A1-MD233 + *Ppd-A1b* + ***Ppd-D1a*** *vrn-A1-MD233* + *Ppd-A1b* + ***Ppd-D1b***	****	****	****	**	****	****	****	****
vrn-A1-SS8641 + *Ppd-A1b* + ***Ppd-D1a*** *vrn-A1-SS8641* + *Ppd-A1b* + ***Ppd-D1b***	****	****	****	****	****	****	****	****
vrn-A1-MD233 + *Ppd-A1a* + ***Ppd-D1a*** *vrn-A1-MD233* + *Ppd-A1a* + ***Ppd-D1b***	***	****			**	*	****	
vrn-A1-SS8641 + *Ppd-A1a* + ***Ppd-D1a*** *vrn-A1-SS8641* + *Ppd-A1a* + ***Ppd-D1b***	****	****	****	****	*	****	****	****
vrn-A1-MD233 + *Ppd-A1b* + *Ppd-D1b* ***vrn-A1-SS8641*** + *Ppd-A1b* + *Ppd-D1b*								
vrn-A1-MD233 + *Ppd-A1a* + *Ppd-D1a* ***vrn-A1-SS8641*** + *Ppd-A1a* + *Ppd-D1a*		***	**	***		****		****

background (Table 2.7, rows five and six), suggesting that *Ppd-D1a* effects on photoperiod response overpower effects of allelic difference at *Ppd-A1*.

Effects of different *Ppd-D1* alleles were found to be significant in both a *Ppd-A1b* photoperiod sensitive background (Table 2.7, rows seven and eight), and in a *Ppd-A1a* PI background (Table 2.7, rows nine and ten). In a *Ppd-A1a* background, *Ppd-D1* allele effects were significant in all locations when tested in a *vrn-A1-SS8641* background, and were significant in five out of eight environments when tested in a *vrn-A1-MD233* background (Table 2.7, rows nine and ten). *Ppd-D1* allele effects were highly significant ($p < 0.01$) in all environments when tested in a *Ppd-A1b* background, and were extremely significant ($p < 0.0001$) in all locations when tested with a *Ppd-A1b* and *vrn-A1-SS8641* background (Table 2.7, rows seven and eight). The stronger effects of allelic differences in *Ppd-D1* as compared to *Ppd-A1*, and the fact that significant *Ppd-D1* effects are present in both a photoperiod sensitive (*Ppd-A1b*) and insensitive (*Ppd-A1a*) background, whereas *Ppd-A1* effects were only significant in a sensitive *Ppd-D1b* background, support the conclusion taken from the QTL mapping results (Table 2.6), that effects of allelic differences in *Ppd-D1* have stronger effects than those at *Ppd-A1*.

However, mean comparisons testing PI of one photoperiod allele in a sensitive background at the other allele (*Ppd-A1a* + *Ppd-D1b* vs. *Ppd-A1b* + *Ppd-D1a*) only detected significant differences in about half of the comparisons tested (Table 2.7, rows one and two). Significant differences were detected at three locations when tested in a *vrn-A1-MD233* background (Table 2.7, row one), and were detected in

four locations when tested in a *vrn-A1-SS8641* background. When simply looking at mean heading date of DHs carrying the different alleles (Table 2.6), DHs carrying the *Ppd-D1a* allele headed 1-3 days earlier than those with the *Ppd-A1a* allele at five locations: 2012 Salisbury, MD; 2012 9 de Julio, ARG; 2013 Clarksville, MD; 2013 Queenstown, MD; and 2014 Kinston, NC (Table 2.6). Mean heading date for *Ppd-A1a* genotypes had the same mean heading date as *Ppd-D1a* genotypes in three environments: 2011 Salisbury, MD; 2014 Clarksville, MD; and 2014 Queenstown, MD (Table 2.6). *Ppd-A1a* and *Ppd-D1a* genotypes headed 1-9 days earlier than their photoperiod sensitive counterparts, *Ppd-A1b* and *Ppd-D1b* (Table 2.6). This suggests that while allelic differences in *Ppd-D1* have stronger effects than those in *Ppd-A1*, these differences are minimized when examined together rather than separately, and have relatively similar effects at the population scale.

Additional QTL were discovered in association with heading date in the field that were not located in same regions as *Ppd-1* genes. Three QTL were mapped in more than one environment (Table 2.5). A QTL on chromosome 2B, at about 63 cM, was detected in three environments: 2013 Clarksville, MD with an LOD score of 5.9; 2014 Clarksville, MD with an LOD score of 5.2; and 2013 Queenstown, MD with and LOD score of 6.6. A QTL on chromosome 7A, at about 55 cM, was detected in two environments: 2013 Clarksville, MD with an LOD score of 3.6 and 2013 Queenstown, MD with an LOD score of 3.5. A QTL on chromosome 5B, at about 66 cM, was detected in two environments: 2013 Clarksville, MD with an LOD score of 3.8; and 2014 Kinston, NC with an LOD score of 4.4. These QTL may represent

other genes that control heading date, though to a lesser extent than the major photoperiod genes. It is difficult to tell if they are earliness per se QTL, as photoperiod and vernalization effects must be removed to accurately measure *Eps* effects.

Most environments had sufficient durations of cold to satisfy all vernalization requirements, but there still appeared to be minor vernalization effects on heading date in the population, especially in warmer environments. A QTL near the *VRN-A1* locus on chromosome 5A was found in only one environment: 2013 Queenstown, MD, with an LOD score of 5.59 (Table 2.5). This QTL was located between flanking markers Xsnp3845 and Xsnp3865. While the assays described in Table 2.1 did not detect any polymorphism between the parents in the *VRN-A1* gene for previously described alleles, it is possible that there is polymorphism in other regions in or near this gene that were not explored using these assays. To further explore this, the DH lines were classified by whether they exhibited MD233 or SS8641 alleles at polymorphic markers flanking this QTL. These were referred to as their *vrn-A1* 'haplotype' and were used for further comparisons. Genotypes with the *vrn-A1* haplotype from SS8641 had mean heading dates 1-2 days later than those carrying the MD233 allele in five environments: 2012 Salisbury, MD; 2012 9 de Julio, ARG; 2013 Clarksville, MD; 2013 Queenstown, MD; and 2014 Kinston, NC (Table 2.4). When genotypes were considered as a combination of alleles at all three flowering time loci, DH lines with *vrn-A1-SS8641+Ppd-A1a+Ppd-D1a* had mean heading dates of an average of 1.75 days earlier than DH lines with the *vrn-A1-MD233+Ppd-*

A1a+Ppd-D1a combination (Table 2.6). In multiple mean comparisons tested, there were significant effects of *vrn-A1* haplotype at four locations, ranging from highly significant $p < 0.01$ to extremely significant ($p < 0.0001$) when tested in a PI (*Ppd-A1a + Ppd-D1a*) background (Table 2.7, row 12). These results also suggests that there may be undetected polymorphism between MD233 and SS8641 at or near the *VRN-A1* locus.

Table 2.8. Pearson correlation coefficients (r) between heading date and grain yield at all locations with yield plots. All correlations calculated using PROC CORR in SAS 9.3.

Environment	correlation coefficient (r)	P value
2013 Clarksville, MD	-0.35	<.0001
2014 Clarksville, MD	0.03	0.6512
2013 Queenstown, MD	-0.43	<.0001
2014 Queenstown, MD	-0.29	<.0001
2014 Kinston, NC	-0.07	0.2875

Correlation coefficients were calculated between heading date and grain yield (Table 2.7). Significant negative correlations were observed in three environments, ranging from -0.29 to -0.43, where earlier heading was correlated with higher grain yield. In two environments, however, no significant correlations were found, suggesting that the correlation between heading date and grain yield is highly dependent on environmental conditions within each location-year.

Greenhouse Experiments

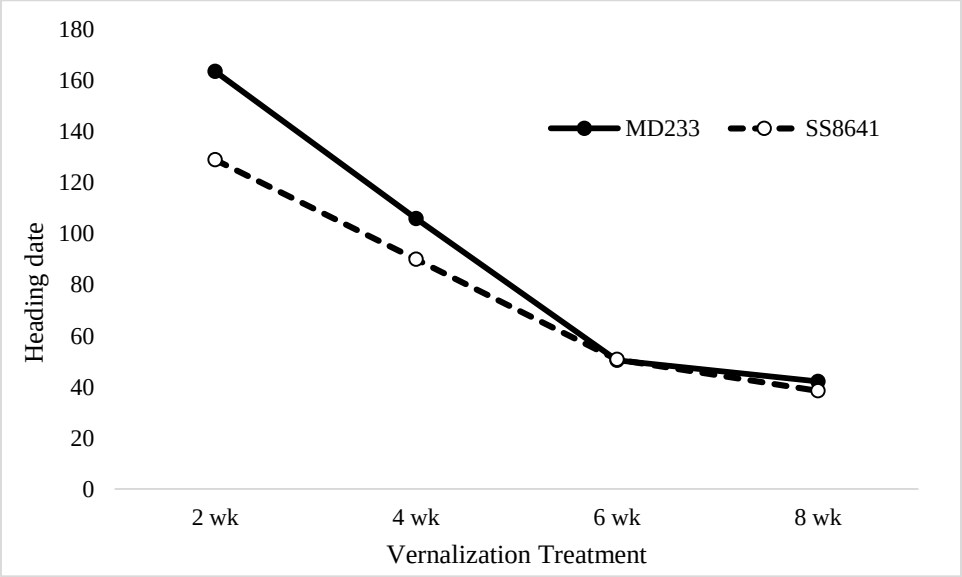

Figure 2.9. Effect of vernalization duration in days from transplanting to heading of MD233 and SS8641 in 2014 Greenhouse Study.

Although MD233 and SS8641 are both winter wheat cultivars, they responded differently to vernalization. The delay in days from transplanting to heading of MD233 was greater than was observed for SS8641 in the 2- and 4-week vernalization treatments (Figure 2.9). There was still a slight response to vernalization beyond 6 weeks of vernalization, about 10 days for both cultivars (Figure 2.9). However, differences between cultivars were minimized in the 6- and 8-week treatments, indicating that the vernalization requirements of both MD233 and SS8641 had been satisfied in these treatments, though additional vernalization still further accelerated heading. Therefore, the 6-week treatment was not repeated in the 2015 greenhouse experiment.

Summary statistics for days from transplanting to heading the 2014 and 2015 greenhouse experiments are reported in Tables 2.9 and 2.10, respectively. Frequencies of DHs for days from transplanting to heading in the 2014 greenhouse experiment is shown in Figure 2.10, frequencies of DHs for the 2015 greenhouse experiment are shown in Figure 2.11. Ranges for days from transplanting to heading decreased with increased vernalization treatment, with a range of 117 days in the 2-week treatment to a range of 35 days in the 8-week treatment in 2014 (Table 2.9, Figure 2.10), and a range of 112 days in the 2-week treatment to a range of 27 days in the 8-week treatment in 2015 (Table 2.10, Figure 2.11). This decreased range with increased vernalization is likely due to the decreased segregation in vernalization response in the population, as more DHs have their vernalization requirements satisfied with longer vernalization treatments.

QTL mapping results are reported in Tables 2.11 and 2.12. Three QTL were detected in both the 2014 and 2015 greenhouse experiments. One QTL, on chromosome 7D at around 120 cM, mapped in the 2-week vernalization treatments only, with an LOD score of 4.3 in 2014 and an LOD score of 3.5 in 2015. Two QTL on chromosome 5A were detected in both the 2- and 4-week treatments in 2014 and 2015. The first QTL was located near the centromere, from 53-57 cM, with LOD scores ranging from 3.2 to 10.6. The second QTL was located at 107-108 cM and was also detected in the 6-week treatment in 2014 and the 8-week treatment in 2015, with LOD scores ranging from 8.99 to 21.44.

The QTL at 107-108 cM on chromosome 5A is in the same genomic region as

Table 2.9. Summary Statistics for days from transplanting to heading (Zadoks 59) in 2014 greenhouse vernalization experiment. F-values and P-values were calculated using the MIXED procedure in SAS.

Vernalization Treatment	Parental Means		DHs							
	MD233	SS8641	Mean	SD	Range	Minimum	Maximum	CV%	F-value	P-value
2 weeks	163	129	123	28.9	117	59	176	23.5	15.25	<.0001
4 weeks	106	90	82	24.1	113	40	153	29.2	17.90	<.0001
6 weeks	51	51	50	8.3	59	24	83	16.7	23.41	<.0001
8 weeks	42	39	42	4.6	35	32	67	10.8	9.45	<.0001

Table 2.10. Summary Statistics for days from transplanting to heading (Zadoks 59) in 2015 greenhouse vernalization experiment. F-values and P-values were calculated using the MIXED procedure in SAS.

Vernalization Treatment	Irrigation	Parental Means		DHs							
		MD233	SS8641	Mean	SD	Range	Minimum	Maximum	CV%	F-value	P-value
2 weeks	drip	174	149	157	17.9	112	83	195	11.4	12.57	<.0001
4 weeks	manual	116	83	96	13.4	60	62	122	13.9	29.94	<.0001
8 weeks	manual	60	55	59	4.8	27	49	76	8.1	14.69	<.0001

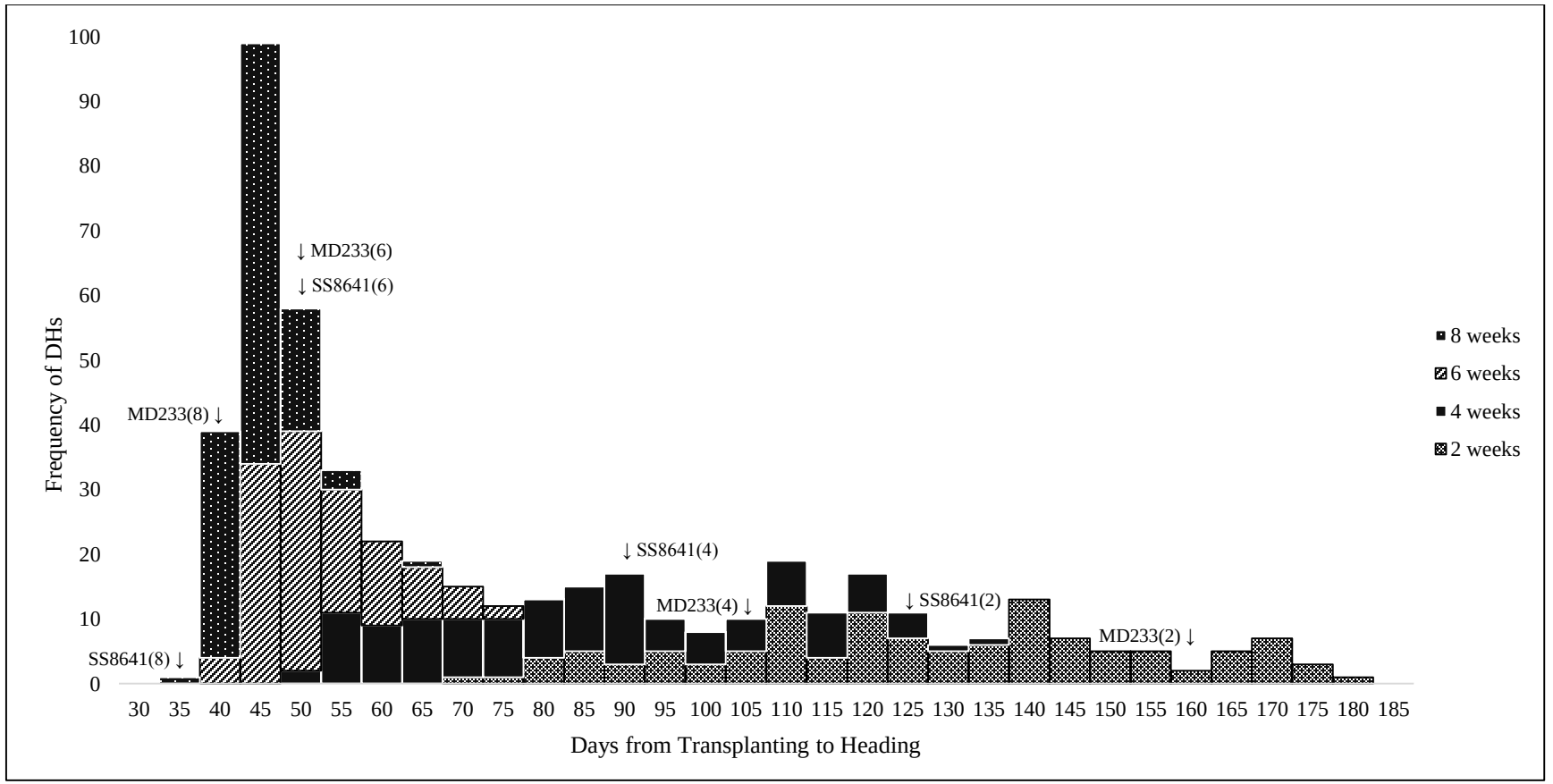

Figure 2.10. Frequency of DHs for days from transplanting to heading (Zadoks 59) in 2014 vernalization greenhouse experiment.

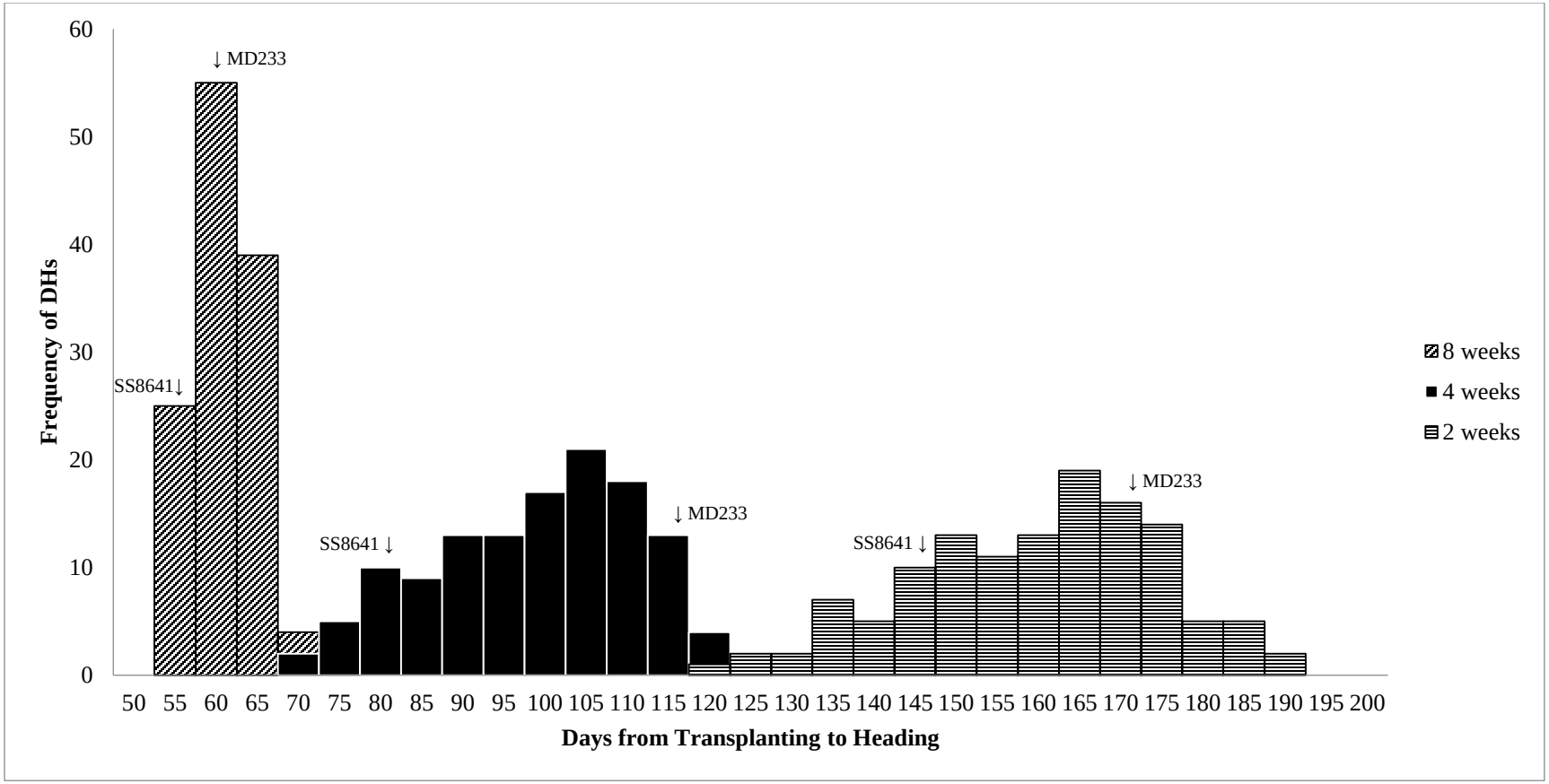

Figure 2.11. Frequency of DHs for days from transplanting to heading (Zadoks 59) in 2015 vernalization greenhouse experiment.

Table 2.11. QTL mapping results from 2014 greenhouse vernalization experiment.

Vernalization Treatment	Chromosome	Position (cM)	Left Marker	Right Marker	LOD	PVE%	Additive Effect
2 week	5A	54	Xsnp49	Xgwm304	9.34	16.34	-10.82
2 week	5A	107	Xsnp3833	Xsnp3863	8.99	15.50	-10.53
2 week	2B	77	Xsnp2635	Xsnp2646	5.03	7.98	7.55
2 week	7D	123	Xgwm111	Xsnp4937	4.29	6.74	6.90
4 week	5A	57	Xsnp3837	Xsnp3838	3.20	4.52	-4.62
4 week	5A	107	Xsnp3833	Xsnp3863	19.28	37.68	-13.35
4 week	1B	49	Xsnp2073	Xsnp2110	5.31	7.80	6.01
6 week	5A	107	Xsnp3833	Xsnp3863	17.99	40.85	-5.04
6 week	5A	178	Xsnp3849	Xsnp3841	5.90	10.94	-2.58
6 week	6B	64	Xsnp4421	Xsnp4451	3.24	5.42	1.82
8 week	5A	166	Xsnp3761	Xsnp3862	7.72	19.36	-1.63
8 week	2D	78	Xsnp2844	Xsnp2877	11.98	33.26	-2.14

Table 2.12. QTL mapping results from 2015 greenhouse vernalization experiment.

Vernalization Treatment	Irrigation	Chromosome	Position (cM)	Left Marker	Right Marker	LOD	PVE%	Additive Effect
2 week	drip	1A	0	Xwmc496	Xsnp1970	3.56	3.94	3.02
2 week	drip	2A	15	Xsnp2445	Xsnp2480	5.76	6.70	3.95
2 week	drip	5A	53	Xsnp218	Xsnp49	10.59	13.46	-5.62
2 week	drip	5A	107	Xsnp3833	Xsnp3863	10.87	13.92	-5.74
2 week	drip	1B	29	Xsnp2213	Xsnp1707	3.03	3.43	2.81
2 week	drip	2B	65	Xsnp2773	Xgwm319	5.39	6.35	3.83
2 week	drip	5B	53	Xsnp4083	Xsnp3988	4.96	6.24	3.80
2 week	drip	2D	54	Xsnp2862	XPpdD1	6.04	7.95	-4.31
2 week	drip	7D	119	Xsnp4945	Xsnp4932	3.49	3.88	2.99
4 week	manual	5A	54	Xsnp49	Xgwm304	5.14	7.35	-3.38
4 week	manual	5A	107	Xsnp3833	Xsnp3863	21.44	42.41	-8.14
4 week	manual	1B	31	Xsnp1707	Xgwm11	3.13	4.27	2.55
4 week	manual	5B	68	Xsnp4061	Xsnp4027	3.25	4.42	2.60
8 week	manual	2A	17	XPpdA1	Xsnp2461	10.22	18.92	1.80
8 week	manual	5A	108	Xsnp3863	Xsnp3845	10.63	19.94	-1.86
8 week	manual	2D	57	Xsnp2862	XPpdD1	15.24	32.40	-2.36

Table 2.13. Mean heading date for DHs with different genotypes and allele combinations in 2014 greenhouse vernalization experiment. Heading date was measured as days from transplanting to heading (Zadoks 59).

Genotype	No. of Lines	Vernalization Treatment			
		2 weeks	4 weeks	6 weeks	8 weeks
MD233 (*Ppd-A1a*, *Ppd-D1b*)		163	101	50	42
SS8641 (*Ppd-A1b*, *Ppd-D1a*)		129	95	51	39
DHs	124	123	82	50	42
vrn-A1-MD233	50	141	100	56	43
vrn-A1-SS8641	67	111	70	46	42
Ppd-A1a-MD233	68	122	80	50	41
Ppd-A1b-SS8641	56	128	86	50	44
Ppd-D1a-SS8641	54	121	85	51	41
Ppd-D1b-MD233	69	128	82	50	44
vrn-A1-MD233 + Ppd-A1a + Ppd-D1a	12	133	99	57	42
vrn-A1-MD233 + Ppd-A1a + Ppd-D1b	16	140	96	55	43
vrn-A1-MD233 + Ppd-A1b + Ppd-D1a	13	132	103	55	41
vrn-A1-MD233 + Ppd-A1b + Ppd-D1b	9	154	102	54	48
vrn-A1-SS8641 + Ppd-A1a + Ppd-D1a	16	105	69	45	39
vrn-A1-SS8641 + Ppd-A1a + Ppd-D1b	21	111	66	45	41
vrn-A1-SS8641 + Ppd-A1b + Ppd-D1a	11	110	69	44	41
vrn-A1-SS8641 + Ppd-A1b + Ppd-D1b	18	114	73	48	45

Table 2.14. Mean heading date for DHs with different genotypes and allele combinations in 2015 greenhouse vernalization experiment. Heading date was measured as days from transplanting to heading (Zadoks 59).

Genotype	No. of Lines	Vernalization Treatment		
		2 wk drip	4 wk manual	8 wk manual
MD233 (*Ppd-A1a*, *Ppd-D1b*)		174	116	60
SS8641 (*Ppd-A1b*, *Ppd-D1a*)		149	83	55
DHs	123	157	96	59
vrn-A1-MD233	49	165	106	60
vrn-A1-SS8641	67	151	89	57
Ppd-A1a-MD233	68	154	95	57
Ppd-A1b-SS8641	55	161	98	60
Ppd-D1a-SS8641	54	153	94	56
Ppd-D1b-MD233	68	160	98	60
vrn-A1-MD233 + Ppd-A1a + Ppd-D1a	12	160	105	59
vrn-A1-MD233 + Ppd-A1a + Ppd-D1b	16	163	106	60
vrn-A1-MD233 + Ppd-A1b + Ppd-D1a	13	165	104	58
vrn-A1-MD233 + Ppd-A1b + Ppd-D1b	8	175	112	65
vrn-A1-SS8641 + Ppd-A1a + Ppd-D1a	26	144	86	54
vrn-A1-SS8641 + Ppd-A1a + Ppd-D1b	21	152	87	57
vrn-A1-SS8641 + Ppd-A1b + Ppd-D1a	11	144	83	55
vrn-A1-SS8641 + Ppd-A1b + Ppd-D1b	18	159	95	62

Table 2.15. Multiple mean comparisons between DHs carrying different allele combinations across all greenhouse experiments, calculated using PROC GLM with Tukey-Kramer adjustment in SAS. Bolded alleles indicate those whose effects are being compared in each test. Significance level of mean comparison is indicated by stars, where * = 0.01 < p < 0.05; ** = 0.001 < p < 0.01; *** = 0.001 < p < 0.001; **** = p < 0.0001.

	Vernalization Treatment						
	2014				2015		
Mean Comparison	2-week	4-week	6-week	8-week	2-week	4-week	8-week
vrn-A1-MD233 + ***Ppd-A1a*** + *Ppd-D1b*				***			****
vrn-A1-MD233 + *Ppd-A1b* + ***Ppd-D1a***							
vrn-A1-SS8641 + ***Ppd-A1a*** + *Ppd-D1b*					*		
vrn-A1-SS8641 + *Ppd-A1b* + ***Ppd-D1a***							
vrn-A1-MD233 + ***Ppd-A1a*** + *Ppd-D1b*				****	***	*	****
vrn-A1-MD233 + ***Ppd-A1b*** + *Ppd-D1b*							
vrn-A1-SS8641 + ***Ppd-A1a*** + *Ppd-D1b*			**	****	**	****	****
vrn-A1-SS8641 + ***Ppd-A1b*** + *Ppd-D1b*							
vrn-A1-MD233 + ***Ppd-A1a*** + *Ppd-D1a*							
vrn-A1-MD233 + ***Ppd-A1b*** + *Ppd-D1a*							
vrn-A1-SS8641 + ***Ppd-A1a*** + *Ppd-D1a*							*
vrn-A1-SS8641 + ***Ppd-A1b*** + *Ppd-D1a*							
vrn-A1-MD233 + *Ppd-A1b* + ***Ppd-D1a***	**			****	*	****	****
vrn-A1-MD233 + *Ppd-A1b* + ***Ppd-D1b***							
vrn-A1-SS8641 + *Ppd-A1b* + ***Ppd-D1a***			**	****	****	****	****
vrn-A1-SS8641 + *Ppd-A1b* + ***Ppd-D1b***							
vrn-A1-MD233 + *Ppd-A1a* + ***Ppd-D1a***							
vrn-A1-MD233 + *Ppd-A1a* + ***Ppd-D1b***							
vrn-A1-SS8641 + *Ppd-A1a* + ***Ppd-D1a***					**		****
vrn-A1-SS8641 + *Ppd-A1a* + ***Ppd-D1b***							
vrn-A1-MD233 + *Ppd-A1b* + *Ppd-D1b*	****	****	***	***	****	****	****
vrn-A1-SS8641 + *Ppd-A1b* + *Ppd-D1b*							
vrn-A1-MD233 + *Ppd-A1a* + *Ppd-D1a*	****	****	****	**	****	****	****
vrn-A1-SS8641 + *Ppd-A1a* + *Ppd-D1a*							

the *VRN-A1* gene, and as the QTL reported on chromosome 5A in the 2013 Queenstown, MD field environment. This QTL was the most consistently detected QTL across vernalization treatments and years in the greenhouse experiments. In the 4-week vernalization treatment, this QTL explained 42.4% of variation (LOD = 21.4) in 2015 and 37.7% of variation (LOD = 19.3) in 2014 (Tables 2.10 and 2.11). This locus also showed effects in the 2-week treatment (LOD = 8.99 in 2014 and 10.87 in 2015), 6-week treatment (LOD = 17.99), and 8-week treatment (LOD = 10.63 in 2015). These results support the hypothesis that there is polymorphism between the two parents of the population in the *VRN-A1* gene region that was not detected using several KASP marker assays described in Table 2.1.

ANOVA of the three-way allele combinations, at *vrn-A1* + *Ppd-A1* + *Ppd-D1* loci found significant differences ($p < 0.0001$) between allele combination classes in all vernalization treatments in 2014 and 2015. Therefore, multiple mean comparisons were calculated for these allele combinations for all treatments in both years, and are reported in Table 2.15. Significant differences were detected in mean comparisons testing effects of *Ppd-A1* alleles in a *Ppd-D1b* background (Table 2.15, rows three and four), and mean comparisons testing *Ppd-D1* allele effects in a *Ppd-A1b* background (Table 2.15, rows seven and eight) in the 8-week treatment in 2014 and all treatments in 2015. The detection of these differences in all treatments in 2015, but not in 2014, likely was due to the increased overall variation in days from transplanting to heading recorded in the 2014 experiments. The most significant differences, however, were found in mean comparisons testing vrn-A1 effects in both

photoperiod sensitive (*Ppd-A1b + Ppd-D1b*) and insensitive (*Ppd-A1a + Ppd-D1a*) backgrounds (Table 2.15, rows 11 and 12). In 2014, highly significant ($p < 0.01$) effects of *vrn-A1* haplotype were detected in the 6- and 8-week treatments, and extremely significant ($p < 0.0001$) effects were detected in the 2- and 4-week treatments. In 2015, extremely significant ($p < 0.0001$) effects were detected in all vernalization treatments (Table 2.15, rows 11 and 12). These results support those of the QTL mapping results, suggesting that there is polymorphism in the *VRN-A1* region underlying differential response to vernalization in this population.

These effects can be seen when comparing mean heading date for different alleles and allele combinations, as reported in Table 2.13 for the 2014 experiments and Table 2.14 for the 2015 experiments. In the 4-week vernalization treatment in 2014, DH lines with the *vrn-A1-MD233* haplotype showed a delay in heading of 30 days as compared to DHs with the *vrn-A1-SS8641* haplotype. When in combination with photoperiod insensitivity alleles, DHs with the *vrn-A1-MD233+Ppd-A1a+Ppd-D1a* haplotype headed 30 days later than DHs with the *vrn-A1-SS8641+Ppd-A1a+Ppd-D1a* haplotype; and in combination with photoperiod sensitivity alleles, DHs with the *vrn-A1-MD233+Ppd-A1b+Ppd-D1b* headed 29 days later than those with the *vrn-A1-SS8641+Ppd-A1b+Ppd-D1b* haplotype (Table 2.13). Differences were smaller in 2015, but DH lines with the *vrn-A1-MD233* haplotype still headed on average 17 days later than those with the *vrn-A1-SS8641* haplotype (Table 2.14).

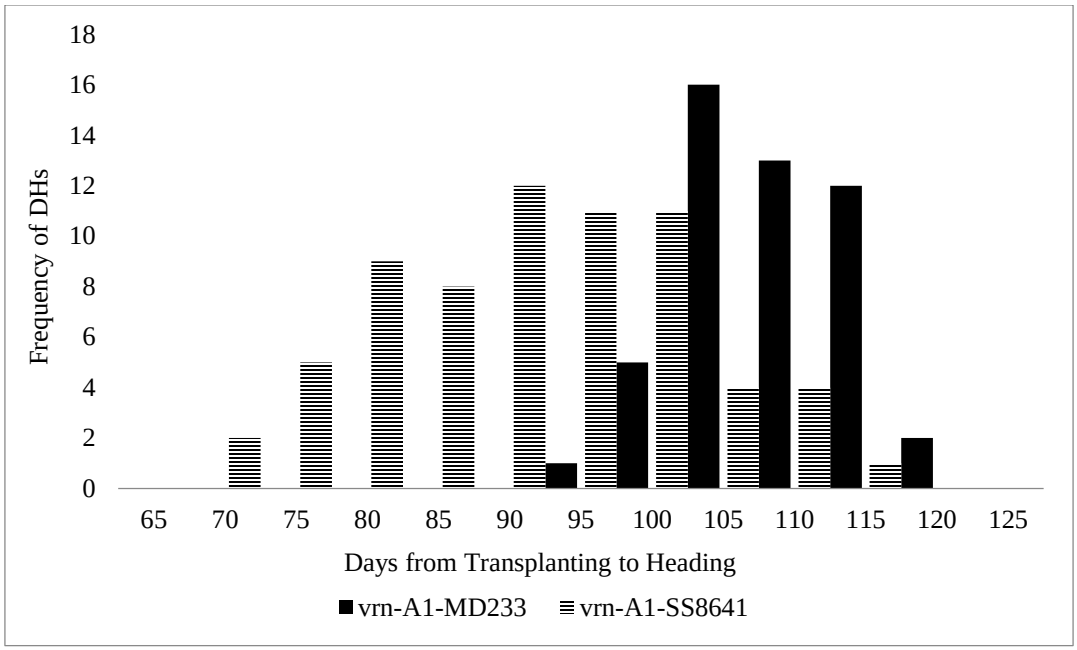

Figure 2.12. Frequency of DHs for days from transplanting to heading in 2015 4-week vernalization treatment classified based on *VRN-A1* haplotype.

Effects of *vrn-A1* haplotype was further investigated by comparing the frequencies of heading dates among DH lines when classified by their *vrn-A1* haplotype in the 4-week vernalization treatment in 2015 (Figure 2.12). While there is some overlap in heading date between the *vrn-A1-MD233* and *vrn-A1-SS8641* haplotypes, there are two separate normal curves for the two different *vrn-A1* haplotype classes. The mean number of days from transplanting to heading of DH lines carrying the *vrn-A1-MD233* haplotype headed 106 days after transplanting on average, whereas lines carrying the *vrn-A1-SS8641* haplotype headed 89 days after transplanting on average. Although no previously-described alleles in the *VRN-A1* gene associated with earlier flowering were detected using the assays described in Table 2.1, the collective results

from the greenhouse trials of this study present strong evidence that there is genetic polymorphism between the *vrn-A1* genes of MD233 and SS8641, where the SS8641 allele is associated with earlier heading in short vernalization treatments.

Allele Discovery in *VRN-A1*

Potential copy number variation of the *VRN-A1* gene was explored using quantitative PCR following the protocols of Diaz et al. (2012). Haploid copy number was determined from differential expression between *VRN-A1* and an internal positive control, *TaCO*, and was calculated as delta CT, where delta CT = $2^{-(\text{VrnA1-TaCO})}$. Control line 'Claire' had a mean delta CT value of 0.77 and was determined to have a haploid copy number of one; control 'Malacca' had a mean delta CT value of 1.36 and was determined to have a haploid copy number of two; control 'Hereward' had a mean delta CT value of 1.85 and was determined to have a haploid copy number of three (Figure 2.13). MD233 had a mean delta CT value of 1.96 and SS8641 had a mean delta CT value of 2.07; therefore, both MD233 and SS8641 were determined to both have three haploid copies of *VRN-A1* (Figure 2.13). These results confirm that copy number variation is not a source of genetic variation associated with the heading date QTL at this locus.

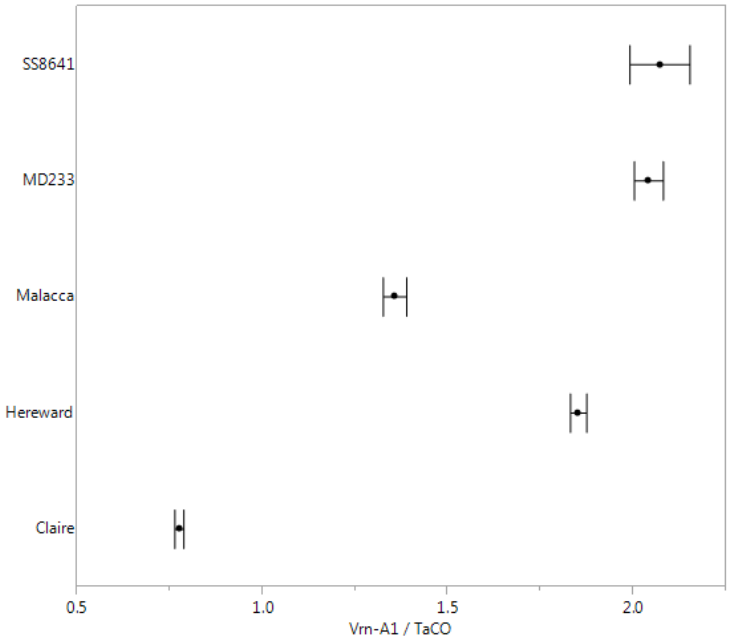

Figure 2.13. Copy number variation of MD233, SS8641, and control lines. Haploid copy number was determined based on *Vrn-A1*/*TaCO* ratio, calculated as ΔCT.

Sequencing results of a ~600 bp portion of the *VRN-A1* first intron that includes the RIP-3 binding region of MD233 and SS8641 were aligned to each other and and the vrn-A1 winter allele of 'Triple Dirk C' (TDC; AY747600.1) using Clustal Omega (Sievers et al. 2011). Three SNPs were found in the alignments against TDC: C→T at bp 3236, G→A at bp 3259, and A→G at bp 3529 (bp referring to those reported in AY747600.1). However, at all three SNPs, MD233 and SS8641 had the same alleles, both differing from TDC. Therefore, these SNPs are not believed to be associated with the difference in heading date mapped to this locus. Further, the results of a BLAST search found 100% alignment of this ~600 bp segment with cultivars Hereward and Malacca, which differ significantly in their heading date, suggesting that these loci are not major determinants of heading date

(Diaz et al. 2012). None of the SNPs that disrupted binding of the TaGRP2 repressor in the *VRN-D4* gene and *VRN-A1* alleles of wheat varieties Jagger, Claire, and Chinese Spring were found in either MD233 or SS8641 (Kippes et al. 2015). Therefore, disruption of TaGRP2 protein binding is not the source of genetic variation associated with the heading date QTL at this locus.

Discussion

My study identified genetic loci associated with heading date both in natural field environments and under reduced vernalization treatments in the greenhouse. Five QTL were mapped in more than one field environment: two QTL, on chromosomes 2A and 2D, were found in all eight environments; one QTL, on chromosomes 2B, was found in three environments; and two QTL, on chromosomes 7A and 5B, were found in two environments (Table 2.5). The two QTL found in all field environments had major effects: the QTL in chromosome 2A explained up to 16.8% of variation in heading date (in 2013 Queenstown, MD), and the QTL on chromosome 2D explained up to 40% of variation in heading date (in 2014 Queenstown, MD). In the reduced vernalization greenhouse experiments, three QTL were detected in at least one vernalization treatment in both 2014 (Table 2.11) and 2015 (Table 2.12). One QTL, on chromosome 7D, was mapped in the 2-week treatment of both years. A QTL, in the centromeric region of chromosome 5A, was mapped in both the 2-week and 4-week treatments in both 2014 and 2015. Lastly, one QTL was mapped in the 2-, 4-, and 6-week treatments in 2014 and all treatments

(2-, 4-, 8-week) in 2015. This QTL had major effects, explaining up to 42.4% of variation (4-week treatment in 2015). Based on its chromosome location and the magnitude of effects, this QTL may be associated with polymorphism in the *VRN-A1* gene, known to have strong effects on heading date in reduced vernalization environments. The results of both the field and greenhouse experiments and QTL mapping validated effects of known major genes and identified previously-unreported genetic regions influencing heading date.

Photoperiod Effects

Photoperiod insensitivity (PI) from *Ppd-D1a* has been widely employed in breeding materials around the world. It was first transferred into European wheats in the 1930s from the Japanese variety 'Akakomugi,' and was long used as the main source of PI (Worland 1996). In a diverse panel of 683 globally-sourced cultivars, the *Ppd-D1a* allele was present in 57% of cultivars and played the most important role in flowering time, explaining 28% of the phenotypic variance (Kiss et al. 2014). However, there has been much less research quantifying the effects of variation in the other *Ppd-1* genes, particularly *Ppd-A1*, on flowering time, or how multiple PI alleles perform in conjunction with each other. This study provides quantification of how *Ppd-A1a* affects flowering time across different field environments and its effects in combination with *Ppd-D1a*.

It was historically believed that PI from *Ppd-A1a* was the least potent of the *Ppd-1* PI alleles, with PI from *Ppd-D1a* being the strongest and PI from *Ppd-B1a*

being intermediate (Worland 1996). Similarly, my results support the conclusion that *Ppd-A1* effects are not as strong as those caused by *Ppd-D1*, although PI from *Ppd-A1a* still has a significant effect and the mean effect of *Ppd-A1a* is only significantly different from *Ppd-D1a* in half of the environments and backgrounds tested (Table 2.7, rows one and two). QTL mapping results indicated that allelic variation in *Ppd-A1* explained about half as much of the variation in heading date as allelic variation in *Ppd-D1*, with *Ppd-A1* explaining 14% and *Ppd-D1* explaining 30% on average across eight field locations. In 2013 Clarksville, MD, however, *Ppd-A1* had slightly stronger effect on PI than *Ppd-D1*. Here, *Ppd-A1* explained 14% of variation and *Ppd-D1* explained only 12%; however, the total variation in heading date at in this environment were very small (Tables 2.4 and 2.5).

Mean comparisons of different combinations of alleles in three major flowering time loci that were segregating in the population detected significant effects of *Ppd-A1* allele in a photoperiod sensitive *Ppd-D1b* background (Table 2.7, rows three and four), but did not detect significant effects of *Ppd-A1* allele in a photoperiod insensitive *Ppd-D1a* background (Table 2.7, rows five and six). However, significant effects of *Ppd-D1* allele were detected in both photoperiod sensitive (*Ppd-A1b*) and photoperiod insensitive (*Ppd-A1a*) backgrounds (Table 2.7, rows 7-10). These results again assert that PI from *Ppd-A1a* has significant effects, but that the effects of PI from *Ppd-D1a* are stronger. Mean comparisons of allelic combinations with PI from one locus and sensitivity from the other (*Ppd-A1a* + *Ppd-D1b* compared to *Ppd-A1b* + *Ppd-D1a*) only found significant differences between genetic sources of PI in half

of the locations tested (Table 2.7, rows one and two), suggesting that the difference of effects from *Ppd-A1* and *Ppd-D1* are not very large.

In other studies, *Ppd-A1a* and *Ppd-D1a* alleles have been found to have very similar effects on flowering time. In near-isogenic BC_2F_4 lines developed using either synthetic hexaploid lines or chromosome substitution lines as donors for specific *Ppd-1* alleles in uniform photoperiod sensitive backgrounds, *Ppd-A1a* and *Ppd-D1a* were found to have comparable reducing effects on flowering time. *Ppd-A1* had a mean allele effect of -38 days and *Ppd-D1* had a mean allele effect of -24 to -42 days, depending on *Ppd-D1a* allele donor, in a greenhouse experiment under short (8 h) photoperiod as compared to lines of the same genetic background with no PI alleles introgressed (Bentley et al. 2013). The *Ppd-D1a* allele donated by cultivar 'Soissons' had a mean reduction effect of 42 days, while the allele donated by 'Ciano67' had a mean reduction of 24 days. These results suggest that the genetic background of PI alleles in the same gene can have a varying effect on its influence on heading date, and that this may be a bigger determinant of the allele's effect on earliness than which *Ppd-1* gene the allele resides in.

In the present study, I found that the combination of PI from *Ppd-A1a* and *Ppd-D1a* resulted in the earliest heading genotypes. DH lines that combined *Ppd-A1a* and *Ppd-D1a* PI alleles headed two to sixteen days earlier than DHs with combined PS alleles *Ppd-A1b* and *Ppd-D1b* (Table 2.6). The lesser effects were found at the more northern latitudes (Clarksville, MD, 39°15'31.44"N), while greater

variation in photoperiod effects was found at lower latitudes (9 de Julio, ARG, 35°28'53.39"S and Salisbury, MD, 38°22'14.48"N).

As climate trends rise, it will become very useful to stack multiple sources of PI to allow for increasingly early flowering times, enabling this cold-adapted crop to flower and mature before the onset of hot, dry summer conditions. In this study, earlier heading was found to be strongly correlated with higher yields in three out of five of the environments (Table 2.7). Increased yields have long been correlated with earlier flowering time, especially in hot climates, and will probably become stronger if global warming trends continue (Worland 1996; Mondal et al. 2015).

Vernalization Effects

In field environments, effects of allelic diversity in *VRN-1* loci generally do not have as large of an effect on the earliness of flowering as allelic diversity in *Ppd-1* loci (Kiss et al. 2014; Gomez et al. 2014). My research also supports this conclusion, as my QTL mapping detected a QTL in the same genomic region as a vernalization locus in only one of the eight environments analyzed (2013 Queenstown, MD, Table 2.6). However, as warming trends continue, vernalization effects will become more apparent as vernalization requirements of winter wheats will be met less often. This will create a difficult situation in fine-tuning flowering time of winter wheat: growing spring-type wheat instead, which does not require vernalization to flower, could cause the crop to flower during winter when it is still too cold and dark for adequate seed set and yield, while growing winter wheats that require long periods of vernalization

may cause the crop to flower too late into the summer due to insufficient vernalization during mild winters. Ideally, breeders could employ vernalization alleles that require some vernalization to induce flowering, but do not require so much vernalization that their requirement cannot be met in shorter, milder winters.

My study appears to have detected such a vernalization allele. In my greenhouse studies, both parents headed essentially at the same time in the fully-vernalized (8-week) treatments, but SS8641 showed higher responsiveness to brief periods (2-weeks, 4-weeks) of vernalization than MD233. In the 2-week vernalization treatment of the 2014 greenhouse experiments, there was a 34 day difference between the parents in days from transplanting to heading. SS8641 reached heading after 129 days, while MD233 took 163 days to reach this growth stage (Table 2.9). After four weeks of vernalization in 2015, SS8641 reached heading after 83 days, whereas MD233 took 116 days, leaving a 33 day gap (Table 2.10). This difference was also seen in the DH population. After four weeks of vernalization in the 2015 greenhouse experiments, DH lines with the SS8641 haplotype in the *VRN-A1* region flowered on average after 89 days, while lines that carried the MD233 haplotype in this region did not reach heading until 106 days, a difference of 17 days (Table 2.14).

The importance of this region in determining heading date in the DH population is supported by my QTL analysis, where a QTL was mapped to a region containing *VRN-A1* on chromosome 5A with an LOD score of 21.4, explaining 42.4% of variation in heading date in the 4-week vernalization treatment of the 2015

greenhouse experiments (Table 2.12). While this locus was also detected in the 2-week treatment (LOD = 10.87) and eight week treatment (LOD = 10.63), the fact that this locus explains twice as much variation in heading date in the 4-week treatment suggests that the difference in responsiveness between the parental alleles in this region is maximized at four weeks of vernalization. SS8641 responds more rapidly to vernalization after four weeks, whereas MD233 still needs a longer duration of vernalization to significantly accelerate this the transition from the vegetative to reproductive phase. While our KASP assays determined SS8641 to carry the recessive *vrn-A1* that classifies it as a winter wheat, our greenhouse results suggest it does not need long durations of vernalization to induce flowering.

Allelic diversity in *VRN-A1* tends to have little effect on heading date in fully-vernalized field environments. An experiment to determine the effects of allelic compositions of the *VRN-1* and *Ppd-1* genes on wheat heading across two autumn-sown field trials in Central Hungary found that winter or spring allele types of the *VRN-A1* and *VRN-B1* genes had no significant effect on heading, while the allele type in *VRN-D1*, *Ppd-B1* and *Ppd-D1* significantly influenced heading (Kiss et al. 2014). The mean heading dates between winter and spring alleles differed by 0.8 days for *VRN-A1*, 0.3 days for *VRN-B1*, and 2.6 days for *VRN-D1* (Kiss et al. 2014). This is fairly consistent with the field experiments in the present study: a QTL in the region of chromosome 5A containing *VRN-A1* was only detected in one environment, and there was only a maximum of 2 days difference between mean heading date of DH lines classified by their *vrn-A1* haplotype in any environment. However, more

pronounced effects were detected in the reduced-vernalization greenhouse experiments, where a QTL with LOD score of 21.4 was detected in the 4-week vernalization treatment in 2015, associated with a 17 day difference in mean heading date between the MD233 and SS8641 *VRN-A1* haplotypes (Table 2.12 and 2.14). Mean comparisons of haplotype in the *vrn-A1* region in my study also found highly significant effects in both photoperiod sensitive (*Ppd-A1b* + *Ppd-D1b*) and insensitive (*Ppd-Aa* + *Ppd-D1a*) backgrounds (Table 2.15, rows 11 and 12).

In contrast, a study which compared *VRN-1* allele effects on heading time between a pre-vernalized treatment (seeds imbibed for 8 weeks at 4˚C prior to planting) and natural vernalization in South Perth, Western Australia, found that allelic diversity in *VRN-A1* had nearly twice the effect as allelic diversity in *VRN-B1* or *VRN-D1* when comparing heading date response to vernalization treatment. In terms of delayed heading, average effect of the winter genotype compared with the spring genotype in this comparison, was 76.8 degree days for *VRN-A1*, 33.8 degree days for *VRN-B1* and 43.6 degree days for *VRN-D1* (Zheng et al. 2013). While no comparisons to allelic diversity in other *VRN-1* genes could be made in the present study, allelic diversity in *VRN-A1* of the DH population had similarly large effects when comparing shortened vernalization treatments to full vernalization treatments. In the 2014 greenhouse experiment, comparison between the mean days from transplanting to heading between the 8-week and 4-week vernalization treatments showed a difference of 57 days in DH lines with the *vrn-A1-MD233* haplotype between treatments, compared to only a difference in 28 days among DH lines with

the *vrn-A1-SS8641* haplotype (Table 2.13). This was an almost two-fold difference: vernalization reduced difference in days from transplanting to heading nearly twice as much in DH lines carrying the *vrn-A1-MD233* haplotype compared to those with the *vrn-A1-SS8641* haplotype. In 2015, DH lines carrying the *vrn-A1-MD233* haplotype showed a difference of 46 days between the 8-week and 4-week vernalization treatments, while DH lines with the *vrn-A1-SS8641* haplotype showed a difference of 32 days (Table 2.14). Because our KASP assays found both MD233 and SS8641 to have the recessive *vrn-A1* winter allele, these differences are particularly interesting.

Allele Discovery in *VRN-A1*

Spring alleles reported for the VRN-1 genes typically come from genetic variation in the promoter region and first intron of the genes (Yan et al. 2003; Fu et al. 2005). MASWheat (www.maswheat.org) cites 6 major *VRN-A1* alleles: *vrn-A1*, the recessive winter type allele; *Vrn-A1a*, the most potent spring allele, caused by an insertion of a foldback repetitive element and duplicated region in the promoter; *Vrn-A1b*, a spring allele with several SNPs and deletions in the promoter region, typically a 20-bp deletion in the 5' UTR; *Vrn-A1c*, a spring allele with a large deletion in the first intron; *Vrn-A1d*, a spring allele with a 32-bp deletion in the promoter region; and *Vrn-A1e*, a spring allele with a 54-bp deletion in the promoter region (McIntosh et al. 2003; Yan et al. 2003; Fu et al. 2005; maswheat.ucdavis.edu/protocols/Vrn/). Assays for the *vrn-A1*, *Vrn-A1a*, and *Vrn-A1b* alleles were performed in this study (Table 2.1), finding that both MD233 and SS8641 carried the recessive winter allele, *vrn-A1*,

and neither parent had the dominant *Vrn-A1a* or *Vrn-A1b* spring alleles. The *Vrn-A1c* allele is not present in either MD233 or SS8641, because my sequencing results covering ~600 bp of the first intron, which would be a part of this deletion, did not detect any missing sequence (Fu et al. 2005).

Variation in vernalization requirement can be induced among wheats with recessive winter alleles by copy number variation. Plants with increased copy number of *vrn-A1* have an increased vernalization requirement, requiring longer periods of cold to induce flowering (Diaz et al. 2012). My TaqMan® assays, however, found that both MD233 and SS8641 have three haploid copies of *vrn-A1*. Therefore, copy number variation is not the basis of the different responses to vernalization exhibited by these cultivars.

Vernalization response has also been found to be influenced by the disruption of the RIP-3 binding site, where the TaGRP protein, a repressor, binds to *VRN-A1*. SNPs in this region, found in the *VRN-D4* gene and *vrn-A1* alleles of wheat varieties Jagger, Claire, and Chinese Spring, inhibit binding and thus accelerate flowering (Kippes et al. 2015). My sequencing results for a ~600-bp region including the RIP-3 binding region did not detect any of the SNPs associated with earliness that were reported in Kippes et al. (2015). Both parents aligned exactly to each other and with the *vrn-A1* sequence of winter wheat cultivars 'Hereward' (JF965397.1) and 'Malacca' (JF965396.1). Therefore, disruption of the RIP-3 binding site is not responsible for the early responsiveness to vernalization exhibited by SS8641. My

results suggest that SS8641 may possess a previously unreported allele of *vrn-A1* associated with accelerated responsiveness to vernalization.

Another potential genetic cause of the variation in heading date detected in the genomic region of *VRN-A1* that should be explored is variation in the *PHYTOCHROME C* (*PHYC*) gene, which is tightly linked to *VRN-A1* (Chen et al. 2014). At the scale of our QTL mapping analysis, we could not distinctly separate influence from the *VRN-A1* and *PHYC* genes. *PHYC* plays a major regulatory role in accelerating flowering under long day conditions: under long days, tetraploid wheat plants homozygous for loss-of-function mutations in both *PHYC* copies flowered on average 108 days later than wild-type plants (Chen et al. 2014). My greenhouse experiment used long-day photoperiod conditions (16 h), so it is possible that allelic variation in *PHYC* caused the variation in heading date in this genomic region. However, the strong influence of vernalization, with the QTL being strongest in shortly-vernalized treatments, still suggests that allelic variation in *VRN-A1* is the likeliest cause.

Conclusions and Future Directions

This study characterized flowering time in a DH population, focusing on three different genes known to regulate flowering time in wheat, *Ppd-A1*, *Ppd-D1*, and *VRN-A1*. I found that *Ppd-D1* and *Ppd-A1* both have greater effects than *VRN-A1* under field conditions/environments tested, likely because all vernalization requirements were met. Among photoperiod effects, variation in heading date was

explained about twice as much by *Ppd-D1* than by *Ppd-A1*, but insensitivity from both alleles combined provided the earliest flowering time. Earlier flowering time was strongly correlated with increased yield at three of five locations where yield plots were grown. When the population was grown in the greenhouse with four weeks of vernalization, 42.4% of variation in heading date was explained by a genomic region of chromosome 5A containing *VRN-A1*. This suggests that there is polymorphism between the parents of the population at this locus. However, no polymorphism was detected between MD233 and SS8641 using several assays and methods previously described for allelic diversity in this region.

I hypothesize that there is polymorphism within the genomic sequence of the *VRN-A1* gene associated with the difference in heading date that has not yet been detected in this study, likely in the promoter region or first intron. To further investigate this, I propose doing a qRT-PCR assay to quantify the expression of *VRN-A1* in MD233, SS8641, and early and late DH lines, in plants given 0-weeks and 4-weeks of vernalization. If there are significant differences in *VRN-A1* expression between parents and early/late lines, this would confirm that the difference in heading date associated with this region is caused by polymorphism in *VRN-A1*. In that case, it would be useful to fully sequence the *VRN-A1* gene of both parents to detect the polymorphism and develop a diagnostic marker that could be used to assay breeding materials for the presence of the short-vernalization *VRN-A1* allele present in SS8641.

Appendix

Appendix 1. Marker names with corresponding original names and marker types. GBS names include chromosome, contig, and position within contigs. Contig information can be found in the URGI wheat survey sequence. Map positions were calculated using ICIMapping.

Marker Name	Original name	Marker Type	Chromosome	Position
Xwmc496	wmc496Nd	SSR	1A	0
Xsnp1970	1AL_3962319_3787	GBS	1A	0.86
Xbarc28	barc28Fd	SSR	1A	1.7
Xsnp2005	1AL_3980322_212	GBS	1A	13.57
Xsnp1999	1AL_3977509_3331	GBS	1A	14.44
Xsnp2129	1BL_3887627_66476923	GBS	1A	15.33
Xsnp1997	1AL_3977305_7017	GBS	1A	18.17
Xsnp1855	1AL_3887831_1334	GBS	1A	19.09
Xsnp939	IWA4538	9kSNP	1A	20.77
Xsnp1452	IWA6934	9kSNP	1A	21.58
Xsnp1895	1AL_3913666_5712	GBS	1A	22.42
Xsnp1983	1AL_3974671_4753	GBS	1A	23.28
Xsnp1943	1AL_3950628_1605	GBS	1A	28.06
Xsnp1834	1AL_3870162_3374	GBS	1A	29.97
Xsnp2001	1AL_3978061_4251	GBS	1A	30.98
Xsnp1953	1AL_3953856_4923	GBS	1A	36.89
Xsnp1940	1AL_3948476_6940	GBS	1A	37.69
Xsnp1993	1AL_3977030_86	GBS	1A	38.7
Xsnp1316	IWA6152	9kSNP	1A	41.16
Xsnp1977	1AL_3969959_2032	GBS	1A	43.64
Xsnp1840	1AL_3873756_1633	GBS	1A	48.66
Xsnp1889	1AL_3907913_15073	GBS	1A	50.37
Xsnp1862	1AL_3891249_1544	GBS	1A	51.27
Xsnp1823	1AL_2936299_1558	GBS	1A	53.84
Xsnp1931	1AL_3941071_3672	GBS	1A	54.83
Xsnp1986	1AL_3975469_1517	GBS	1A	55.64
Xsnp1996	1AL_3977287_1198	GBS	1A	58.73
Xsnp1950	1AL_3952293_6360	GBS	1A	59.6
Xsnp1868	1AL_3894014_3875	GBS	1A	62.28
Xsnp1995	1AL_3977278_1163	GBS	1A	63.19
Xsnp2227	1DL_2206847_14787	GBS	1A	67.71
Xsnp2477	2AS_5308609_11662	GBS	2A	0
Xsnp2432	2AS_5218356_643	GBS	2A	2.68

Marker Name	Original name	Marker Type	Chromosome	Position
Xsnp4490	6DL_3328699_11778	GBS	2A	8.06
Xsnp2445	2AS_5254682_4662	GBS	2A	9.11
Xsnp2480	2AS_5309087_9086	GBS	2A	15.27
Xsnp2471	2AS_5306357_2235	GBS	2A	16.1
XPpdA1	Ppd-A1prodel	KASP	2A	16.92
Xsnp2461	2AS_5289049_8858	GBS	2A	19.51
Xsnp2466	2AS_5302874_2821	GBS	2A	24.7
Xsnp2427	2AS_5204705_2355	GBS	2A	25.53
Xsnp2479	2AS_5309065_8848	GBS	2A	27.23
Xsnp2423	2AS_5196777_2088	GBS	2A	28.21
Xsnp1327	IWA6250	9kSNP	2A	31.04
Xsnp2481	2AS_5310156_1591	GBS	2A	33.56
Xsnp2436	2AS_5228280_4935	GBS	2A	36.32
Xsnp2448	2AS_5260825_4791	GBS	2A	41.7
Xsnp2475	2AS_5307952_3491	GBS	2A	49.38
Xsnp2431	2AS_5217292_209	GBS	2A	50.24
Xsnp87	IWA534	9kSNP	2A	51.08
Xsnp2323	2AL_6357025_932	GBS	2A	51.94
Xsnp768	IWA3842	9kSNP	2A	52.8
Xsnp2400	2AL_6437618_10530	GBS	2A	53.72
Xsnp2268	2AL_5107209_192	GBS	2A	55.7
Xsnp2366	2AL_6407053_3453	GBS	2A	56.74
Xsnp2320	2AL_6354607_3366	GBS	2A	57.76
Xsnp2404	2AL_6439119_6478	GBS	2A	59.47
Xsnp2377	2AL_6427513_2027	GBS	2A	60.29
Xsnp81	IWA510	9kSNP	2A	63.55
Xsnp2409	2AL_6439975_20430	GBS	2A	66.33
Xsnp2390	2AL_6435732_3539	GBS	2A	69.19
Xsnp2351	2AL_6388541_5469	GBS	2A	70.05
Xsnp2277	2AL_6316154_6468	GBS	2A	71.79
Xsnp2372	2AL_6420089_5912	GBS	2A	73.54
Xsnp2394	2AL_6435992_27	GBS	2A	74.43
Xsnp2375	2AL_6422946_2164	GBS	2A	78.28
Xsnp2365	2AL_6405818_6387	GBS	2A	79.33
Xsnp2382	2AL_6433528_540	GBS	2A	84.11
Xsnp2401	2AL_6437689_8365	GBS	2A	85.96
Xsnp2339	2AL_6376905_3016	GBS	2A	88.88
Xsnp2397	2AL_6436455_8982	GBS	2A	89.87
Xsnp2381	2AL_6431038_4873	GBS	2A	91.97

Marker Name	Original name	Marker Type	Chromosome	Position
Xsnp2321	2AL_6355802_8344	GBS	2A	92.9
Xsnp2313	2AL_6350115_2943	GBS	2A	97.15
Xsnp2405	2AL_6439487_9872	GBS	2A	98
Xsnp2406	2AL_6439895_1953	GBS	2A	99.87
Xsnp2363	2AL_6403331_8280	GBS	2A	104.6
Xsnp2315	2AL_6351340_262	GBS	2A	105.47
Xsnp2353	2AL_6390992_49	GBS	2A	108.05
Xsnp2350	2AL_6388048_3408	GBS	2A	108.99
Xsnp2383	2AL_6433629_4880	GBS	2A	109.94
Xsnp2337	2AL_6375566_7626	GBS	2A	110.87
Xsnp2355	2AL_6392472_4146	GBS	2A	111.9
Xsnp2360	2AL_6399661_321	GBS	2A	114.73
Xsnp2362	2AL_6401647_9090	GBS	2A	116.4
Xsnp494	IWA2555	9kSNP	2A	117.22
Xsnp2291	2AL_6330122_7889	GBS	2A	119.7
Xsnp2398	2AL_6437051_2639	GBS	2A	121.4
Xsnp533	IWA2777	9kSNP	2A	123.92
Xsnp3027	3AS_3319009_4498	GBS	3A	0
Xsnp3744	4DL_14114663_56	GBS	3A	0.92
Xsnp3048	3AS_3398062_644	GBS	3A	1.76
Xsnp1466	IWA6977	9kSNP	3A	3.58
Xsnp3049	3AS_3406572_1568	GBS	3A	4.39
Xsnp3021	3AS_3301696_5508	GBS	3A	8.79
Xsnp3059	3AS_3441390_2410	GBS	3A	12.46
Xbarc12	barc12Fd	SSR	3A	13.41
Xsnp3008	3AS_2984591_1278	GBS	3A	14.26
Xsnp2993	3AS_538169_821	GBS	3A	23.18
Xsnp1522	IWA7259	9kSNP	3A	25.1
Xsnp3034	3AS_3355869_8917	GBS	3A	26.74
Xsnp3051	3AS_3418807_1186	GBS	3A	27.73
Xsnp3046	3AS_3390719_201	GBS	3A	28.57
Xsnp3064	3AS_3444703_1047	GBS	3A	31.37
Xsnp3040	3AS_3369915_9060	GBS	3A	32.24
Xsnp3094	3B_9868209_66	GBS	3A	33.1
Xsnp3056	3AS_3437041_3033	GBS	3A	33.95
Xsnp3005	3AS_2457382_276	GBS	3A	34.91
Xsnp3041	3AS_3369973_1380	GBS	3A	45.05
Xsnp2988	3AL_4452804_2208	GBS	3A	79.13
Xsnp3065	3AS_3444782_16976	GBS	3A	115.24

Marker Name	Original name	Marker Type	Chromosome	Position
Xbarc45	barc45Fd	SSR	3A	120.95
Xsnp3037	3AS_3361063_2705	GBS	3A	123.56
Xsnp3023	3AS_3304799_139	GBS	3A	124.4
Xsnp3383	3B_10760555_4469	GBS	3A	126.11
Xsnp3009	3AS_3140772_113	GBS	3A	127.01
Xsnp3052	3AS_3419527_1124	GBS	3A	127.84
Xsnp758	IWA3794	9kSNP	3A	128.65
Xsnp310	IWA1699	9kSNP	3A	129.45
Xsnp4288	6AS_4426056_2566	GBS	3A	131.98
Xsnp1758	IWA8435	9kSNP	3A	134.68
Xsnp1485	IWA7073	9kSNP	3A	136.29
Xsnp2964	3AL_4406528_3920	GBS	3A	137.1
Xsnp2885	3AL_471273_270	GBS	3A	142.07
Xsnp2987	3AL_4452778_444	GBS	3A	143.03
Xsnp2937	3AL_4354018_2106	GBS	3A	144.02
Xsnp4728	7AS_4240223_294	GBS	3A	147.91
Xsnp2968	3AL_4413928_107	GBS	3A	148.86
Xsnp443	IWA2362	9kSNP	3A	152.44
Xsnp2927	3AL_4326475_1019	GBS	3A	153.25
Xsnp2924	3AL_4319573_1631	GBS	3A	154.1
Xsnp2956	3AL_4385948_401	GBS	3A	155.88
Xsnp2950	3AL_4374565_1515	GBS	3A	159.31
Xsnp3313	3B_10683732_816	GBS	3A	160.17
Xsnp2977	3AL_4447320_219	GBS	3A	161.02
Xsnp2900	3AL_4235146_125	GBS	3A	161.89
Xsnp2973	3AL_4441348_1055	GBS	3A	162.85
Xsnp2989	3AL_4454539_1757	GBS	3A	167.97
Xsnp2983	3AL_4449191_960	GBS	3A	169.8
Xsnp2990	3AL_4456364_278	GBS	3A	173.94
Xsnp2905	3AL_4249917_1899	GBS	3A	179.73
Xsnp2979	3AL_4448404_3263	GBS	3A	180.66
Xsnp445	IWA2372	9kSNP	3A	181.49
Xsnp2984	3AL_4451049_2150	GBS	3A	187.83
Xsnp2934	3AL_4352445_3732	GBS	3A	188.69
Xsnp2970	3AL_4416797_4181	GBS	3A	189.54
Xsnp2920	3AL_4305396_1063	GBS	3A	197.45
Xsnp2960	3AL_4391858_3335	GBS	3A	200.45
Xsnp2948	3AL_4370942_771	GBS	3A	201.43
Xsnp2951	3AL_4378466_9399	GBS	3A	206.45

Marker Name	Original name	Marker Type	Chromosome	Position
Xsnp2971	3AL_4419050_1730	GBS	3A	215.86
Xsnp2909	3AL_4263029_395	GBS	3A	216.84
Xsnp3634	4AS_6011855_802	GBS	4A	0
Xsnp3632	4AS_6010640_35237	GBS	4A	1.92
Xsnp3623	4AS_5971673_14471	GBS	4A	10.56
Xsnp1057	IWA4981	9kSNP	4A	13.12
Xsnp3614	4AS_5934912_3551	GBS	4A	19.03
Xsnp3636	4AS_6013627_24611	GBS	4A	48.96
Xsnp3576	4AL_7169775_2147	GBS	4A	51.53
Xsnp3508	4AL_7103930_9565	GBS	4A	52.39
Xsnp3637	4AS_6014112_1611	GBS	4A	53.39
Xsnp3590	4AL_7173814_6086	GBS	4A	54.25
Xsnp3444	4AL_3841322_2777	GBS	4A	58.34
Xsnp318	IWA1720	9kSNP	4A	80.68
Xsnp309	IWA1692	9kSNP	4A	81.49
Xsnp3604	4AL_7175497_315	GBS	4A	84.08
Xbarc170	barc170Pd	SSR	4A	84.95
Xsnp836	IWA4142	9kSNP	4A	88.18
Xsnp3566	4AL_7157490_6094	GBS	4A	93.76
Xsnp3597	4AL_7174549_3892	GBS	4A	94.72
Xsnp910	IWA4425	9kSNP	4A	97.5
Xsnp3545	4AL_7140513_2820	GBS	4A	99.37
Xsnp3573	4AL_7163808_8551	GBS	4A	100.28
Xsnp3574	4AL_7167769_1762	GBS	4A	102.94
Xsnp753	IWA3756	9kSNP	4A	103.79
Xsnp3551	4AL_7143684_1192	GBS	4A	104.63
Xsnp3490	4AL_7090465_7483	GBS	4A	105.53
Xsnp3595	4AL_7174083_3024	GBS	4A	111.62
Xsnp3462	4AL_7063503_8494	GBS	4A	114.19
Xsnp3572	4AL_7161240_7897	GBS	4A	115.12
Xsnp3568	4AL_7158864_3727	GBS	4A	116.07
Xsnp3608	4AL_7176389_26698	GBS	4A	116.92
Xsnp3535	4AL_7129067_4737	GBS	4A	121.52
Xsnp3447	4AL_5262151_1457	GBS	4A	122.54
Xsnp3464	4AL_7064270_2484	GBS	4A	135.31
Xsnp3547	4AL_7140728_9572	GBS	4A	138.38
Xsnp3606	4AL_7175623_18776	GBS	4A	139.25
Xsnp3575	4AL_7168953_2823	GBS	4A	140.24
Xsnp3542	4AL_7138052_166	GBS	4A	142.02

Marker Name	Original name	Marker Type	Chromosome	Position
Xsnp3488	4AL_7088131_1401	GBS	4A	146.5
Xsnp3607	4AL_7176109_4853	GBS	4A	154.74
Xsnp3486	4AL_7088065_3379	GBS	4A	155.68
Xsnp3602	4AL_7175161_2771	GBS	4A	156.57
Xsnp3512	4AL_7106133_7959	GBS	4A	157.43
Xsnp4975	7DS_3949538_3306	GBS	4A	158.28
Xsnp3874	5AS_1519130_167	GBS	5A	0
Xsnp3872	5AS_1513496_11975	GBS	5A	1.98
Xsnp3869	5AS_1464255_7054	GBS	5A	5.02
Xsnp3879	5AS_1547910_486	GBS	5A	6.8
Xsnp3877	5AS_1528895_1701	GBS	5A	15.75
Xsnp621	IWA3197	9kSNP	5A	20.76
Xsnp1749	IWA8356	9kSNP	5A	21.58
Xsnp1368	IWA6463	9kSNP	5A	22.38
Xsnp279	IWA1569	9kSNP	5A	24
Xsnp3878	5AS_1542667_723	GBS	5A	48.68
Xsnp617	IWA3190	9kSNP	5A	50.35
Xsnp842	IWA4149	9kSNP	5A	51.97
Xsnp218	IWA1301	9kSNP	5A	52.79
Xsnp49	IWA333	9kSNP	5A	53.59
Xgwm304	gwm304Fd	SSR	5A	54.41
Xsnp996	IWA4736	9kSNP	5A	55.31
Xsnp3837	5AL_2791539_9640	GBS	5A	56.15
Xsnp3838	5AL_2793993_2759	GBS	5A	57.13
Xbarc100	barc100Fd	SSR	5A	59.99
Xsnp4843	7BL_6718065_1071	GBS	5A	67.26
Xsnp3819	5AL_2755881_3156	GBS	5A	68.25
Xsnp3789	5AL_2678682_64	GBS	5A	71.22
Xsnp3844	5AL_2798538_722	GBS	5A	77.06
Xsnp3851	5AL_2805861_1111	GBS	5A	77.93
Xsnp4167	5DL_4584184_14443	GBS	5A	78.9
Xsnp3760	5AL_460494_596	GBS	5A	79.86
Xsnp3839	5AL_2794409_6138	GBS	5A	80.92
Xsnp3812	5AL_2748687_5315	GBS	5A	81.96
Xsnp3856	5AL_2807652_8947	GBS	5A	83.94
Xsnp3776	5AL_1881421_4336	GBS	5A	84.89
Xsnp3852	5AL_2806281_983	GBS	5A	85.81
Xsnp3843	5AL_2797497_3896	GBS	5A	86.65

Marker Name	Original name	Marker Type	Chromosome	Position
Xsnp3820	5AL_2758417_1165	GBS	5A	87.54
Xsnp2008	1AS_612486_1691	GBS	5A	94.06
Xsnp4472	6DL_3218827_3531	GBS	5A	97.91
Xsnp3855	5AL_2807509_1664	GBS	5A	98.79
Xsnp856	IWA4207	9kSNP	5A	99.6
Xsnp3867	5AL_2812590_39455	GBS	5A	101.24
Xsnp3836	5AL_2788883_2077	GBS	5A	102.06
Xsnp3833	5AL_2784434_4621	GBS	5A	102.9
Xsnp3863	5AL_2809951_162	GBS	5A	107.37
Xsnp3845	5AL_2803630_4943	GBS	5A	108.24
Xsnp3865	5AL_2811200_3157	GBS	5A	125.37
Xsnp3802	5AL_2739429_4461	GBS	5A	127.06
Xsnp3783	5AL_2670044_1359	GBS	5A	129
Xsnp3859	5AL_2808837_1616	GBS	5A	134.4
Xsnp3853	5AL_2806290_2571	GBS	5A	136.06
Xsnp3835	5AL_2787690_1567	GBS	5A	143.12
Xsnp3761	5AL_630370_6383	GBS	5A	165.57
Xsnp3862	5AL_2809320_1256	GBS	5A	170.5
Xsnp3787	5AL_2673208_4938	GBS	5A	171.34
Xsnp663	IWA3391	9kSNP	5A	172.2
Xsnp3747	4DL_14325871_3401	GBS	5A	173.96
Xsnp3849	5AL_2805844_635	GBS	5A	176.59
Xsnp3841	5AL_2795190_2671	GBS	5A	186.19
Xsnp3803	5AL_2739515_6175	GBS	5A	187.02
Xsnp3775	5AL_1841010_125	GBS	5A	187.95
Xsnp3860	5AL_2809039_6225	GBS	5A	190.04
Xsnp4296	6AS_4429106_3407	GBS	6A	0
Xsnp4276	6AS_4399358_1451	GBS	6A	13.66
Xsnp4243	6AS_4344367_2948	GBS	6A	19.95
Xsnp4298	6AS_4429679_3186	GBS	6A	20.83
Xsnp4271	6AS_4393178_1994	GBS	6A	23.59
Xsnp4435	6BS_3017345_790	GBS	6A	25.59
Xsnp4280	6AS_4406278_1705	GBS	6A	27.76
Xsnp4247	6AS_4349633_8257	GBS	6A	28.63
Xsnp4259	6AS_4367214_4457	GBS	6A	36.95
Xsnp4286	6AS_4414744_1278	GBS	6A	37.94
Xsnp4290	6AS_4428136_1099	GBS	6A	38.86
Xsnp4299	6AS_4431389_7433	GBS	6A	40.85
Xsnp4245	6AS_4345745_12203	GBS	6A	41.65

Marker Name	Original name	Marker Type	Chromosome	Position
Xsnp367	IWA1956	9kSNP	6A	42.49
Xsnp4278	6AS_4403930_3409	GBS	6A	43.29
Xsnp4489	6DL_3320513_3120	GBS	6A	44.27
Xsnp4265	6AS_4383134_9547	GBS	6A	45.14
Xsnp4183	6AL_5706007_1624	GBS	6A	45.96
Xsnp4216	6AL_5820289_1958	GBS	6A	47.62
Xsnp4217	6AL_5822404_1804	GBS	6A	49.34
Xsnp4226	6AL_5831789_1113	GBS	6A	50.2
Xsnp4225	6AL_5831597_5940	GBS	6A	51.13
Xsnp4211	6AL_5801261_10328	GBS	6A	51.93
Xsnp4186	6AL_5747296_6651	GBS	6A	75.04
Xsnp4222	6AL_5830501_7494	GBS	6A	78.31
Xsnp492	IWA2539	9kSNP	6A	79.92
Xsnp4197	6AL_5774271_4179	GBS	6A	80.77
Xsnp473	IWA2481	9kSNP	6A	81.62
Xsnp4228	6AL_5833398_2845	GBS	6A	83.23
Xsnp4219	6AL_5828239_2711	GBS	6A	92.6
Xsnp70	IWA442	9kSNP	6A	93.42
Xsnp4364	6BL_4400867_516	GBS	6A	94.22
Xsnp4207	6AL_5795879_1254	GBS	6A	95.05
Xsnp4725	7AS_4238512_3061	GBS	7A	0
Xsnp4766	7AS_4253469_222	GBS	7A	2.11
Xsnp1398	IWA6642	9kSNP	7A	3.01
Xsnp4732	7AS_4244678_1009	GBS	7A	3.9
Xsnp4779	7AS_4256951_10891	GBS	7A	5.6
Xsnp4764	7AS_4252764_11481	GBS	7A	6.45
Xsnp4752	7AS_4249067_2709	GBS	7A	7.45
Xsnp4717	7AS_4222765_2598	GBS	7A	8.42
Xsnp4736	7AS_4245898_2288	GBS	7A	9.32
Xsnp4723	7AS_4236024_838	GBS	7A	10.33
Xsnp4727	7AS_4239160_8874	GBS	7A	12.77
Xsnp4665	7AS_2072047_1105	GBS	7A	13.6
Xsnp4682	7AS_4107657_565	GBS	7A	14.55
Xsnp4718	7AS_4224058_429	GBS	7A	15.51
Xsnp4759	7AS_4251617_1228	GBS	7A	18.09
Xsnp4771	7AS_4253880_1441	GBS	7A	25.7
Xsnp4773	7AS_4254599_64	GBS	7A	26.63
Xsnp4777	7AS_4256424_440	GBS	7A	31.07
Xsnp4741	7AS_4246617_2852	GBS	7A	32.89

Marker Name	Original name	Marker Type	Chromosome	Position
Xsnp4739	7AS_4246389_3735	GBS	7A	35.41
Xsnp4697	7AS_4183259_787	GBS	7A	36.48
Xsnp4768	7AS_4253633_1895	GBS	7A	37.6
Xsnp1302	IWA6088	9kSNP	7A	38.54
Xsnp4762	7AS_4252748_1108	GBS	7A	39.37
Xsnp4754	7AS_4250432_1538	GBS	7A	46.63
Xsnp4734	7AS_4244795_3943	GBS	7A	47.54
Xsnp4667	7AS_4050162_593	GBS	7A	48.47
Xsnp4715	7AS_4221213_1765	GBS	7A	49.32
Xsnp4722	7AS_4235586_1908	GBS	7A	50.17
Xsnp4690	7AS_4172444_990	GBS	7A	51.02
Xsnp4668	7AS_4050568_393	GBS	7A	51.87
Xsnp4749	7AS_4248307_2865	GBS	7A	53.64
Xsnp324	IWA1751	9kSNP	7A	54.52
Xbarc127	barc127Vd	SSR	7A	55.34
Xsnp1376	IWA6507	9kSNP	7A	57.08
Xsnp4745	7AS_4246978_1250	GBS	7A	58.8
Xsnp4774	7AS_4255252_1667	GBS	7A	59.73
Xsnp4767	7AS_4253483_3267	GBS	7A	60.76
Xsnp4763	7AS_4252760_13498	GBS	7A	61.61
Xsnp4746	7AS_4247020_4843	GBS	7A	71.75
Xsnp4675	7AS_4073295_163	GBS	7A	73.57
Xsnp4776	7AS_4256393_3907	GBS	7A	77.71
Xsnp849	IWA4181	9kSNP	7A	78.54
Xsnp4775	7AS_4256219_6243	GBS	7A	80.96
Xsnp1553	IWA7419	9kSNP	7A	84.45
Xsnp1674	IWA7942	9kSNP	7A	85.25
Xsnp4770	7AS_4253826_1634	GBS	7A	86.87
Xsnp4733	7AS_4244756_7038	GBS	7A	88.52
Xsnp4758	7AS_4251365_5387	GBS	7A	90.24
Xsnp4757	7AS_4251205_1192	GBS	7A	91.21
Xsnp4761	7AS_4252699_2366	GBS	7A	92.15
Xsnp4772	7AS_4254221_72	GBS	7A	94.81
Xsnp4547	7AL_4432944_1558	GBS	7A	95.72
Xsnp4535	7AL_4373898_4825	GBS	7A	96.61
Xsnp4660	7AL_4561213_3219	GBS	7A	101.02
Xsnp4637	7AL_4554227_5600	GBS	7A	103
Xsnp4567	7AL_4466188_3090	GBS	7A	105.35
Xsnp4946	7DL_3367231_172	GBS	7A	106.27

Marker Name	Original name	Marker Type	Chromosome	Position
Xsnp4546	7AL_4432236_469	GBS	7A	107.1
Xsnp4624	7AL_4550762_896	GBS	7A	107.9
Xsnp4612	7AL_4539901_1981	GBS	7A	109.63
Xsnp1385	IWA6562	9kSNP	7A	110.46
Xsnp4523	7AL_1108355_364	GBS	7A	112.13
Xsnp4584	7AL_4485479_10037	GBS	7A	113
Xsnp4935	7DL_3320969_21094	GBS	7A	114.74
Xsnp4622	7AL_4549513_434	GBS	7A	115.69
Xsnp4639	7AL_4554415_13489	GBS	7A	117.39
Xsnp1181	IWA5489	9kSNP	7A	118.34
Xsnp321	IWA1725	9kSNP	7A	119.95
Xsnp4593	7AL_4500731_8231	GBS	7A	120.76
Xsnp4588	7AL_4492038_5593	GBS	7A	121.62
Xsnp4620	7AL_4546220_912	GBS	7A	123.29
Xgwm282	gwm282Pd	SSR	7A	124.13
Xsnp4563	7AL_4457312_294	GBS	7A	127.64
Xsnp4936	7DL_3331520_593	GBS	7A	129.32
Xsnp4602	7AL_4512458_22643	GBS	7A	137.23
Xsnp4659	7AL_4560757_4741	GBS	7A	138.06
Xsnp4658	7AL_4558219_441	GBS	7A	139.02
Xsnp4606	7AL_4530188_6012	GBS	7A	149.06
Xsnp4570	7AL_4471025_1016	GBS	7A	150.82
Xsnp4623	7AL_4549909_2675	GBS	7A	152.57
Xsnp4536	7AL_4386143_534	GBS	7A	154.24
Xsnp4556	7AL_4445689_979	GBS	7A	155.06
Xsnp4557	7AL_4446013_813	GBS	7A	156.2
Xsnp4947	7DL_3373580_5763	GBS	7A	159.06
Xsnp1727	IWA8204	9kSNP	7A	159.94
Xsnp4608	7AL_4532833_2327	GBS	7A	160.89
Xwmc273	wmc273Fd	SSR	7A	167.37
Xsnp4655	7AL_4557387_2760	GBS	7A	170.66
Xsnp4643	7AL_4555463_1359	GBS	7A	171.5
Xsnp2200	1BS_3467668_3931	GBS	1B	0
Xsnp2221	1BS_3484468_10138	GBS	1B	0.93
Xsnp2217	1BS_3484067_14330	GBS	1B	3.81
Xsnp2205	1BS_3477882_7381	GBS	1B	7.78
Xsnp4503	6DS_2071140_3886	GBS	1B	12.38
Xsnp2181	1BS_3458552_2656	GBS	1B	18.5
Xsnp2218	1BS_3484153_4290	GBS	1B	19.38

Marker Name	Original name	Marker Type	Chromosome	Position
Xsnp2180	1BS_3458076_11479	GBS	1B	21.27
Xsnp2209	1BS_3482301_1437	GBS	1B	22.11
Xsnp2186	1BS_3459873_17200	GBS	1B	23.09
Xsnp2206	1BS_3480191_3942	GBS	1B	24.19
Xsnp2213	1BS_3482821_1928	GBS	1B	25.09
Xsnp1707	IWA8084	9kSNP	1B	30.94
Xgwm11	gwm11Pd	SSR	1B	31.87
Xsnp2071	1BL_3809495_103089202	GBS	1B	32.84
Xsnp767	IWA3837	9kSNP	1B	33.8
Xsnp2130	1BL_3889244_64749925	GBS	1B	34.61
Xsnp2073	1BL_3809495_117686160	GBS	1B	39.55
Xsnp2110	1BL_3855100_76178312	GBS	1B	49.19
Xsnp854	IWA4198	9kSNP	1B	50.01
Xsnp2121	1BL_3876159_73759641	GBS	1B	50.81
Xsnp2053	1BL_2970142_13728132	GBS	1B	52.68
Xsnp2132	1BL_3893620_70537839	GBS	1B	54.54
Xsnp2092	1BL_3813560_79583224	GBS	1B	58.86
Xsnp2064	1BL_3798857_60461582	GBS	1B	59.73
Xsnp2087	1BL_3809495_61566497	GBS	1B	60.55
Xsnp2115	1BL_3865925_75214146	GBS	1B	61.39
Xsnp2117	1BL_3868800_74155622	GBS	1B	63.12
Xsnp2080	1BL_3809495_20302209	GBS	1B	63.97
Xsnp2114	1BL_3861063_74831512	GBS	1B	64.91
Xsnp3227	3B_10575480_10462	GBS	1B	66.78
Xsnp2128	1BL_3886594_67200727	GBS	1B	67.71
Xsnp2126	1BL_3885136_66354414	GBS	1B	68.58
Xsnp4928	7BS_3165082_107	GBS	1B	71.19
Xsnp2107	1BL_3850458_73461928	GBS	1B	74.13
Xsnp2106	1BL_3850458_73460439	GBS	1B	75.08
Xsnp2084	1BL_3809495_31590257	GBS	1B	84.54
Xsnp2113	1BL_3857019_75864099	GBS	1B	86.25
Xsnp2091	1BL_3809802_79375982	GBS	1B	87.13
Xsnp2052	1BL_2500121_12277290	GBS	1B	87.94
Xsnp1777	IWA8542	9kSNP	1B	117.37
Xsnp2059	1BL_3795374_41583290	GBS	1B	124.77
Xsnp2131	1BL_3892683_69588750	GBS	1B	125.64
Xsnp2116	1BL_3867808_74689679	GBS	1B	128.88
Xsnp2067	1BL_3802551_64689280	GBS	1B	133.23
Xsnp2127	1BL_3886068_66500558	GBS	1B	141.65

Marker Name	Original name	Marker Type	Chromosome	Position
Xbarc80	barc80Vd	SSR	1B	144.13
Xsnp2779	2BS_5243472_3117	GBS	2B	0
Xsnp2750	2BS_5206442_3261	GBS	2B	0.89
Xsnp2771	2BS_5239924_12595	GBS	2B	10.17
Xsnp2780	2BS_5245350_1701	GBS	2B	17.29
Xsnp3734	4BS_4904601_1034	GBS	2B	19.9
Xsnp2743	2BS_5198867_18223	GBS	2B	24.68
Xsnp456	IWA2407	9kSNP	2B	25.51
Xsnp746	IWA3722	9kSNP	2B	33.65
Xsnp2785	2BS_5246460_6069	GBS	2B	34.46
Xsnp2778	2BS_5242975_9575	GBS	2B	36.2
Xsnp2769	2BS_5234121_5768	GBS	2B	46.43
Xbarc10	barc10Nd	SSR	2B	47.26
Xsnp2744	2BS_5200256_4769	GBS	2B	58.33
Xsnp774	IWA3868	9kSNP	2B	59.14
Xsnp2705	2BS_3514149_4373	GBS	2B	60.04
Xsnp2752	2BS_5211499_1299	GBS	2B	61.14
Xsnp2786	2BS_5247378_16667	GBS	2B	62.24
Xsnp2777	2BS_5242970_3502	GBS	2B	63.19
Xsnp2773	2BS_5242129_6102	GBS	2B	64.05
Xgwm319	gwm319Vd	SSR	2B	66.13
Xsnp2767	2BS_5233701_6070	GBS	2B	66.96
Xsnp2591	2BL_8018724_14746	GBS	2B	69.02
Xsnp2569	2BL_7993505_9892	GBS	2B	70.93
Xsnp2688	2BL_8090690_11510	GBS	2B	71.8
Xsnp2697	2BL_8092406_5191	GBS	2B	72.62
Xsnp2598	2BL_8026857_2110	GBS	2B	74.23
Xsnp2686	2BL_8089568_16543	GBS	2B	75.07
Xsnp2635	2BL_8061064_1749	GBS	2B	76.92
Xsnp2646	2BL_8071971_14150	GBS	2B	77.8
Xsnp2607	2BL_8033452_7955	GBS	2B	78.61
Xsnp3413	3B_10772655_4568	GBS	2B	79.48
Xsnp2659	2BL_8079933_5233	GBS	2B	80.35
Xsnp2698	2BL_8092457_7836	GBS	2B	82.04
Xsnp2571	2BL_7993650_114	GBS	2B	86.36
Xsnp2667	2BL_8084207_8316	GBS	2B	87.44
Xsnp2668	2BL_8084228_12492	GBS	2B	88.26
Xsnp2696	2BL_8092402_18755	GBS	2B	89.11
Xsnp2515	2BL_7944092_5682	GBS	2B	89.99

Marker Name	Original name	Marker Type	Chromosome	Position
Xsnp2515	2BL_7944092_5682	GBS	2B	89.99
Xsnp1176	IWA5460	9kSNP	2B	90.84
Xsnp2694	2BL_8092363_4315	GBS	2B	92.53
Xsnp2648	2BL_8072178_2131	GBS	2B	93.51
Xsnp2615	2BL_8042673_1160	GBS	2B	94.5
Xsnp2682	2BL_8089334_583	GBS	2B	95.53
Xsnp2619	2BL_8044149_1112	GBS	2B	97.41
Xsnp2670	2BL_8084644_3918	GBS	2B	98.31
Xsnp2523	2BL_7946466_1428	GBS	2B	100.16
Xsnp2620	2BL_8044538_4111	GBS	2B	102.05
Xsnp2665	2BL_8083153_1876	GBS	2B	103.82
Xsnp2633	2BL_8059131_6835	GBS	2B	105.8
Xsnp2614	2BL_8039831_30516	GBS	2B	107.72
Xsnp2649	2BL_8072721_11163	GBS	2B	109.85
Xsnp2585	2BL_8011702_3034	GBS	2B	115.94
Xsnp681	IWA3474	9kSNP	2B	116.78
Xsnp2666	2BL_8084010_12487	GBS	2B	119.41
Xsnp2723	2BS_5174017_1762	GBS	2B	122.07
Xsnp2574	2BL_7995697_7525	GBS	2B	123.72
Xsnp448	IWA2377	9kSNP	2B	125.36
Xsnp2603	2BL_8030377_647	GBS	2B	130.28
Xsnp2586	2BL_8011970_1993	GBS	2B	132.26
Xsnp2600	2BL_8028363_11925	GBS	2B	133.93
Xsnp2679	2BL_8087489_6421	GBS	2B	134.84
Xsnp2599	2BL_8027088_1327	GBS	2B	137.06
Xsnp2802	2DL_9842762_4578	GBS	2B	138.1
Xsnp2496	2BL_7897228_15139	GBS	2B	138.99
Xsnp2663	2BL_8082340_6500	GBS	2B	139.83
Xsnp3074	3B_4479612_412	GBS	3B	0
Xsnp599	IWA3103	9kSNP	3B	1.72
Xsnp3407	3B_10767253_14045	GBS	3B	4.25
Xbarc147	barc147Nd	SSR	3B	5.05
Xsnp3328	3B_10699215_3620	GBS	3B	9.15
Xsnp3421	3DL_6939290_326	GBS	3B	13.5
Xsnp3318	3B_10689659_456	GBS	3B	15.45
Xsnp3156	3B_10475931_978	GBS	3B	17.37
Xsnp3404	3B_10765972_8647	GBS	3B	18.23
Xsnp3411	3B_10771504_818	GBS	3B	19.26
Xsnp3399	3B_10765208_4307	GBS	3B	20.26

Marker Name	Original name	Marker Type	Chromosome	Position
Xsnp3070	3B_3612672_1223	GBS	3B	21.32
Xsnp3288	3B_10649889_464	GBS	3B	22.36
Xsnp3405	3B_10766170_3098	GBS	3B	23.3
Xsnp3389	3B_10762174_1463	GBS	3B	27.16
Xsnp3344	3B_10725169_490	GBS	3B	31.01
Xsnp3253	3B_10610499_1037	GBS	3B	35.33
Xsnp3349	3B_10730729_1056	GBS	3B	41.79
Xsnp3367	3B_10749124_15377	GBS	3B	42.7
Xsnp3320	3B_10691623_2391	GBS	3B	43.5
Xsnp3335	3B_10706474_9184	GBS	3B	44.34
Xsnp3119	3B_10416442_2670	GBS	3B	46.25
Xsnp3395	3B_10763657_1258	GBS	3B	47.27
Xsnp3387	3B_10761943_8766	GBS	3B	48.13
Xsnp3415	3B_10776024_3607	GBS	3B	49.94
Xsnp1539	IWA7353	9kSNP	3B	51.63
Xsnp3408	3B_10767366_9873	GBS	3B	52.44
Xbarc164	barc164Nd	SSR	3B	53.24
Xsnp3205	3B_10551630_648	GBS	3B	55.05
Xsnp3385	3B_10760970_7259	GBS	3B	55.87
Xsnp3146	3B_10454210_856	GBS	3B	56.74
Xsnp3382	3B_10760374_7126	GBS	3B	57.58
Xsnp3372	3B_10757392_10848	GBS	3B	60.88
Xsnp611	IWA3170	9kSNP	3B	61.87
Xsnp3192	3B_10529003_6926	GBS	3B	62.68
Xsnp3381	3B_10759531_14302	GBS	3B	63.63
Xsnp3393	3B_10763186_2310	GBS	3B	64.51
Xsnp3368	3B_10751565_2457	GBS	3B	66.22
Xsnp3153	3B_10470501_10205	GBS	3B	67.1
Xsnp887	IWA4324	9kSNP	3B	68.75
Xsnp3410	3B_10769285_4136	GBS	3B	72.53
Xsnp3416	3B_10776028_6083	GBS	3B	73.41
Xsnp3386	3B_10760995_4122	GBS	3B	74.3
Xsnp3247	3B_10602795_2863	GBS	3B	75.36
Xsnp3312	3B_10683632_6031	GBS	3B	76.22
Xsnp1697	IWA8043	9kSNP	3B	79.62
Xsnp187	IWA1094	9kSNP	3B	80.42
Xsnp3342	3B_10723152_5820	GBS	3B	81.25
Xsnp3112	3B_10397959_8732	GBS	3B	85.57
Xsnp3864	5AL_2811106_3038	GBS	3B	87.33

Marker Name	Original name	Marker Type	Chromosome	Position
Xsnp3299	3B_10668771_462	GBS	3B	88.23
Xsnp3345	3B_10727035_88	GBS	3B	93.05
Xsnp3289	3B_10650537_5714	GBS	3B	93.92
Xsnp3160	3B_10479329_10560	GBS	3B	97.29
Xsnp3174	3B_10497886_16083	GBS	3B	98.11
Xsnp3397	3B_10763720_953	GBS	3B	101.54
Xsnp3417	3B_10777129_7917	GBS	3B	102.42
Xsnp3418	3B_10777870_7419	GBS	3B	107.24
Xsnp3175	3B_10499271_1684	GBS	3B	109.04
Xsnp3401	3B_10765455_669	GBS	3B	128.18
Xsnp3358	3B_10738302_4609	GBS	3B	129.14
Xsnp3400	3B_10765212_4397	GBS	3B	130
Xsnp326	IWA1756	9kSNP	3B	130.93
Xsnp3406	3B_10766972_9821	GBS	3B	131.78
Xsnp3403	3B_10765610_565	GBS	3B	132.78
Xsnp3181	3B_10503783_781	GBS	3B	134
Xsnp3730	4BS_4872427_2077	GBS	4B	0
Xsnp3739	4BS_4943667_6325	GBS	4B	17.14
Xsnp3732	4BS_4885981_3715	GBS	4B	25.92
Xsnp3741	4BS_4955467_2552	GBS	4B	36.93
Xsnp3742	4BS_4959487_4643	GBS	4B	51.62
Xsnp3736	4BS_4914868_9201	GBS	4B	57.59
Xsnp3740	4BS_4949465_4044	GBS	4B	58.74
Xsnp3656	4BL_6964273_1010	GBS	4B	61.1
Xsnp3737	4BS_4921445_8198	GBS	4B	64.16
Xsnp3751	4DL_14470936_8599	GBS	4B	66.75
Xsnp3660	4BL_6970390_1123	GBS	4B	68.46
Xsnp3727	4BL_7041842_9706	GBS	4B	70.17
Xsnp3688	4BL_7008688_477	GBS	4B	71.1
Xsnp3652	4BL_6959768_11162	GBS	4B	72.05
Xsnp3699	4BL_7024693_15741	GBS	4B	73.04
Xsnp3705	4BL_7032318_702	GBS	4B	73.93
Xsnp3721	4BL_7037907_1029	GBS	4B	74.83
Xsnp1656	IWA7854	9kSNP	4B	77.33
Xsnp1430	IWA6808	9kSNP	4B	78.15
Xsnp3729	4BS_1307481_452	GBS	4B	78.96
Xsnp4930	7BS_3166889_15400	GBS	4B	79.93
Xbarc163	barc163Nd	SSR	4B	80.88
Xsnp3638	4BL_369038_75	GBS	4B	81.95

Marker Name	Original name	Marker Type	Chromosome	Position
Xsnp1366	IWA6461	9kSNP	4B	84.61
Xsnp3725	4BL_7040734_12257	GBS	4B	86.39
Xsnp3645	4BL_6850619_728	GBS	4B	88.42
Xsnp3716	4BL_7036878_356	GBS	4B	133.64
Xsnp3711	4BL_7035020_8671	GBS	4B	134.51
Xsnp4140	5BS_2278291_5314	GBS	5B	0
Xsnp4114	5BS_2241856_1193	GBS	5B	0.89
Xsnp4142	5BS_2281878_2847	GBS	5B	11.42
Xsnp48	IWA332	9kSNP	5B	12.23
Xsnp4152	5BS_2294711_10012	GBS	5B	13.84
Xsnp625	IWA3211	9kSNP	5B	15.6
Xsnp4150	5BS_2294326_1146	GBS	5B	16.58
Xsnp4155	5BS_2297920_4611	GBS	5B	17.65
Xsnp4120	5BS_2246258_742	GBS	5B	18.69
Xsnp4130	5BS_2262029_2346	GBS	5B	19.52
Xsnp3884	5BL_3411937_867	GBS	5B	20.33
Xsnp4079	5BL_10922543_7815	GBS	5B	21.24
Xsnp4016	5BL_10876890_4135	GBS	5B	22.12
Xsnp3964	5BL_10834284_8855	GBS	5B	22.97
Xsnp330	IWA1776	9kSNP	5B	24.96
Xsnp3882	5BL_339996_1440	GBS	5B	25.81
Xsnp4168	5DL_4587964_1887	GBS	5B	27.42
Xsnp4028	5BL_10886215_8167	GBS	5B	28.32
Xsnp3901	5BL_10785394_219	GBS	5B	29.47
Xsnp3997	5BL_10861422_6677	GBS	5B	30.47
Xsnp4092	5BL_10926855_30617	GBS	5B	31.3
Xsnp725	IWA3645	9kSNP	5B	32.23
Xsnp4005	5BL_10868635_991	GBS	5B	33.04
Xsnp4018	5BL_10878617_6729	GBS	5B	34.08
Xsnp4014	5BL_10875057_7890	GBS	5B	35.03
Xsnp3975	5BL_10841969_2471	GBS	5B	36.73
Xsnp3963	5BL_10834259_495	GBS	5B	37.68
Xsnp3891	5BL_8633401_2511	GBS	5B	38.77
Xsnp3973	5BL_10841439_11807	GBS	5B	44.9
Xsnp4062	5BL_10917962_4026	GBS	5B	45.92
Xsnp446	IWA2373	9kSNP	5B	46.74
Xsnp4083	5BL_10923028_862	GBS	5B	47.61
Xsnp3988	5BL_10852584_5912	GBS	5B	57.47
Xsnp1006	IWA4793	9kSNP	5B	58.29

Marker Name	Original name	Marker Type	Chromosome	Position
Xsnp823	IWA4103	9kSNP	5B	59.09
Xsnp4059	5BL_10915544_8072	GBS	5B	64.76
Xsnp4061	5BL_10917817_3505	GBS	5B	66.42
Xsnp4027	5BL_10884756_2450	GBS	5B	68.1
Xsnp4017	5BL_10878230_15117	GBS	5B	69.78
Xsnp4049	5BL_10907688_3566	GBS	5B	71.45
Xsnp4090	5BL_10924912_8638	GBS	5B	72.29
Xsnp4060	5BL_10916640_14409	GBS	5B	73.21
Xsnp4072	5BL_10921302_15511	GBS	5B	74.2
Xsnp4085	5BL_10923595_1436	GBS	5B	78.17
Xsnp4058	5BL_10913899_282	GBS	5B	79.15
Xsnp4050	5BL_10908775_610	GBS	5B	80.91
Xsnp4020	5BL_10879329_11196	GBS	5B	82.63
Xsnp4068	5BL_10920136_11384	GBS	5B	83.55
Xsnp4012	5BL_10872742_1600	GBS	5B	94.73
Xsnp1356	IWA6416	9kSNP	5B	96.46
Xsnp549	IWA2856	9kSNP	5B	98.92
Xsnp3983	5BL_10849486_812	GBS	5B	100.61
Xsnp797	IWA3984	9kSNP	5B	101.45
Xsnp794	IWA3972	9kSNP	5B	102.25
Xsnp4086	5BL_10923712_6962	GBS	5B	103.2
Xsnp4089	5BL_10924587_14089	GBS	5B	104.12
Xsnp29	IWA197	9kSNP	5B	106.71
Xbarc59	barc59Vd	SSR	5B	108.35
Xsnp4077	5BL_10922184_4499	GBS	5B	113.04
Xsnp4011	5BL_10872018_3053	GBS	5B	114.66
Xsnp4073	5BL_10921419_3669	GBS	5B	117.92
Xsnp3970	5BL_10840305_3724	GBS	5B	118.76
Xsnp4753	7AS_4250076_4895	GBS	5B	122.4
Xsnp435	IWA2322	9kSNP	5B	123.21
Xsnp4434	6BS_3015089_462	GBS	6B	0
Xsnp4381	6BS_2382089_3037	GBS	6B	0.85
Xsnp4456	6BS_3045731_3453	GBS	6B	2.74
Xsnp107	IWA666	9kSNP	6B	3.64
Xsnp4445	6BS_3026386_3531	GBS	6B	4.52
Xsnp4444	6BS_3026386_1714	GBS	6B	5.57
Xsnp4453	6BS_3042865_5315	GBS	6B	9.66
Xsnp4437	6BS_3018441_9034	GBS	6B	14.06
Xsnp4433	6BS_3014202_2832	GBS	6B	14.99

Marker Name	Original name	Marker Type	Chromosome	Position
Xsnp4436	6BS_3017682_61	GBS	6B	16.67
Xsnp4419	6BS_2980973_1601	GBS	6B	17.51
Xsnp4458	6BS_3047124_3482	GBS	6B	20.34
Xsnp4398	6BS_2945993_5225	GBS	6B	21.24
Xsnp4402	6BS_2948526_2724	GBS	6B	22.95
Xsnp4420	6BS_2982232_3167	GBS	6B	28.1
Xsnp4424	6BS_2989241_1219	GBS	6B	36.42
Xsnp4413	6BS_2971926_3904	GBS	6B	41.4
Xsnp4380	6BS_1815865_3388	GBS	6B	48.79
Xsnp4418	6BS_2980939_1278	GBS	6B	57.8
Xbarc101	barc101Fd	SSR	6B	60.74
Xsnp4793	7BL_6505483_1409	GBS	6B	61.59
Xsnp4421	6BS_2983594_1675	GBS	6B	62.45
Xsnp4451	6BS_3040589_9326	GBS	6B	64.17
Xsnp1683	IWA7962	9kSNP	6B	64.98
Xsnp4405	6BS_2953728_521	GBS	6B	65.83
Xsnp4358	6BL_4395814_376	GBS	6B	66.76
Xsnp4312	6BL_4221522_2029	GBS	6B	87.94
Xsnp1438	IWA6853	9kSNP	6B	93.8
Xsnp416	IWA2212	9kSNP	6B	96.22
Xsnp1703	IWA8072	9kSNP	6B	98.64
Xsnp4326	6BL_4291725_2242	GBS	6B	101.37
Xsnp4360	6BL_4397743_2024	GBS	6B	106.35
Xsnp4359	6BL_4397705_3655	GBS	6B	108
Xsnp4352	6BL_4374248_2376	GBS	6B	108.89
Xsnp1582	IWA7556	9kSNP	6B	110.7
Xsnp4357	6BL_4394660_814	GBS	6B	112.39
Xsnp4875	7BS_340844_212	GBS	7B	0
Xsnp4925	7BS_3163910_1729	GBS	7B	4.14
Xsnp4886	7BS_3037778_408	GBS	7B	5.09
Xsnp4921	7BS_3163051_6541	GBS	7B	13.91
Xsnp1693	IWA8007	9kSNP	7B	18.16
Xsnp4906	7BS_3121171_4350	GBS	7B	19.01
Xsnp4874	7BS_335942_68	GBS	7B	21.05
Xsnp4913	7BS_3144089_5377	GBS	7B	27.4
Xsnp4924	7BS_3163477_2926	GBS	7B	33.37
Xsnp4895	7BS_3089818_8962	GBS	7B	35.08
Xsnp400	IWA2105	9kSNP	7B	45.3
Xsnp4914	7BS_3144965_1801	GBS	7B	47

Marker Name	Original name	Marker Type	Chromosome	Position
Xsnp4923	7BS_3163281_540	GBS	7B	56.59
Xsnp4927	7BS_3164331_4293	GBS	7B	57.58
Xsnp489	IWA2534	9kSNP	7B	58.41
Xsnp4929	7BS_3165930_665	GBS	7B	59.38
Xsnp4883	7BS_3020366_1047	GBS	7B	60.31
Xsnp4808	7BL_6641908_1159	GBS	7B	62.05
Xsnp838	IWA4145	9kSNP	7B	62.91
Xsnp4852	7BL_6739556_386	GBS	7B	63.77
Xsnp4943	7DL_3352559_4358	GBS	7B	84.23
Xsnp4830	7BL_6688517_964	GBS	7B	87.06
Xsnp4872	7BL_6751455_4478	GBS	7B	91.19
Xsnp4869	7BL_6750359_4298	GBS	7B	92.05
Xsnp4855	7BL_6742737_2778	GBS	7B	92.89
Xsnp4840	7BL_6716171_1125	GBS	7B	94.03
Xsnp4780	7BL_267652_92	GBS	7B	95.14
Xsnp4865	7BL_6747975_4407	GBS	7B	101.05
Xsnp4867	7BL_6749334_1159	GBS	7B	102.81
Xsnp881	IWA4306	9kSNP	7B	103.63
Xsnp4833	7BL_6696170_4616	GBS	7B	105.43
Xsnp4839	7BL_6714218_2379	GBS	7B	106.31
Xsnp4810	7BL_6644774_480	GBS	7B	108.26
Xsnp4864	7BL_6747440_206	GBS	7B	109.11
Xsnp2525	2BL_7948745_11182	GBS	7B	130.29
Xsnp4860	7BL_6744829_4359	GBS	7B	137.3
Xsnp4831	7BL_6693640_2774	GBS	7B	151.56
Xsnp1066	IWA5001	9kSNP	7B	152.44
Xsnp4801	7BL_6568837_100	GBS	7B	153.24
Xsnp4785	7BL_4654046_81	GBS	7B	154.13
Xsnp4838	7BL_6709603_1964	GBS	7B	155.09
Xsnp1065	IWA5000	9kSNP	7B	155.9
Xsnp4804	7BL_6631440_3856	GBS	7B	157.56
Xsnp4940	7DL_3335671_2579	GBS	7B	177.83
Xsnp1304	IWA6094	9kSNP	1D	0
Xsnp2252	1DS_1903999_4020	GBS	1D	4.28
Xsnp606	IWA3124	9kSNP	1D	5.15
Xsnp2238	1DS_1881378_6074	GBS	1D	14.58
Xsnp2237	1DS_1877942_12021	GBS	1D	17.17
Xsnp1642	IWA7797	9kSNP	1D	18
Xsnp2240	1DS_1883270_672	GBS	1D	22.4

Marker Name	Original name	Marker Type	Chromosome	Position
Xsnp2239	1DS_1882647_1575	GBS	1D	26.45
Xsnp2251	1DS_1903643_13166	GBS	1D	27.29
Xsnp2255	1DS_1914087_1537	GBS	1D	50.01
Xsnp2256	1DS_1914495_3816	GBS	1D	50.82
Xsnp2244	1DS_1890379_6849	GBS	1D	52.59
Xsnp2229	1DL_2227188_3400	GBS	1D	53.43
Xsnp2235	1DL_2273917_4020	GBS	1D	55.25
Xsnp2231	1DL_2251128_416	GBS	1D	60.02
Xsnp2224	1DL_1414308_108	GBS	1D	68.26
Xsnp2234	1DL_2273598_7600	GBS	1D	73.28
Xsnp2232	1DL_2262988_3689	GBS	1D	85.55
Xsnp2870	2DS_5383098_16018	GBS	2D	0
Xsnp2854	2DS_5364086_1065	GBS	2D	5.77
Xsnp2819	2DS_4881294_131	GBS	2D	9.44
Xsnp2868	2DS_5382354_2100	GBS	2D	12.5
Xsnp2881	2DS_5390826_7647	GBS	2D	13.44
Xsnp2823	2DS_5303895_671	GBS	2D	19.61
Xsnp2882	2DS_5390971_8013	GBS	2D	20.5
Xgwm261	gwm261Nd	SSR	2D	25.67
Xsnp2810	2DS_1166935_168	GBS	2D	27.54
Xsnp2875	2DS_5386510_5609	GBS	2D	28.51
Xsnp2850	2DS_5351730_1417	GBS	2D	29.35
Xsnp2862	2DS_5375380_1169	GBS	2D	47
PpdD1	TaPpdDD002	KASP	2D	61.7
Xsnp2869	2DS_5382880_5243	GBS	2D	76.39
Xsnp2844	2DS_5342105_4599	GBS	2D	77.44
Xsnp2877	2DS_5389644_3961	GBS	2D	78.54
Xsnp2848	2DS_5351475_6429	GBS	2D	79.51
Xsnp634	IWA3248	9kSNP	2D	80.41
Xsnp2863	2DS_5375976_5855	GBS	2D	81.25
Xsnp2876	2DS_5387030_10613	GBS	2D	82.13
Xsnp522	IWA2722	9kSNP	2D	85.56
Xsnp2808	2DL_9908282_8445	GBS	2D	88.53
Xsnp2804	2DL_9864848_2667	GBS	2D	89.39
Xsnp1766	IWA8487	9kSNP	2D	91.23
Xsnp2809	2DL_9908584_75	GBS	2D	95.51
Xsnp2806	2DL_9900717_5277	GBS	2D	96.39
Xsnp179	IWA1072	9kSNP	2D	99.73
Xsnp2790	2DL_9727927_2650	GBS	2D	105.01

Marker Name	Original name	Marker Type	Chromosome	Position
Xsnp2807	2DL_9903734_1425	GBS	2D	107.77
Xsnp2788	2DL_4349500_161	GBS	2D	108.7
Xsnp2805	2DL_9877430_14537	GBS	2D	109.51
Xsnp2795	2DL_9813904_943	GBS	2D	112.49
Xsnp708	IWA3571	9kSNP	2D	119.39
Xsnp1745	IWA8325	9kSNP	2D	125.93
Xsnp4980	BS00065928	KASP	3D	0
Xsnp3431	3DS_2571866_1401	GBS	3D	16.62
Xsnp3434	3DS_2603133_61	GBS	3D	18.61
Xsnp3425	3DS_451487_186	GBS	3D	28.13
Xsnp3427	3DS_2233625_836	GBS	3D	34.97
Xsnp3430	3DS_2569686_2858	GBS	3D	35.8
Xsnp3432	3DS_2577014_1698	GBS	3D	36.65
Xsnp942	IWA4559	9kSNP	3D	38.26
Xsnp786	IWA3929	9kSNP	3D	39.08
Xsnp3419	3DL_6862069_373	GBS	3D	47.56
Xsnp3422	3DL_6949138_157	GBS	3D	56.04
Xsnp3187	3B_10517682_6066	GBS	3D	72.74
Xsnp3753	4DS_2294270_678	GBS	4D	0
Xsnp3752	4DS_2286922_3696	GBS	4D	10.24
Xsnp3754	4DS_2302886_964	GBS	4D	14.02
Xsnp4981	BS00036421	KASP	4D	55.79
Xsnp3750	4DL_14442270_2725	GBS	4D	62.55
Xsnp3748	4DL_14366503_1367	GBS	4D	63.42
Xsnp3743	4DL_6952434_82	GBS	4D	76.77
Xsnp4177	5DS_2767092_1122	GBS	5D	0
Xsnp4179	5DS_2782975_3120	GBS	5D	3.45
Xsnp1751	IWA8360	9kSNP	5D	6.71
Xsnp4175	5DS_2730791_8400	GBS	5D	22.14
Xsnp198	IWA1172	9kSNP	5D	23.75
Xsnp4156	5DL_74079_2181	GBS	5D	24.6
Xsnp4173	5DS_131747_281	GBS	5D	27.14
Xsnp4178	5DS_2782527_6993	GBS	5D	28.12
Xgdm136	gdm136Fd	SSR	5D	47.9
Xsnp4172	5DL_4607882_1952	GBS	5D	56.32
Xsnp4171	5DL_4605624_9145	GBS	5D	78.89
Xsnp876	IWA4274	9kSNP	5D	89.52
Xsnp4170	5DL_4604235_7923	GBS	5D	94.58
Xsnp4157	5DL_1208228_231	GBS	5D	117.64

Marker Name	Original name	Marker Type	Chromosome	Position
Xsnp1271	IWA5970	9kSNP	5D	124.35
Xsnp4163	5DL_4529496_20413	GBS	5D	125.27
Xsnp4162	5DL_4508888_3320	GBS	5D	139.36
Xsnp4169	5DL_4588938_1981	GBS	5D	165.6
Xsnp4166	5DL_4561264_559	GBS	5D	178.6
Xsnp553	IWA2877	9kSNP	5D	179.45
Xsnp4521	6DS_2123217_2578	GBS	6D	0
Xsnp4501	6DS_2068362_1361	GBS	6D	1.01
Xsnp4513	6DS_2102292_5249	GBS	6D	5.1
Xsnp4508	6DS_2081875_1712	GBS	6D	14.21
Xsnp4496	6DS_1919110_1843	GBS	6D	29.19
Xsnp4504	6DS_2072139_8001	GBS	6D	30.03
Xsnp4515	6DS_2104699_481	GBS	6D	30.9
Xsnp4512	6DS_2098523_128	GBS	6D	31.89
Xsnp4518	6DS_2114456_29	GBS	6D	51.43
Xsnp4482	6DL_3297209_3422	GBS	6D	60.45
Xsnp814	IWA4042	9kSNP	6D	66.41
Xsnp4470	6DL_3214335_2089	GBS	6D	67.25
Xsnp4491	6DL_3329775_3397	GBS	6D	71.34
Xsnp4484	6DL_3300954_10135	GBS	6D	129.96
Xsnp4488	6DL_3315387_4801	GBS	6D	131.79
Xsnp4485	6DL_3304331_696	GBS	6D	136.11
Xsnp4465	6DL_2631344_795	GBS	6D	137
Xsnp4487	6DL_3315130_4117	GBS	6D	138.8
Xsnp4468	6DL_3206411_930	GBS	6D	139.67
Xsnp4483	6DL_3300954_8654	GBS	6D	141.35
Xsnp4486	6DL_3311975_19081	GBS	6D	142.16
Xsnp230	IWA1384	9kSNP	6D	144.64
Xsnp4977	7DS_3962731_625	GBS	7D	0
Xsnp4976	7DS_3955977_943	GBS	7D	0.9
Xsnp4967	7DS_3905453_8238	GBS	7D	7.25
Xsnp4978	7DS_3966794_3169	GBS	7D	62.18
Xsnp4954	7DS_3583569_83	GBS	7D	70.59
Xsnp4973	7DS_3940684_560	GBS	7D	86.88
Xsnp3420	3DL_6915964_5472	GBS	7D	93.43
XRc	Rc	morphological	7D	106.74
Xsnp4942	7DL_3343962_3908	GBS	7D	118.04
Xsnp4945	7DL_3364893_8951	GBS	7D	118.86
Xsnp4932	7DL_381629_250	GBS	7D	119.69

Marker Name	Original name	Marker Type	Chromosome	Position
Xsnp4966	7DS_3905335_3571	GBS	7D	121.46
Xgwm111	gwm111Vd	SSR	7D	122.46
Xsnp4937	7DL_3332751_1874	GBS	7D	125.75
Xsnp1759	IWA8436	9kSNP	7D	145.66
Xsnp4949	7DL_3391526_3377	GBS	7D	233.57
Xsnp4941	7DL_3340905_8547	GBS	7D	235.51
Xsnp4934	7DL_3318693_750	GBS	7D	241.42
Xsnp4944	7DL_3353775_2814	GBS	7D	244.9
Xsnp4948	7DL_3388502_2021	GBS	7D	256.41
Xsnp420	IWA2226	9kSNP	7D	259.8

Bibliography

Andrés, F. & Coupland, G., 2012. The genetic basis of flowering responses to seasonal cues. *Nature Reviews Genetics*, 13(9), pp.627–639. Available at: http://dx.doi.org/10.1038/nrg3291.

Beales, J. et al., 2007. A Pseudo-Response Regulator is misexpressed in the photoperiod insensitive Ppd-D1a mutant of wheat (Triticum aestivum L .). *Theoretical and Applied Genetics*, 115, pp.721–733.

Bentley, A.R. et al., 2013. Short, natural, and extended photoperiod response in BC2F4 lines of bread wheat with different Photoperiod-1 (Ppd-1) alleles. *Journal of Experimental Botany*, 64(7), pp.1783–1793.

Botstein, D. et al., 1980. Construction of a Genetic Linkage Map in Man Using Restriction Fragment Length Polymorphisms. *American Journal of Human Genetics*, 32, pp.314–331.

Bushuk, W., 1998. Wheat breeding for end-product use. *Euphytica*, 100, pp.137–145.

Cavanagh, C.R. et al., 2013. Genome-wide comparative diversity uncovers multiple targets of selection for improvement in hexaploid wheat landraces and cultivars. *Proceedings of the National Academy of Sciences*, 110(20), pp.8057–8062.

Chen, A. et al., 2014. PHYTOCHROME C plays a major role in the acceleration of wheat flowering under long-day photoperiod. *Proceedings of the National Academy of Science*, 111(28), pp.10037–10044.

Chouard, P., 1960. Vernalization and its relations to dormancy. *Annual Review of Plant Physiology*, 11, pp.191–238.

Collard, B.C.Y. et al., 2005. An introduction to markers , quantitative trait loci (QTL) mapping and marker-assisted selection for crop improvement : The basic concepts. *Euphytica*, 142, pp.169–196.

Collard, B.C.Y. & Mackill, D.J., 2008. Marker-assisted selection: an approach for precision plant breeding in the twenty-first century. *Philospohical Transactions of the Royal Society*, 363, pp.557–572.

Diaz, A. et al., 2012. Copy Number Variation Affecting the Photoperiod-B1 and Vernalization-A1 Genes Is Associated with Altered Flowering Time in Wheat (Triticum aestivum). *PloS one*, 7(3), p.e33234: 1–11.

Distelfeld, A., Li, C. & Dubcovsky, J., 2009. Regulation of flowering in temperate cereals. *Current Opinion in Plant Biology*, pp.1–7. Available at: http://dx.doi.org/10.1016/j.pbi.2008.12.010.

Doerge, R., 2002. Mapping and analysis of quantitative trait loci in experimental populations. *Nature Reviews Genetics*, 3, pp.43–52.

Dubcovsky, J., 2004. Marker-Assisted Selection in Public Breeding Programs: The Wheat Experience. In *Genomics and Plant Breeding Symposium*. pp. 1895–1898.

Dubcovsky, J. & Dvorak, J., 2007. Genome Plasticity a Key Factor. *Science*, 316, pp.1862–1866.

Dvorak, J. et al., 1998. The structure of the Aegilops tauschii genepool and the evolution of hexaploid wheat. *Theoretical and Applied Genetics*, 97, pp.657–670.

Elshire, R.J. et al., 2011. A Robust , Simple Genotyping-by-Sequencing (GBS) Approach for High Diversity Species. *PloS one*, 6(5), p.e19379.

Feldman, M. & Kislev, M.E., 2015. Domestication of emmer wheat and evolution of free-threshing tetraploid wheat. *Israel Journal of Plant Sciences*, 55(October), pp.207–221.

Fu, D. et al., 2005. Large deletions within the first intron in VRN-1 are associated with spring growth habit in barley and wheat. *Molecular Genetics and Genomics*, 273(1), pp.54–65. Available at: http://link.springer.com/10.1007/s00438-004-1095-4.

Geldermann, H., 1975. Investigations on Inheritance of Quantitative Characters in Animals by Gene Markers. *Theoretical and Applied Genetics*, 46, pp.319–330.

Gomez, D. et al., 2014. Effect of Vrn-1, Ppd-1 genes and earliness per se on heading time in Argentinean bread wheat cultivars. *Field Crops Research*, 158, pp.73–81. Available at: http://dx.doi.org/10.1016/j.fcr.2013.12.023.

Guedira, M. et al., 2014. Vernalization Duration Requirement in Soft Winter Wheat is Associated with Variation at the Locus. *Crop Science*, 54(5), p.1960. Available at: https://www.crops.org/publications/cs/abstracts/54/5/1960.

Hartl, D.L. & Jones, E.W., 2001. *Genetics: Analysis of genes and genomes*, Jones & Bartlett Publishers.

He, J. et al., 2014. Genotyping-by-sequencing (GBS), an ultimate marker-assisted selection (MAS) tool to accelerate plant breeding. *Frontiers in Plant Science*, 5, p.Article 484.

Irish, V.F. & Sussex, M., 1990. Function of the apetala-1 Gene during Arabídopsis Floral Development. *The Plant Cell*, 2, pp.741–753.

Kamran, A., Iqbal, M. & Spaner, D., 2014. Flowering time in wheat (Triticum aestivum L .): a key factor for global adaptability. *Euphytica*, 197, pp.1–26.

Kang, J. et al., 2011. Exotic Scab Resistance Quantitative Trait Loci Effects on Soft Red Winter Wheat. *Crop Science*, 51, pp.924–933.

Kato, K. & Wada, T., 1999. Genetic Analysis and Selection Experiment for Narrow-Sense Earliness in Wheat by Using Segregating Hybrid Progenies. *Breeding Science*, 49, pp.233–238.

Kato, K. & Yokoyama, H., 1992. Geographical variation in heading characters among wheat landraces , Triticum aestivum L ., and its implication for their adaptability. *Theoretical and Applied Genetics*, 84, pp.259–265.

Kippes, N. et al., 2015. Identification of the *VERNALIZATION 4* gene reveals the origin of spring growth habit in ancient wheats from South Asia. *Proceedings of the National Academy of Sciences*, 112(39), pp.E5401–E5410. Available at: http://www.pnas.org/lookup/doi/10.1073/pnas.1514883112.

Kiss, T. et al., 2014. Allele frequencies in the VRN-A1 , VRN-B1 and VRN-D1 vernalization response and PPD-B1 and PPD-D1 photoperiod sensitivity genes, and their effects on heading in a diverse set of wheat cultivars (Triticum aestivum L.). *Molecular Breeding*, 34, pp.297–310.

Knox, J. et al., 2012. Climate change impacts on crop productivity in Africa and South Asia. *Environmental Research Letters*, 7(034032), pp.1–8.

Lander, E.S. & Botstein, L., 1989. Mapping Mendelian Factors Underlying Quantitative Traits Using RFLP Linkage Maps. *Genetics*, 121, pp.185–199.

Laurie, D.A. & Bennett, M.D., 1988. The production of haploid wheat plants from wheat x maize crosses. *Theoretical and Applied Genetics*, 76, pp.393–397.

Li, C. & Dubcovsky, J., 2008. Wheat FT protein regulates VRN1 transcription through interactions with FDL2. *The Plant Journal*, 55, pp.543–554.

Marcussen, T. et al., 2014. Ancient hybridizations among the ancestral genomes of bread wheat. *Science*, 345(6194), p.1250092; 1–4.

McIntosh, R. et al., 2003. Catalogue of Gene Symbols for Wheat. In N. Pogna et al., eds. *Proceedings of the 10th International Wheat Genetics Symposium*. Instituto Sperimentale per la Cerealicoltura Rome, Paestum, Italy. Available at: http://wheat.pw.usda.gov/ggpages/wgc/2003/.

Mondal, S. et al., 2015. Characterization of Heat- and Drought-Stress Tolerance in High-Yielding Spring Wheat. *Crop Science*, 55, pp.1552–1562.

Nakamichi, N. et al., 2005. Pseuo-Response Regulators, PRR9, PRR7, and PRR5, Together Play Essential Roles Close to the Circadian Clock of Arabidopsis thaliana. *Plant Cell Physiology*, 46(5), pp.686–698.

Nishida, H. et al., 2013. Structural variation in the 5 0 upstream region of photoperiod-insensitive alleles Ppd - A1a and Ppd - B1a identified in hexaploid wheat (Triticum aestivum L .), and their effect on heading time. *Molecular Breeding*, 31, pp.27–37.

Pallotta, M. A., P., Warner, R. L., Fox, H., Kuchel, S. J., eries, J., and Langridge, P. (2003). Marker assisted wheat breeding in the southern region of Australia. *In* "Proceedings of the Tenth International Wheat Genetics Symposium", pp. 789-791, 1-6 September, 2003. Paestum, Italy.

Paterson, A., 1996. Physical mapping and map-based cloining: Bridging the gap between DNA markers and genes. In *Genome Mapping in Plants*. RG Landes Co, Austin: Academic Press, pp. 55–62.

Paterson, A.H. et al., 1988. Resolution of quantitative traits into Mendelian factors by using a complete linkage map of restriction fragment length polymorphisms. *Nature*, 335, pp.721–726.

Peng, J.H., Sun, D. & Nevo, E., 2011. Domestication evolution, genetics and genomics in wheat. *Molecular Breeding*, 28, pp.281–301.

Petersen, G. et al., 2006. Phylogenetic relationships of Triticum and Aegilops and evidence for the origin of the A , B , and D genomes of common wheat (Triticum aestivum). *Molecular Phylogenetics and Evolution*, 39, pp.70–82.

Poland, J. a et al., 2012. Development of high-density genetic maps for barley and wheat using a novel two-enzyme genotyping-by-sequencing approach. *PloS one*, 7(2), p.e32253. Available at: http://journals.plos.org/plosone/article?id=10.1371/journal.pone.0032253.

Putterill, J. et al., 1995. The CONSTANS Gene of Arabidopsis Promotes Flowering and Encodes a Protein Showing Similarities to Zinc Finger Transcription Factors. *Cell*, 80, pp.847–857.

Reynolds, M. et al., 2009. Raising yield potential in wheat. *Journal of Experimental Botany*, 60(7), pp.1899–1918.

Roder, M.S. et al., 1998. A microsatellite map of wheat. *Genetics*, 149(4), pp.2007–2023.

Schmid, K.J. et al., 2003. Large-Scale Identification and Analysis of Genome-Wide Single-Nucleotide Polymorphisms for Mapping in Arabidopsis thaliana. *Genome Research*, 13, pp.1250–1257.

Shitsukawa, N. et al., 2007. The einkorn wheat (Triticum monococcum) mutant , maintained vegetative phase , is caused by a deletion in the VRN1 gene. *Genes & Genetic Systems*, 82, pp.167–170.

Sievers, F. et al., 2011. Fast,scalable generation of high-quality protein multiple sequence alignments using Clustal Omega. *Molecular Systems Biology*, 7, pp.539.

Snape, J.W. et al., 2001. Waiting for fine times : genetics of flowering time in wheat. *Euphytica*, 119, pp.185–190.

Somers, D.J., Isaac, P. & Edwards, K., 2004. A high-density microsatellite consensus map for bread wheat (Triticum aestivum L.). *Theoretical and applied genetics*, 109(6), pp.1105–1114.

Song, Q.J. et al., 2005. Development and mapping of microsatellite (SSR) markers in wheat. *Theoretical and Applied Genetics*, 110(3), pp.550–560.

Southern, E., 1975. Detection of specific sequences among DNA fragments separated by gel electrophoresis. *Journal of Molecular Biology*, 98(3), pp.503–17.

Suarez-Lopez, P. et al., 2001. CONSTANS mediates between the circadian clock and the control of flowering in Arabidopsis. *Nature*, 410(April), pp.1116–1120.

Tanksley, S.D., 1993. Mapping Polygenes. *Annual Review of Genetics*, 27, pp.205–233.

Tranquilli, G. & Dubcovsky, J., 2000. Epistatic Interaction Between Vernalization Genes Vrn-Am1 and Vrn-Am2 in Diploid Wheat. *Heredity*, 91(4), pp.304–306.

Turner, A. et al., 2005. The Pseudo-Response Regulator Ppd-H1 Provides Adaptation to Photoperiod in Barley. *Science*, 310(5750), pp.1031–1034.

Valverde, F. et al., 2004. Photoreceptor Regulation of CONSTANS Protein in Photoperiodic Flowering. *Science*, 303, pp.1003–1006.

Vos, P. et al., 1995. AFLP : a new technique for DNA fingerprinting. *Nucleic Acids Research*, 23(21), pp.4407–4414.

Wheeler, T. & von Braun, J., 2013. Climate Change Impacts on Global Food Security. *Science*, 341(August), pp.1773–1775.

Wilhelm, E.P., Turner, A.S. & Laurie, D. a., 2009. Photoperiod insensitive Ppd-A1a mutations in tetraploid wheat (Triticum durum Desf.). *Theoretical and Applied Genetics*, 118(2), pp.285–294. Available at: http://link.springer.com/10.1007/s00122-008-0898-9.

Wilkinson, P.A. et al., 2012. CerealsDB 2.0: an integrated resource for plant breeders and scientists. *BMC bioinformatics*, 13(1), p.219.

Winter, P. & Kahl, G., 1995. Molecular marker technologies for plant improvement. *World Journal of Microbiology & Biotechnology*, 11, pp.438–448.

Worland, A.J., 1996. The influence of flowering time genes on environmental adaptability in European wheats Vernalization sensitivity. *Euphytica*, 89, pp.49–57.

Worland, A.J. et al., 1998. The influence of photoperiod genes on the adaptability of European winter wheats. *Euphytica*, 100, pp.385–394.

Xiao, J. et al., 2014. O-GlcNAc-mediated interaction between VER2 and TaGRP2 elicits TaVRN1 mRNA accumulation during vernalization in winter wheat. *Nature Communications*, 5, p.4572. Available at: http://dx.doi.org/10.1038/ncomms5572.

Xu, Y., 2010. *Molecular Plant Breeding* 1st ed., CAB International.

Yan, L. et al., 2003. Positional cloning of the wheat vernalization gene VRN1. *Proceedings of the National Academy of Sciences*, 100(10), pp.6263–6268.

Yan, L. et al., 2006. The wheat and barley vernalization gene VRN3 is an orthologue of FT. *Proceedings of the National Academy of Sciences*, 103(51), pp.19581–19586.

Yan, L. et al., 2004. The Wheat VRN2 Gene Is a Flowering Repressor Down-Regulated by Vernalization. *Science*, 303, pp.1640–1644.

Zadoks, J.C., Chang, T.T. & Konzak, C.F., 1974. A decimal code for the growth stages of cereals. *Weed Research*, 14, pp.415–421.

Zheng, B. et al., 2013. Quantification of the effects of VRN1 and Ppd-D1 to predict spring wheat (Triticum aestivum) heading time across diverse environments. *Journal of Experimental Botany*, 64(12), pp.3747–3761.

Zikhali, M. et al., 2014. Validation of a 1DL earliness per se (eps) flowering QTL in bread wheat (Triticum aestivum). *Molecular Breeding*, 34, pp.1023–1033.